

Spring 2009

Temporal variation, regional sources, and removal processes of volatile organic compounds in New England

Rachel S. Russo

University of New Hampshire, Durham

Follow this and additional works at: <https://scholars.unh.edu/dissertation>

Recommended Citation

Russo, Rachel S., "Temporal variation, regional sources, and removal processes of volatile organic compounds in New England" (2009). *Doctoral Dissertations*. 485.

<https://scholars.unh.edu/dissertation/485>

This Dissertation is brought to you for free and open access by the Student Scholarship at University of New Hampshire Scholars' Repository. It has been accepted for inclusion in Doctoral Dissertations by an authorized administrator of University of New Hampshire Scholars' Repository. For more information, please contact nicole.hentz@unh.edu.

TEMPORAL VARIATION, REGIONAL SOURCES, AND REMOVAL PROCESSES
OF VOLATILE ORGANIC COMPOUNDS IN NEW ENGLAND

BY

Rachel S. Russo

Bachelor of Science in Physics, Rensselaer Polytechnic Institute, 2001

Master of Science in Earth Science: Geochemical Systems,

University of New Hampshire, 2005

DISSERTATION

Submitted to the University of New Hampshire

in Partial Fulfillment of

the Requirements for the Degree of

Doctor of Philosophy

in

Earth and Environmental Science

May, 2009

UMI Number: 3363729

Copyright 2009 by
Russo, Rachel S.

INFORMATION TO USERS

The quality of this reproduction is dependent upon the quality of the copy submitted. Broken or indistinct print, colored or poor quality illustrations and photographs, print bleed-through, substandard margins, and improper alignment can adversely affect reproduction.

In the unlikely event that the author did not send a complete manuscript and there are missing pages, these will be noted. Also, if unauthorized copyright material had to be removed, a note will indicate the deletion.

UMI[®]

UMI Microform 3363729
Copyright 2009 by ProQuest LLC
All rights reserved. This microform edition is protected against
unauthorized copying under Title 17, United States Code.

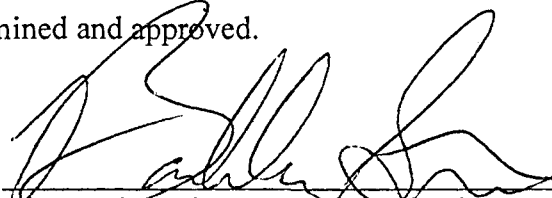
ProQuest LLC
789 East Eisenhower Parkway
P.O. Box 1346
Ann Arbor, MI 48106-1346

All Rights Reserved

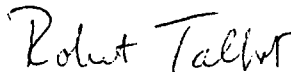
© 2009

Rachel S. Russo

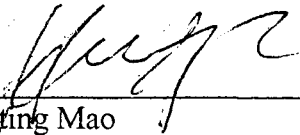
This dissertation has been examined and approved.



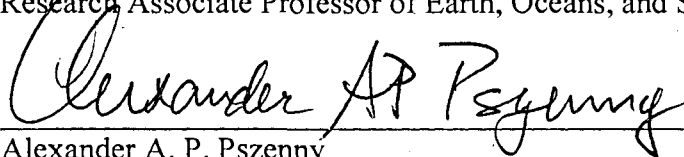
Dissertation Director, Barkley C. Sive
Research Associate Professor of Earth, Oceans, and Space



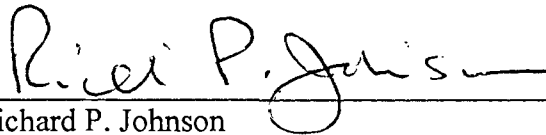
Robert W. Talbot
Research Professor of Earth Sciences and Earth, Oceans,
and Space



Huijing Mao
Research Associate Professor of Earth, Oceans, and Space



Alexander A. P. Pszenny
Research Associate Professor of Earth, Oceans, and Space



Richard P. Johnson
Professor of Chemistry

April 16, 2009
Date

ACKNOWLEDGEMENTS

Financial support for this work was provided through the Office of Oceanic and Atmospheric Research at the National Oceanic and Atmospheric Administration as part of AIRMAP. Additional support for the research conducted on Appledore Island was provided by the National Science Foundation.

TABLE OF CONTENTS

ACKNOWLEDGEMENTS.....	iv
LIST OF TABLES.....	ix
LIST OF FIGURES.....	x
ABSTRACT.....	xiii

CHAPTER	PAGE
1. INTRODUCTION	1
2. LONG-TERM MEASUREMENTS OF NONMETHANE HYDROCARBONS AND HALOCARBONS IN NEW HAMPSHIRE: SEASONAL VARIATIONS AND REGIONAL SOURCES	
2.1 Introduction.....	4
2.2 Sampling and Analytical Methods.....	6
2.2.1 Daily Canister Samples.....	6
2.2.2 Daily Canister Sample Data Set.....	9
2.2.3 Thompson Farm Automated Gas Chromatograph	10
2.2.4 Standards and Calibration	11
2.3 Seasonal and Interannual Variability	13
2.3.1 Anthropogenic Nonmethane Hydrocarbons	13
2.3.2 Isoprene.....	16
2.3.3 Halocarbons	18
2.4 NMHC Source Identification.....	24
2.4.1 Comparison with Tracers and Source Signatures	24

2.4.2 Ambient Ratios: Compounds with Similar Lifetimes.....	30
2.4.3 Ambient Ratios: Compounds with Different Lifetimes.....	33
2.5 Regional Emission Rates of NMHCs	36
2.6 Comparison with the 2002 EPA National Emissions Inventory.....	41
2.7 Summary.....	44
3. TEMPORAL VARIABILITY, SOURCES, AND SINKS OF C ₁ -C ₅ ALKYL NITRATES IN COASTAL NEW ENGLAND	
3.1 Introduction.....	45
3.2 Experimental.....	48
3.2.1 NEAQS 2002	48
3.2.1.1 Thompson Farm GC System.....	48
3.2.1.2 GC System on the NOAA R/V <i>Ronald H. Brown</i>	49
3.2.2 Canister Samples.....	49
3.2.2.1 Great Bay Experiment.....	49
3.2.2.2 Thompson Farm Daily Canister Samples	51
3.2.3 Measurement Intercomparison.....	52
3.2.4 Ancillary Measurements	52
3.3 Temporal Variation of Alkyl Nitrates at Thompson Farm	54
3.3.1 Seasonal Variation	55
3.3.2 Diurnal Variation	59
3.4 Sources of Alkyl Nitrates in Coastal New England.....	66
3.4.1 Inland/Coastal Environment: Thompson Farm.....	67
3.4.2 Marine Environment: Measurements onboard the NOAA R/V <i>Ronald H. Brown</i>	70

3.4.3 Estuarine Environment: Great Bay Experiment	72
3.5 Alkyl Nitrate/Parent Hydrocarbon Relationships	74
3.6 Summary	81
4. CHLORINE ATOM CONCENTRATIONS AND CONTRIBUTIONS TO VOC OXIDATION DURING SUMMER 2004 AND 2005 AT INLAND AND OFFSHORE COASTAL NEW ENGLAND SITES	
4.1 Introduction.....	83
4.2 Experimental.....	86
4.2.1 Sampling Sites	86
4.2.2 Sample Collection and Analysis at Thompson Farm: July-August 2004 and 2005	87
4.2.3 Appledore Island Canister Samples: July-August 2004 and 2005	87
4.2.3.1 Canister Sample Collection.....	87
4.2.3.2 Laboratory Analysis of Canister Samples.....	88
4.2.4 Proton Transfer Reaction-Mass Spectrometer	89
4.2.5 Data	89
4.3 Comparison of Source Regions, Meteorology, and Trace Gases at TF and AI during July-August 2004 and 2005.....	90
4.3.1 Source Regions	90
4.3.2 Interannual Variability in Meteorological Conditions.....	93
4.3.3 Interannual Variability in VOC Distributions at TF and AI.....	95
4.4 Estimates of Chlorine Atom Concentrations	100
4.4.1 Lifetime-Variability Relationship.....	100
4.4.2 Comparison between [Cl] Estimates at TF and AI in 2004 and 2005.....	105

4.4.3 Comparison to [Cl] Estimates based on Hydrocarbon Ratios	107
4.5 VOC Contributions to OH and Cl Removal over Coastal NH	109
4.6 DMS Trends and Oxidation	116
4.6.1 Diurnal Cycle and Removal Mechanisms of DMS at AI	116
4.6.2 Comparison with Previous Studies	121
4.7 Summary	122
LIST OF REFERENCES	124

LIST OF TABLES

Table 2.1. Monthly mean, standard deviation (SD), median, number of samples (N), and range of NMHC mixing ratios (pptv) at TF during January 2004-February 2008	21
Table 2.2. Annual C ₂ HCl ₃ and C ₂ Cl ₄ statistics (pptv), and the rate of decrease (pptv/year) in the annual background mixing ratios	24
Table 2.3. Emission rates (molecules cm ⁻² s ⁻¹) of C ₃ -C ₈ NMHCs calculated using measurements made by the TF GC and the winter 2006 daily canister data.....	39
Table 2.4. Emission rates (Mg/year) of benzene, toluene, ethylbenzene, xylenes, and ethyne extrapolated from the TF rates (Table 2.3) and from the 2002 EPA National Emissions Inventory for New Hampshire and New England	43
Table 3.1. Seasonal mean, standard deviation (SD), median, and number of samples (N) of alkyl nitrates at TF during winter and summer 2002	56
Table 3.2. Monthly mean, standard deviation (SD), and median alkyl nitrate mixing ratios (pptv), and number of samples (N) at TF during January 2004-February 2008.....	57
Table 3.3. Dry deposition fluxes (nmol m ⁻² hr ⁻¹), velocities (V _d) (cm s ⁻¹), and lifetimes (days) of alkyl nitrates during winter and summer 2002 at TF.....	65
Table 3.4. Mean mixing ratios of alkyl nitrates (pptv) in the northeast (NE, 0-90°), southeast (SE, 90-180°), southwest (SW, 180-270°), and northwest (NW, 270-360°) transport sectors during winter and summer 2002.....	68
Table 3.5. Values of the rate constants and branching ratios used to produce the predicted photochemical evolution curves in Figure 3.8	76
Table 4.1. Median mixing ratios of VOCs (pptv), CO (ppbv), and CH ₄ (ppmv) in the five transport sectors at TF and AI in (a) 2004 and (b) 2005.....	98
Table 4.2. VOC, CO, and CH ₄ rate constants for reaction with OH and Cl.....	101
Table 4.3. Estimated chlorine atom concentrations (molecules cm ⁻³) in the five transport sectors at TF and AI in 2004 and 2005	104
Table 4.4. The loss rates (molecules cm ⁻³ s ⁻¹) and kinetic reactivity of VOCs, CO, and CH ₄ in the (a) marine and (b) NW sectors at TF and AI in 2004 and 2005.....	112

LIST OF FIGURES

Figure 2.1. Location of the UNH AIRMAP Atmospheric Observing Station at Thompson Farm in Durham, New Hampshire, and (inset) the sampling sites used during the Great Bay Experiment (Chapter 3)	7
Figure 2.2. Per carbon response factors (PCRF) of (a) ethane, (b) ethyne, (c) propane, (d) propene, (e) n-butane, (f) 1-butene, (g) benzene, and (h) toluene in various standards analyzed in the UNH laboratory during 2004-2008.....	12
Figure 2.3. Time series of NMHCs (pptv) at TF during January 2004-February 2008: (a) ethane, propane, (b) n-butane, i-butane, (c) i-pentane, n-pentane, n-hexane, (d) ethene, ethyne, benzene, (e) propene, 1-butene, (f) toluene, ethylbenzene, and (g) m+p-xylene, o-xylene.....	15
Figure 2.4. (a) Time series of isoprene (pptv) at TF. (b) Hourly average temperature (°C) during June-August of 2004, 2005, 2006, and 2007	17
Figure 2.5. (a) Time series of C ₂ Cl ₄ and C ₂ HCl ₃ (pptv) at TF. Monthly mean mixing ratios of (b) C ₂ HCl ₃ and (c) C ₂ Cl ₄	20
Figure 2.6. Correlations between (a) ethyne and CO (ppbv) and (b) propene and 1-butene.....	26
Figure 2.7. Correlations between (a) n-butane and propane, (b) n-butane and i-butane, and (c) n-pentane and i-pentane.....	27
Figure 2.8. Correlations between (a) toluene and ethylbenzene, (b) o-xylene, and m+p-xylene, and (c) m+p-xylene and ethylbenzene	28
Figure 2.9. Correlations between ethyne and (a) propane and (b) benzene.....	32
Figure 2.10. Time series of the (a) ethyne/CO (pptv/ppbv) and toluene/benzene ratios and (b) propane/ethane and C ₂ HCl ₃ /C ₂ Cl ₄ ratios	34
Figure 2.11. Comparison between (a) propane, (b) ethyne, (c) benzene, and (d) toluene measurements made by the automated TF GC system and the daily canister samples collected during December 2005-January 2006	37
Figure 3.1. Alkyl nitrate and NMHC measurement intercomparison between the UNH, UCI, U. Miami and U. York (NMHCs only) laboratories	53

Figure 3.2. Time series of (a) MeONO ₂ , EtONO ₂ , 1-PrONO ₂ , (b) 2-PrONO ₂ , 2-BuONO ₂ , and (c) 2-PenONO ₂ , 3-PenONO ₂ (pptv) during winter and summer 2002 at TF	54
Figure 3.3. Time series of (a) MeONO ₂ , EtONO ₂ , 1-PrONO ₂ , (b) 2-PrONO ₂ , 2-BuONO ₂ , and (c) 2-PenONO ₂ , 3-PenONO ₂ (pptv) at TF during January 2004-February 2008.....	55
Figure 3.4. Hourly average (local time) (a) and (b) O ₃ (ppbv), wind speed (m/s), and J_{NO_2} , (c) and (d) MeONO ₂ and EtONO ₂ , (e) and (f) 2-PrONO ₂ and 2-BuONO ₂ in winter (left column) and summer (right column) 2002 at TF.....	60
Figure 3.5. Time series of (a) O ₃ (ppbv) and wind speed (m/s), (b) ethane and propane (pptv), (c) NO _y (ppbv), CO (ppbv), and CO ₂ (ppmv), (d) MeONO ₂ and EtONO ₂ , and (e) 2-PrONO ₂ and 2-BuONO ₂ (pptv) during June 6-16, 2002	62
Figure 3.6. Ambient air and surface seawater mixing ratios (pptv) of (a, b) MeONO ₂ and (c, d) 2-PrONO ₂ collected in the Gulf of Maine onboard the NOAA R/V <i>Ronald H. Brown</i> during NEAQS 2002.....	71
Figure 3.7. (a) O ₃ (ppbv), CO ₂ (ppmv), (b) wind speed (m/s), wind direction, and J_{NO_2} at TF from August 18 at 16:00 to August 19, 2003 at 22:00. (c-i) Alkyl nitrate mixing ratios (pptv) at four sites throughout the Great Bay estuary and at TF	73
Figure 3.8. Alkyl nitrate/parent hydrocarbon ratios versus 2-BuONO ₂ /n-butane for winter (left) and summer (right) 2002: (a, b) EtONO ₂ /ethane, (c, d) 2-PrONO ₂ /propane, (e, f) 1-PrONO ₂ /propane, (g, h) 3-PenONO ₂ /n-pentane, and (i, j) 2-PenONO ₂ /n-pentane.....	77
Figure 4.1. (a) Location of the UNH Atmospheric Observing Stations at TF (Durham, NH) and AI (ME). (b) Examples of HYSPLIT backward trajectories for each of the five source regions	91
Figure 4.2. Time series of ethane (pptv) at TF and AI in (a) 2004 and (b) 2005	92
Figure 4.3. Hourly average (a) temperature (°C), (b) J_{NO_2} (s ⁻¹), (c) wind speed (m/s), (d) O ₃ (ppbv), and (e) CO (ppbv) at TF and AI in 2004 and 2005.....	94
Figure 4.4. Hourly average (a) propane, (b) i-butane, (c) n-butane, (d) i-pentane, (e) n-pentane, (f) ethyne, (g) benzene, and (h) toluene mixing ratios (pptv) at TF and AI in 2004 and 2005	97
Figure 4.5. Lifetime-variability relationships for NMHCs in the five transport sectors at TF in (a) 2004 and (c) 2005 and at AI in (b) 2004 and (d) 2005	103

Figure 4.6. $\ln(\text{NMHC}/\text{NMHC}_0)$ versus k_{OH} and k_{Cl} correlations at (a) AI in the marine sector during 2004, (b) AI during July 13-14, 2004, and at TF during (c) July 13-14, 2004, and (d) August 12-13, 2004.....	108
Figure 4.7. VOC, CO, and CH_4 loss rates with respect to reaction with OH and Cl during 2004 at TF and AI in the (a) marine and (b) NW sectors and during 2005 in the (c) marine and (d) NW sectors	111
Figure 4.8. Hourly average DMS (pptv) and wind speed (m/s) in the marine sector at AI during 2004	117
Figure 4.9. (a) Hourly photolysis frequencies (s^{-1}) and calculated OH concentrations (molecules cm^{-3}), (b) hourly average DMS and (c) ethane mixing ratios (pptv) in the marine sector at AI in 2004	120

ABSTRACT

TEMPORAL VARIATION, REGIONAL SOURCES, AND REMOVAL PROCESSES OF VOLATILE ORGANIC COMPOUNDS IN NEW ENGLAND

by

Rachel S. Russo

University of New Hampshire, May, 2009

This dissertation describes three research projects with the common objective of characterizing the influence of volatile organic compounds (VOCs) on air quality in New England using measurements made over multiple years (2002-2008) and from different sampling locations. The specific objectives include identifying sources (direct emission or secondary production), quantifying mixing ratios, and characterizing the chemical (i.e., oxidation, photolysis) and physical (i.e., transport, mixing) processes which regulate the distributions of VOCs in the troposphere over southeastern New Hampshire.

Chapters 2 and 3 discuss the seasonal and interannual variability of nonmethane hydrocarbons (NMHCs), selected halocarbons, and alkyl nitrates using measurements from canister samples collected at Thompson Farm in Durham, NH throughout January 2004-February 2008. Several anthropogenic and biogenic sources of NMHCs and halocarbons were identified based on correlations with tracer compounds and comparisons with source signatures. Additionally, evidence for the dry deposition of alkyl nitrates at night was observed which is a previously unaccounted for removal mechanism. Analysis of alkyl nitrate/parent hydrocarbon ratios, measurements made onboard the NOAA R/V *Ronald H. Brown* during the 2002 New England Air Quality

Study, and canister samples collected throughout the Great Bay estuary in August 2003 are presented to assess the relative contributions of anthropogenic and marine sources of alkyl nitrates.

The research described in Chapter 4 used measurements of VOCs made at an inland (Thompson Farm) and an offshore (Appledore Island) site to identify evidence of chlorine initiated oxidation of VOCs, estimate chlorine atom (Cl) concentrations during two summers and for different transport sectors, and assess the potential influence of chlorine chemistry on the oxidative capacity of the troposphere over coastal New Hampshire. Comparable Cl concentrations were estimated using a novel technique based on the lifetime-variability relationship of NMHCs and using the traditional NMHC ratio method. Furthermore, the daytime loss of DMS and ethane in the marine sector at AI was reproduced when reaction with both OH and Cl were considered providing supporting evidence for Cl chemistry occurring in this region.

CHAPTER 1

INTRODUCTION

The atmosphere extends from the surface to greater than 100 km above the surface of the Earth. However, the troposphere (the lowest ~8-15 km) contains the majority of the mass in the atmosphere (~90%) and is chemically and physically dynamic because of interactions with the surface (e.g., Brasseur et al., 1999). The natural processes occurring in the troposphere directly influence life (i.e., human, animal, vegetation) and the cycling of chemical constituents throughout the entire atmosphere, the ocean, and the continental biosphere. Human interactions with the environment, through agricultural practices, population growth, industrial and technological development, alter and perturb the chemical state and natural balance of the atmosphere (e.g., Crutzen and Lelieveld, 2001; IPCC, 2007; Schlesinger, 2009).

The radiative budget and oxidation capacity of the atmosphere are significantly influenced by trace components (less than 1% of the atmospheric composition). An important group of trace gases in the atmosphere are volatile organic compounds (VOCs) (including hydrocarbons (RH), organic nitrates, halogenated and oxygenated organic species). VOCs originate from natural (volcanoes, lightning, marine organisms, vegetation, soil, biomass burning) and anthropogenic (combustion, industry, manufacturing, fuel and gasoline use, biomass burning) sources and are removed from the atmosphere (or converted to secondary products) by oxidation, photolysis, wet or dry

deposition, air-sea exchange, soil uptake, or heterogeneous processes (e.g., Roberts, 1990; Altschuler, 1991; Fehsenfeld et al., 1992; Singh and Zimmerman, 1992; Atkinson and Arey, 2003). The hydroxyl radical (OH) initiated oxidation of VOCs removes OH from the atmosphere and produces the peroxy radicals responsible for production of its primary precursor, ozone (O₃). Clearly, the chemical processes involving VOCs in the troposphere are directly linked to the budgets of several compounds, such as carbon monoxide, carbon dioxide, water vapor, methane, and ozone, which play major roles in climate change and air quality.

The chemical composition of the atmosphere is complex and highly variable on temporal (seconds to decades) and spatial (local, regional, continental, global) scales because of the different sources, removal mechanisms, and residence times of the various compounds. Therefore, the budgets (i.e., production and removal processes, mixing ratios) of trace gases need to be studied and characterized for individual regions. For example, the air quality in New England is influenced by local anthropogenic and biogenic sources of VOCs and by emissions that are transported from upwind urban and industrial areas in the U. S. (e.g., de Gouw et al., 2005; Moody et al., 1998; Talbot et al., 2005; Lee et al., 2006; White et al., 2008, 2009; Zhou et al., 2005, 2008). Moreover, the northeast U. S. is a major source region of continental outflow to the North Atlantic. Properly characterizing the relative contributions of transported and local emissions, background mixing ratios, and the processes responsible for variations in the composition of air masses is difficult. Additional complexities arise when studying air quality in coastal regions, such as New England, because of interactions between air masses originating from continental and marine regions.

Ambient measurements of VOCs made at various time scales (diurnal, seasonal, interannual) are required to constrain and identify the physical (mixing, dilution, transport, deposition) and chemical (oxidation, photolysis, decomposition) processes which regulate their behavior. This dissertation is focused on characterizing the influence of VOCs on air quality in New England using multi-year measurements of nonmethane hydrocarbons, halocarbons, and alkyl nitrates. Chapter 2 is focused on analyzing the seasonal and interannual variability of C₂-C₈ NMHCs and two halocarbons from daily canister samples collected throughout January 2004-February 2008 at Thompson Farm in Durham, NH. The specific objectives are to identify sources, describe temporal trends in sources or emissions, estimate emission rates of NMHCs from New England, and compare emission rates from the 2002 EPA National Emissions Inventory with the rates derived from ambient measurements. Chapter 3 discusses the seasonal, interannual, and diurnal variation and sources of alkyl nitrates using four separate data sets collected throughout coastal New Hampshire. Alkyl nitrates are photochemical products of the OH initiated oxidation of the C₂-C₅ alkanes discussed in Chapter 2 and are minor reaction products of the same NMHC-NO_x chemistry which produces tropospheric O₃. The relative contributions of different removal mechanisms of alkyl nitrates are assessed. Chapter 4 compares the relative influence of OH and chlorine initiated oxidation of NMHCs, CO, CH₄, OVOCs, and DMS on the chemical composition of air masses encountered at Thompson Farm and Appledore Island during two summers (July-August 2004 and 2005). Additional objectives include characterizing the interannual variability in meteorological conditions and VOC distributions, estimating chlorine atom concentrations, and describing the diurnal cycle of DMS.

CHAPTER 2

LONG-TERM MEASUREMENTS OF NONMETHANE HYDROCARBONS AND HALOCARBONS IN NEW HAMPSHIRE: SEASONAL VARIATIONS AND REGIONAL SOURCES

2.1 Introduction

Volatile organic compounds (VOCs) (including nonmethane hydrocarbons (NMHCs), alkyl nitrates, oxygenated hydrocarbons, halocarbons) are ubiquitous and important chemical constituents in the atmosphere. Reaction of VOCs with various oxidants (e.g., hydroxyl radical (OH), ozone (O₃), nitrate radical, halogens) produces organic (RO₂) and hydro (HO₂) peroxy radicals which react with nitrogen oxides (NO_x) to produce secondary species, such as tropospheric ozone, organic nitrates, and peroxides, thus regulating the oxidation capacity of the atmosphere. The relative concentrations and speciation of NO_x and NMHCs in a particular region determine whether ozone production or destruction occurs (e.g., Carter, 1994; Sillman and He, 2002; Kleinman et al., 2005). In addition, the partitioning of low volatility VOC oxidation products into the condensed phase produces secondary organic aerosols (e.g., Odum et al., 1997; Kroll and Seinfeld, 2008). Ozone and aerosols are components of photochemical smog, respiratory lung irritants, and harmful to vegetation and crops. Furthermore, several VOCs, such as benzene, toluene, xylenes, and tetrachloroethene, are classified as toxic air pollutants and are subject to federal regulations (U.S. EPA, 2008). Therefore, it is crucial to identify and characterize the atmospheric distributions and

sources of VOCs in order to develop and validate emission inventories, reduce the levels of hazardous air pollutants, and to predict and control O₃ and aerosol concentrations.

Despite the importance of quantifying VOC sources and emissions, information on their regional distributions is highly variable because of several confounding factors, including different atmospheric lifetimes and removal mechanisms, varying meteorological conditions, and distinguishing between local, regional, and distant sources. In order to minimize these complications and to eliminate site-to-site differences, long-term continuous measurements from the same location are necessary. Multi-year measurements of NMHCs and halocarbons at remote and urban North American sites have been reported (e.g., Jobson et al., 1994; Hagerman et al., 1997; Kang et al., 2001; Mohamed et al., 2002; Gautrois et al., 2003; Swanson et al., 2003; McCarthy et al., 2006; Qin et al., 2007), but not for New England since 1994-2001 (Goldstein et al., 1995; Kleiman and Prinn, 2000; Barnes et al., 2003; Lee et al., 2006). These studies have provided baseline data from which to monitor future changes in sources and ambient mixing ratios. Previous research has shown that the trace gas measurements (including O₃, carbon monoxide (CO), nitric oxide (NO), NMHCs, halocarbons, alkyl nitrates) made at Thompson Farm (TF) in Durham, New Hampshire are representative of both inland and coastal New England (e.g., Talbot et al., 2005; Chen et al., 2007; Sive et al., 2007; Mao et al., 2008; Russo et al., 2009; White et al., 2008; Zhou et al., 2005, 2008). Therefore, the TF results can be applied to regional analyses of the short and long-term temporal variability, sources, and sinks of VOCs and to emission inventory evaluation. This is particularly valuable because southern New England, including the seacoast region of New Hampshire, and extending to the southwest through New York and New

Jersey are classified as O₃ nonattainment areas (U.S. EPA, 2003, 2008). Moreover, air masses containing urban and industrial emissions from southern New England, the U. S. East Coast and mid-Atlantic corridor, and the Midwest are transported to New Hampshire. Consequently, TF is ideally situated for studying the chemical composition of air masses transported to the North Atlantic.

In this work, four years of ambient NMHC and halocarbon data from daily canister samples collected at the UNH AIRMAP Thompson Farm site in southeastern New Hampshire are discussed. The primary objectives are to characterize and interpret the seasonal to interannual mixing ratio trends and to identify the sources of C₂-C₈ NMHCs and halocarbons. Additionally, emission rates of the NMHCs are estimated and compared with the 2002 EPA National Emissions Inventory.

2.2 Sampling and Analytical Methods

2.2.1 Daily Canister Samples

A canister sample has been collected nearly every day since January 12, 2004 at the University of New Hampshire AIRMAP Atmospheric Observing Station at Thompson Farm (TF) located in Durham, New Hampshire (43.11°N, 70.95°W, elevation 24 m) (Figure 2.1). Thompson Farm is surrounded by agricultural fields and a mixed deciduous and coniferous forest and is located approximately 20 km inland from the Atlantic Ocean and 100 km north of Boston, MA. The ambient air samples were collected at the top of a 15 m tower next to the manifold inlet for all the instruments housed in the TF trailer. Samples were collected each day between 10:00-15:00 (EST; UTC-5 hours) and are representative of daytime conditions when photochemistry is most active and the boundary layer is likely well mixed. From January-June 2004, samples were collected in

1-liter canisters. Samples have been collected in 2-liter electropolished stainless steel canisters (University of California-Irvine) since June 2004. Prior to sampling, the canisters were prepared by flushing with UHP helium that had passed through an activated charcoal/molecular sieve trap immersed in liquid nitrogen. The canisters were then evacuated to 1×10^{-2} torr.

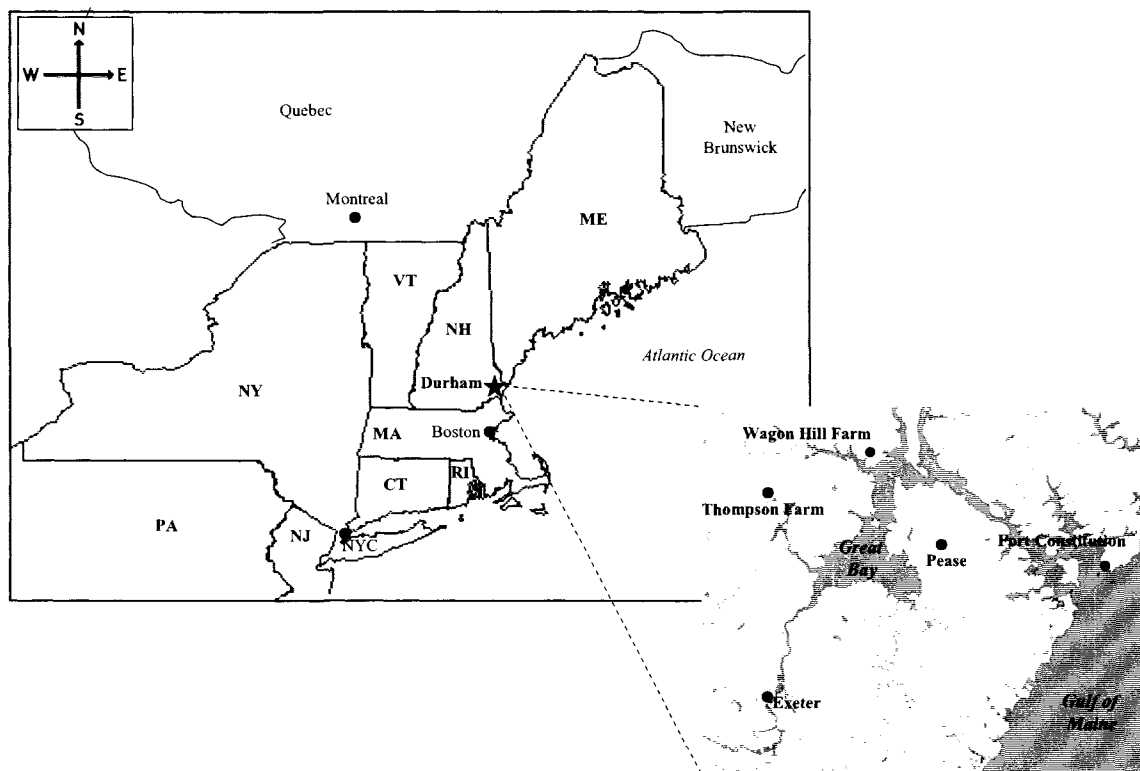


Figure 2.1. Location of the UNH AIRMAP Atmospheric Observing Station at Thompson Farm in Durham, New Hampshire, and (inset) the sampling sites used during the Great Bay Experiment (Chapter 3).

The canister samples were analyzed in the lab at UNH approximately every 1-3 months for C_2 - C_{10} nonmethane hydrocarbons, C_1 - C_5 alkyl nitrates, C_1 - C_2 halocarbons, several oxygenated volatile organic compounds, and selected sulfur compounds. A three

gas chromatograph system in conjunction with flame ionization detection (FID), electron capture detection (ECD), and mass spectrometry (MS) was used for sample analysis. Details of the system configuration used for analysis of the canister samples collected in 2004 and 2005 are given in Sive et al. (2005) and Zhou et al. (2005, 2008). A brief description of the system and modifications made in 2006 are presented here. The samples were analyzed by trapping 1500 cc (STP) of air on a glass bead filled loop immersed in liquid nitrogen. After sample trapping was complete, the loop was isolated, warmed to 80°C, and the sample was injected. Helium carrier gas flushed the contents of the loop and the stream was split into five with each sub-stream feeding a separate GC column. A 25 m x 0.53 mm I.D., 10 µm film thickness CP-Al₂O₃/Na₂SO₄ PLOT column and a 60 m x 0.32 mm I.D., 1 µm film thickness VF-1ms column were connected to FIDs and were used for detecting the C₂-C₁₀ NMHCs. C₁-C₂ halocarbons and C₁-C₅ alkyl nitrates were detected by ECD and separated with a 60 m x 0.25 mm I.D., 1µm film thickness OV-1701 column. C₁-C₂ halocarbons were also measured with a 25 m x 0.25 mm I.D., 3 µm film thickness CP-PoraBond-Q column coupled to a Restek Phase XTI-5 30 m x 0.25 mm I.D., 0.25 µm film thickness column and detected by ECD. Oxygen doping was used for this channel to improve the sensitivity for the methyl halide measurements. A 60 m x 0.25 mm I.D., 1.4 µm film thickness OV-624 column provided separation for the MS which was run in electron impact mode with single ion monitoring for measuring OVOCs and sulfur compounds, as well as duplicate measurements of several halocarbons and NMHCs. A secondary He carrier with a slower flow rate (1 sccm) was used for the MS in order to improve the measurement sensitivity. The OV-1701 ECD channel was used for quantifying C₂Cl₄ and C₂HCl₃, and the C₈ aromatics

were quantified using the MS. A 1500 cc aliquot from one of two working standards was assayed every ninth analysis. The measurement precision (i.e., relative standard deviation (RSD) = (standard deviation of peak areas/average of peak areas) for each compound within a specific standard) for the different compounds was <1-5% for the C₂-C₇ NMHCs, 2-10% for the C₈ aromatics, 3-8% for C₂Cl₄, and 5-10% for C₂HCl₃.

2.2.2 Daily Canister Sample Data Set

Measurements of several classes of NMHCs and two halocarbons are analyzed from the canister samples collected during January 12, 2004 to February 8, 2008. Collection of the daily samples is ongoing. The specific compounds, which represent a wide range of chemical reactivities and sources, are C₂-C₆ alkanes (ethane, propane, i-butane, n-butane, i-pentane, n-pentane, n-hexane), C₂-C₄ alkenes (ethene, propene, 1-butene), C₆-C₈ aromatics (benzene, toluene, ethylbenzene, m+p-xylene, o-xylene), ethyne, isoprene, tetrachloroethene (C₂Cl₄), and trichloroethene (C₂HCl₃). The data for each year and for the combined four year data set was separated into four seasons which are defined as winter: December, January, February; spring: March, April, May; summer: June, July, August; and fall: September, October, November. Note that the data encompasses five winter seasons (2004-2008) and four spring, summer, and fall seasons (2004-2007). Winter includes December of the previous year (i.e., winter 2005 represents December 2004 and January-February 2005). Winter 2004 only includes January 12 to February 29, and winter 2008 is only through February 8. Mixing ratios higher than the 95th percentile for each month were removed in order to ensure that the results were representative of typical conditions and were not skewed by a few outlying data points.

2.2.3 Thompson Farm Automated Gas Chromatograph

Measurements of C₃-C₆ alkanes, ethyne, propene, benzene, toluene, ethylbenzene, m+p-xylene, and o-xylene made once per hour with an automated gas chromatography system during December 2005-January 2006 at TF were also used in this analysis. Details of the four channel (2 FIDs, 1 ECD, 1 MS) GC system, MMR preconcentrator, sample trapping and splitting, calibrations, and instrument control are given in Sive et al. (2005). The system deployed at TF also contained four channels, but VOC detection was made with two FIDs and two ECDs. The MMR preconcentrator system used two independently cooled and controlled stages for sample trapping. The first stage (water management) contained a Silonite-coated stainless steel sample loop and was cooled to -30°C. The second stage (sample enrichment) housed a Silonite-coated stainless steel loop filled with 1 mm diameter glass beads and was cooled to -185°C. After the two stages reached their initial set point temperatures, a 1500 cc aliquot of air was trapped at 200 ccm. After trapping was complete, 100 cc of UHP helium was passed through both loops at a rate of 100 ccm. The glass bead filled loop was then isolated, warmed to 90°C, and the sample was injected. Helium carrier gas flushed the contents of the loop and the stream was split into four with each sub-stream feeding a separate GC column. One 50 m x 0.32 mm I.D., 5 µm film thickness CP-Al₂O₃/Na₂SO₄ PLOT column, one 60 m x 0.32 mm I.D., 1 µm film thickness VF-1ms column, one 60 m x 0.25 mm I.D., 1 µm film thickness OV-1701 column, and a 25 m x 0.25 mm I.D., 3 µm film thickness PoraBond-Q column coupled to a 40 m x 0.25 mm I.D., 1 µm film thickness OV-1 column were used for trace gas separation. The PLOT and VF-1ms columns were connected to FIDs and were used for C₃-C₇ and C₅-C₁₀ NMHC detection, respectively. The OV-1701 and PoraBond-Q/OV-1

columns were connected to ECDs and measured C₁-C₂ halocarbons and C₁-C₅ alkyl nitrates. A 1500 cc aliquot from one of two working standards was assayed every tenth analysis. The precision (i.e., RSD) for each of the hydrocarbons ranged from 3-10%.

2.2.4 Standards and Calibration

In order to ensure that the mixing ratios for samples analyzed at different times are comparable, whole air and synthetic standards were routinely analyzed and calibrated. After every eight canister samples, one of two whole air standards was analyzed in order to quickly notice any analytical problems and to monitor changes in detector sensitivity. Due to overlapping periods when different working standards were being used (e.g., July 2005, Figure 2.2), the response of each detector (i.e., response factors) can be cross referenced, and the mixing ratios in the standards can be recalibrated (if necessary) and verified. Response factors (RF) for each compound in a particular standard were calculated by dividing the detector response (peak area = A) by the mixing ratio (MR) of that compound in the standard ($RF = A/MR$). The per carbon response factors (PCRF) were determined by dividing the response factor by the number of carbon atoms (C) in the particular hydrocarbon ($PCRF = RF/C$).

Examples of the PCRFs for several NMHCs are shown in Figure 2.2 for the analyses when a new standard began to be used and every ~5-7 months when the same two standards were being analyzed. Ethane, propane, n-butane, ethyne, propene, and 1-butene were measured with the PLOT column, and benzene and toluene were measured with the VF-1ms column. The PCRF of the C₂-C₄ NMHCs decreased with increasing carbon number, but remained approximately the same over the four years and did not vary with standard (Figure 2.2a-f). Additionally, the PCRF were fairly constant for the C₃

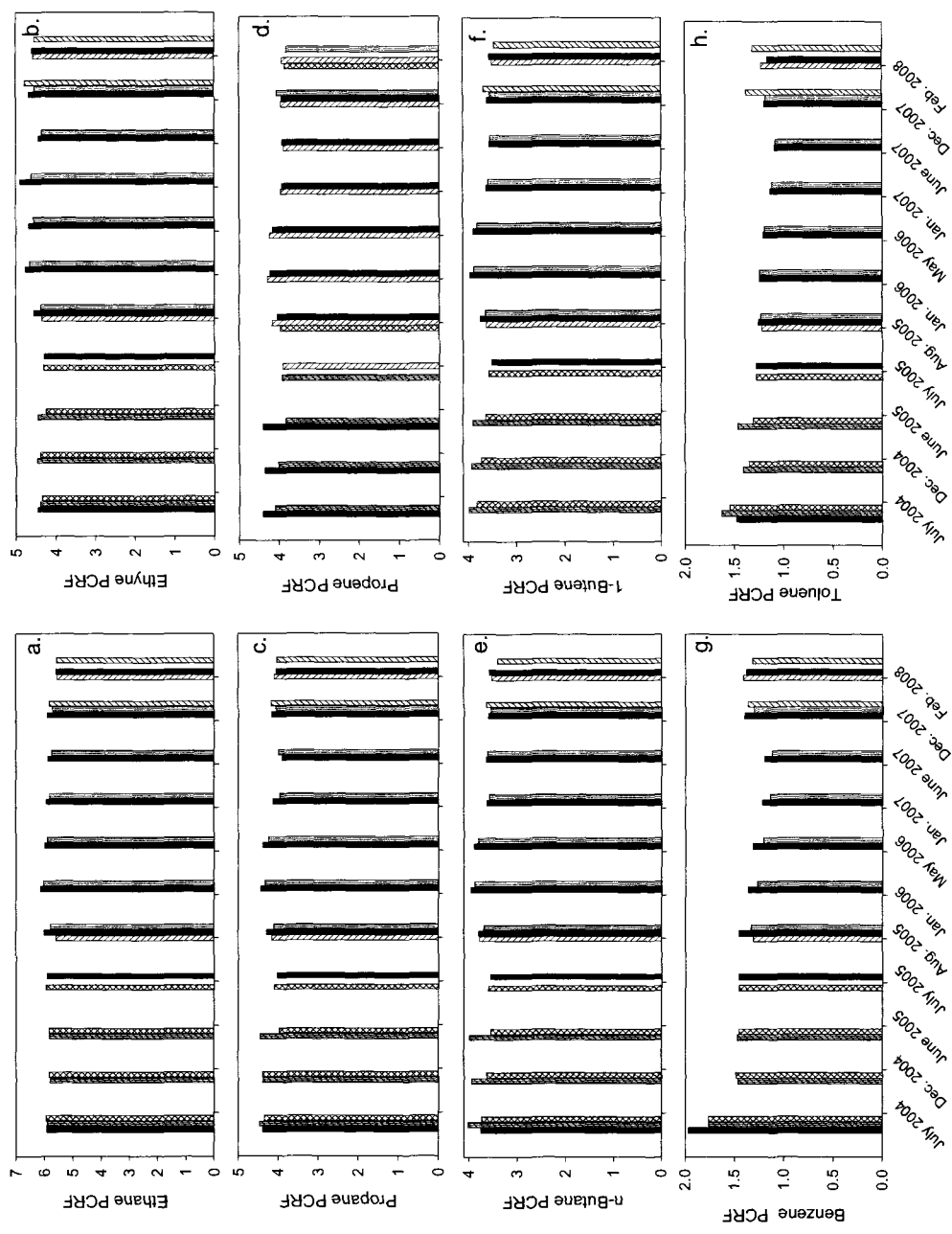


Figure 2.2. Per carbon response factors (PCRF) of (a) ethane, (b) ethyne, (c) propane, (d) propene, (e) n-butane, (f) 1-butene, (g) benzene, and (h) toluene in various standards analyzed in the UNH laboratory during 2004-2008. The labels along the bottom of the figure (pont1, pont2, ccrXY, hppc, DC2) refer to different standards.

(mean \pm standard deviation PCRf $\sim 4.1 \pm 0.18$) and C₄ (3.7 ± 0.16) compounds. The PCRfs for the VF-1ms column were fairly constant for compounds with different carbon numbers within a specific analysis period. For example, in August 2005, the PCRfs for the C₆-C₁₀ NMHCs in ccr21, ccr24, and DC2 were 1.5 ± 0.03 , 1.4 ± 0.03 , and 1.4 ± 0.04 , respectively. In addition, in February 2008, the PCRfs for ccr21, hppc, and DC2 were 1.2 ± 0.04 , 1.3 ± 0.04 , and 1.3 ± 0.07 , respectively. Periodically, the standards used by the automated GC system at TF were returned to the laboratory and analyzed on the canister analysis system. The PCRfs for the TF standards (ex. DC2) were in good agreement ($\pm 5\%$) with the lab standards ensuring that the measurements made by the two independent systems were comparable.

2.3 Seasonal and Interannual Variability

2.3.1 Anthropogenic Nonmethane Hydrocarbons

The highest monthly mean and median mixing ratios of NMHCs (excluding isoprene, section 2.3.2) at TF were observed in the winter (Figure 2.3, Table 2.1). This reflects the slow removal rates from the atmosphere caused by minimum OH radical concentrations. Lower boundary layer heights in winter are conducive to the build up of trace gas concentrations and may also contribute to the wintertime peak mixing ratios. The lowest NMHC mixing ratios were observed in spring to summer when the maximum OH concentrations occur and the photochemical removal of NMHCs is the most rapid. The seasonal variation at TF is consistent with the general tropospheric trend observed at other Northern Hemisphere sites (e.g., Jobson et al., 1994; Bottenheim and Shepherd, 1995; Goldstein et al., 1995; Hagerman et al., 1997; Gautrois et al., 2003; Swanson et al., 2003; Lee et al., 2006; Qin et al., 2007). Furthermore, the summer background mixing

ratios (monthly 10th percentile) of the C₂-C₆ alkanes and ethyne were comparable to background levels measured at Harvard Forest in Massachusetts throughout 1992-2001 (Goldstein et al., 1995; Lee et al., 2006) suggesting that the atmospheric levels of these compounds have not changed considerably since the 1990's.

The longer lived compounds had higher mixing ratios and reached minimum annual mixing ratios later in the year. For example, ethane was the most abundant NMHC (excluding isoprene) all year with peak mixing ratios in winter-early spring (2000-5000 pptv) (Figure 2.3a). Ethane decreased quickly from March to June (300-400 pptv/month), and then decreased more slowly (80-160 pptv/month) until mid-late summer when minimum mixing ratios (1000-2000 pptv) were observed. Mixing ratios of the C₃-C₆ alkanes, alkenes, ethyne, and aromatics began to decrease in mid-late winter and reached minimum levels 2-4 months later (Figure 2.3; Table 2.1). Propane, i-butane, and n-butane mixing ratios were lowest in late spring followed by an increase in early summer before reaching a second minimum in late summer (Figures 2.3a-b). In comparison, minimum mixing ratios of the shorter-lived C₅-C₆ alkanes and toluene occurred earliest (April-May), increased in early summer, and then remained within a similar range through October-November (Figures 2.3c-f; Table 2.1). Contrary to the expected photochemical trend, i-pentane mixing ratios were similar to or higher than the less reactive butanes in summer. The monthly median mixing ratios in June-September of each year for i-pentane, n-butane, and i-butane were 70-120, 70-140, and 50-100 pptv, respectively.

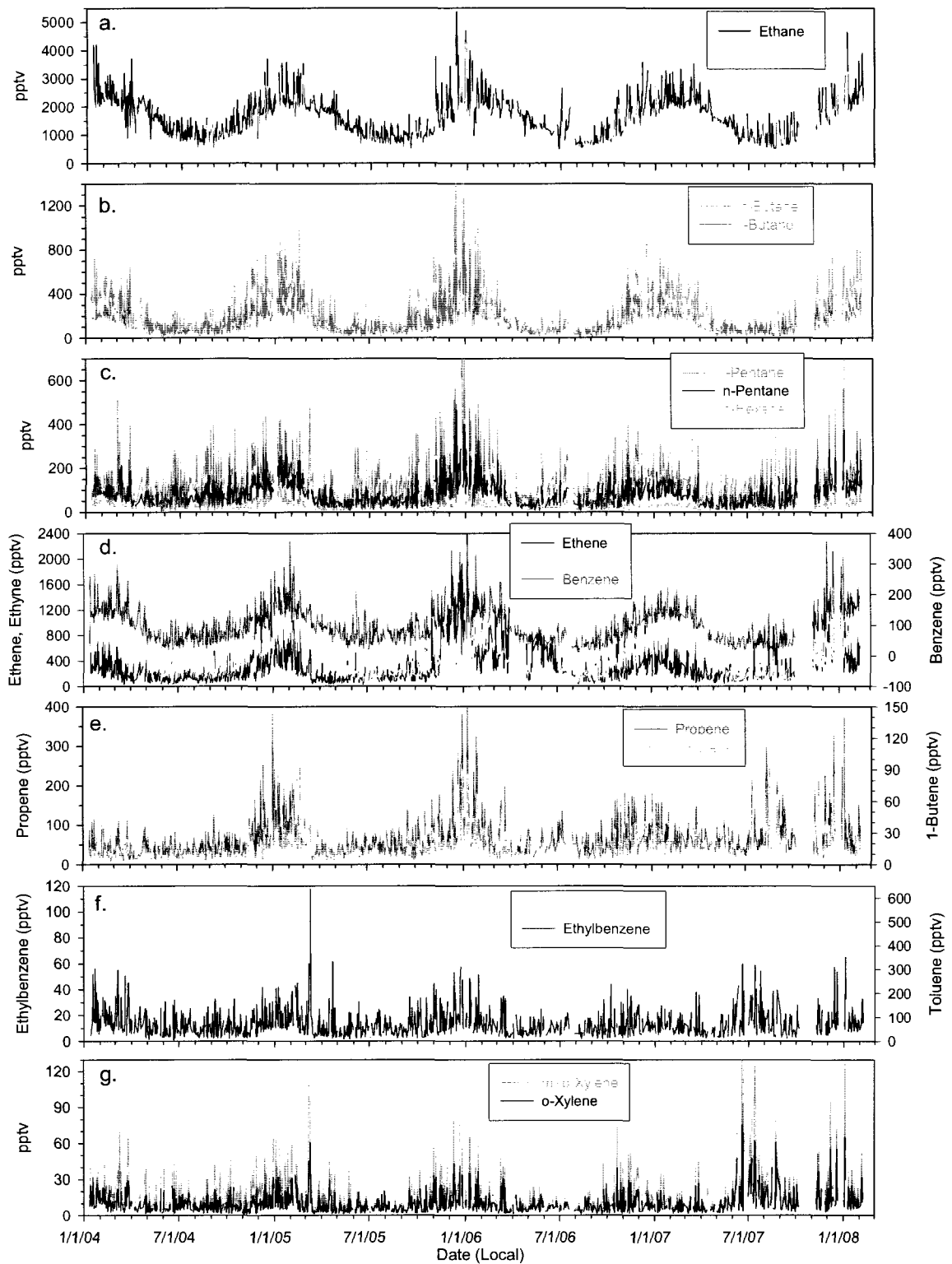


Figure 2.3. Time series of NMHCs (pptv) at TF during January 2004-February 2008: (a) ethane, propane, (b) n-butane, i-butane, (c) i-pentane, n-pentane, n-hexane, (d) ethene, ethyne, benzene, (e) propene, 1-butene, (f) toluene, ethylbenzene, and (g) m+p-xylene, o-xylene.

The lowest mixing ratios of ethene, ethyne, and benzene were reached in late spring to early summer and persisted through late summer (Figure 2.3d, Table 2.1). Despite its order of magnitude shorter lifetime, ethene mixing ratios were often similar to or higher than ethyne in summer, fall, and winter. On average, propene, 1-butene, ethylbenzene, and xylenes (m+p and o) were also highest in winter, lowest in early-mid spring, and increased in early summer (Figures 2.3d-g, Table 2.1). Superimposed on the general seasonal pattern were unique interannual trends reflecting varying sources or emission ratios. For example, a higher and narrower range of propene (~50-80 pptv) and 1-butene (~8-17 pptv) monthly medians was observed in spring 2006 through winter 2008 compared to the previous two years when distinct winter peaks and spring-summer minimum mixing ratios were observed. Additionally, the highest monthly mean and median m+p-xylene and o-xylene mixing ratios of the entire four year study period (~25-40 and 25-35 pptv, respectively), as well as the highest summer toluene (90-140 pptv) and ethylbenzene (14-22 pptv) mixing ratios, were observed in summer 2007 and elevated mixing ratios persisted through winter 2008 (Figures 2.3f-g).

2.3.2 Isoprene

Isoprene is the only NMHC discussed in this work with a predominantly biogenic origin (deciduous plants and trees) (e.g., Fehsenfeld et al., 1992). Isoprene mixing ratios increased rapidly in the beginning of June, remained high through August, and gradually decreased in September-October of each year (Figure 2.4a, Table 2.1). In July-August 2005, 2006, and 2007, isoprene was the most abundant NMHC (monthly mean mixing ratios = 1000-2100 pptv) illustrating the importance of biogenic emissions in this region. In comparison, ethane (the longest lived NMHC) mixing ratios were 800-1250 pptv.

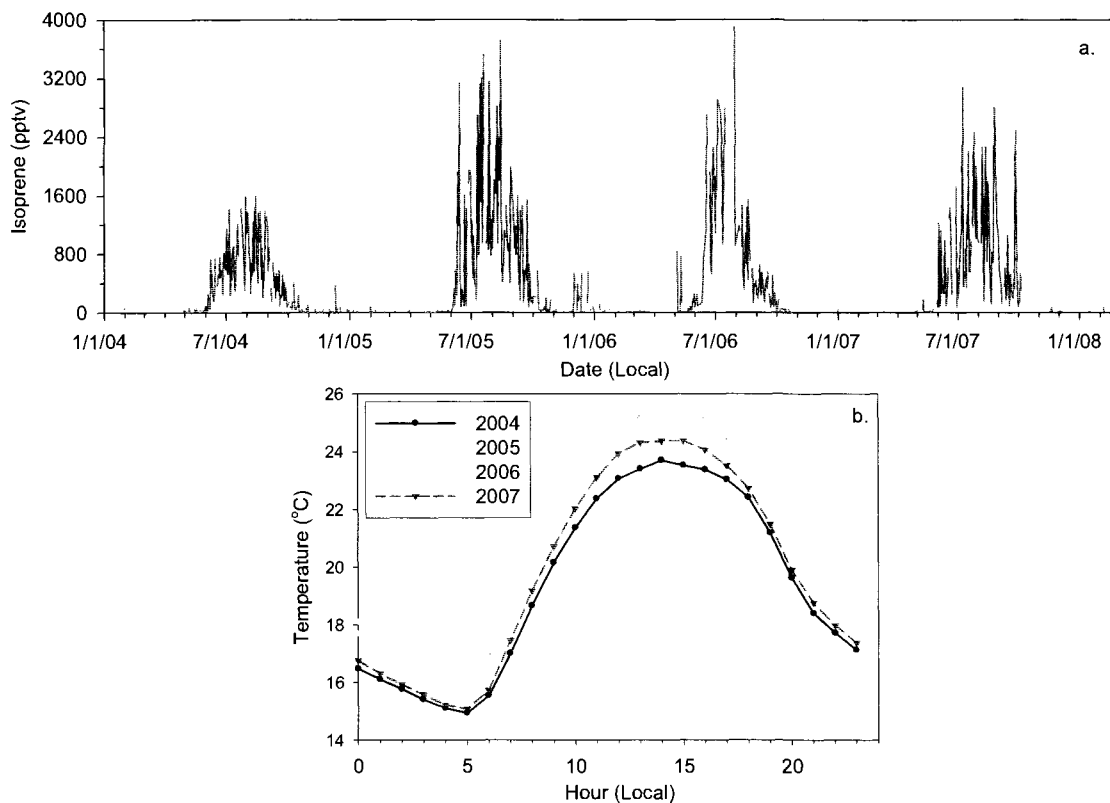


Figure 2.4. (a) Time series of isoprene (pptv) at TF during January 2004-February 2008. (b) Hourly average temperature (°C) during June-August of 2004, 2005, 2006, and 2007.

Isoprene and ambient temperature were positively correlated during summer of each year (Figure 2.4b). The highest isoprene mixing ratios (>3 ppbv) were observed in the warmest summers (2005 and 2006) while the lowest (<1600 pptv) mixing ratios corresponded to the coolest summer (2004). The equation relating isoprene (in ppbv) and the hourly average temperature (T in °C corresponding to the hour the sample was collected) for all of the June-September data was $\log(\text{isoprene}) = 0.074T - 1.91$ ($r^2=0.57$). The equation was nearly the same each individual year, on sunny/clear days, and on cloudy/rainy days. Furthermore, this relationship is consistent with previous studies (Fehsenfeld et al., 1992; Jobson et al., 1994; Goldan et al., 1995; Gong and Demerjian, 1997; Hagerman et al., 1997; Kang et al., 2001) indicating a similar temperature dependence of ambient isoprene mixing ratios at various North American sites. Isoprene

was not correlated with J_{NO_2} (NO_2 photolysis frequency) or with the daily maximum and average photosynthetically active radiation (PAR) (obtained from the UNH weather station <http://www.weather.unh.edu>). This may suggest temperature is a better predictor of isoprene emission rates than sunlight at TF.

2.3.3 Halocarbons

Trichloroethene and tetrachloroethene are primarily emitted from industrial sources (dry cleaning solvents, degreasing agents) (e.g., Wang et al., 1995; McCulloch and Midgley, 1996). It is necessary to monitor the atmospheric trends of C_2HCl_3 and C_2Cl_4 because they are toxic air pollutants and regulated by the EPA (U. S. EPA, 2007), precursors to toxic oxidation products (phosgene, trichloroacetic acid) (e.g., Kindler et al., 1995), and potential sources of chlorine radicals in the troposphere and stratosphere (Schauffler et al., 2003; Thompson et al., 2004). At TF, the shorter-lived (days-weeks) C_2HCl_3 had a similar seasonal variation as the NMHCs with a winter maximum (5-8 pptv) and spring minimum (1-2 pptv). The early summer (3-5 pptv) increase in monthly median mixing ratios implies that evaporative emissions of C_2HCl_3 are important to its atmospheric distribution (Figure 2.5). Monthly median mixing ratios of the longer-lived (months) C_2Cl_4 were fairly uniform. A seasonal variation was apparent in the C_2Cl_4 background (monthly 10th percentile) mixing ratios which were highest in winter (8-9 pptv) and lowest in late summer (3-5 pptv). The C_2Cl_4 mixing ratios at TF are similar to background levels in Massachusetts during 1996-1999 (Kleiman and Prinn, 2000; Barnes et al., 2003). Even though a decrease in ambient C_2Cl_4 mixing ratios has been observed at remote northern hemisphere sites (McCulloch et al., 1999; Blake et al., 2003b; Gautrois et al., 2003; Simpson et al., 2004; Thompson et al., 2004; Simmonds et al., 2006), the

similar mixing ratios in New England suggest that C_2Cl_4 emission rates in more populated areas in the U.S. did not change considerably between the late 1990's and 2004. However, several characteristics of the C_2Cl_4 and C_2HCl_3 trends indicate that their atmospheric mixing ratios have been decreasing throughout 2004-2008. For example, there has been a decrease in the magnitude of peak mixing ratios, and the annual mean, median, and background mixing ratios have decreased with each successive year (Figure 2.5, Table 2.2).

Acknowledging that it is difficult to conduct an accurate trend analysis based on only four years of measurements, an estimate of the rate of decrease in atmospheric mixing ratios of both halocarbons was made. The annual statistics were used in order to minimize the influence of the seasonal variation in C_2HCl_3 and in background C_2Cl_4 . The linear regression through the annual background mixing ratios gave decrease rates of 0.73 ± 0.24 (~10-20 %/year) and 0.27 ± 0.05 (~20-40 %/year) pptv/year for C_2Cl_4 and C_2HCl_3 , respectively (Table 2.2). In comparison, C_2Cl_4 decrease rates (pptv/year) were estimated to be 0.18 ($C_2HCl_3=0.01$) during July 2000-December 2004 at Mace Head, Ireland (Simmonds et al., 2006), 1.0 ($C_2HCl_3=0.1$) in 1991-1996 at Alert, Canada (Gautrois et al., 2003), 0.1-0.4 throughout 1989-2002 along the North American west coast (Simpson et al., 2004), 0.6-1.2 during 1994-1997 in the continental U.S. (Hurst et al., 1998), and 5 %/year in 1995-2003 based on analysis of EPA and NOAA CMDL data at remote U.S. and North American sites (McCarthy et al., 2006). However, it is difficult to make direct comparisons between the trends observed at different location because of the short C_2HCl_3 lifetime, the limited number of previous estimates, and the differences in regional emission rates and regulations.

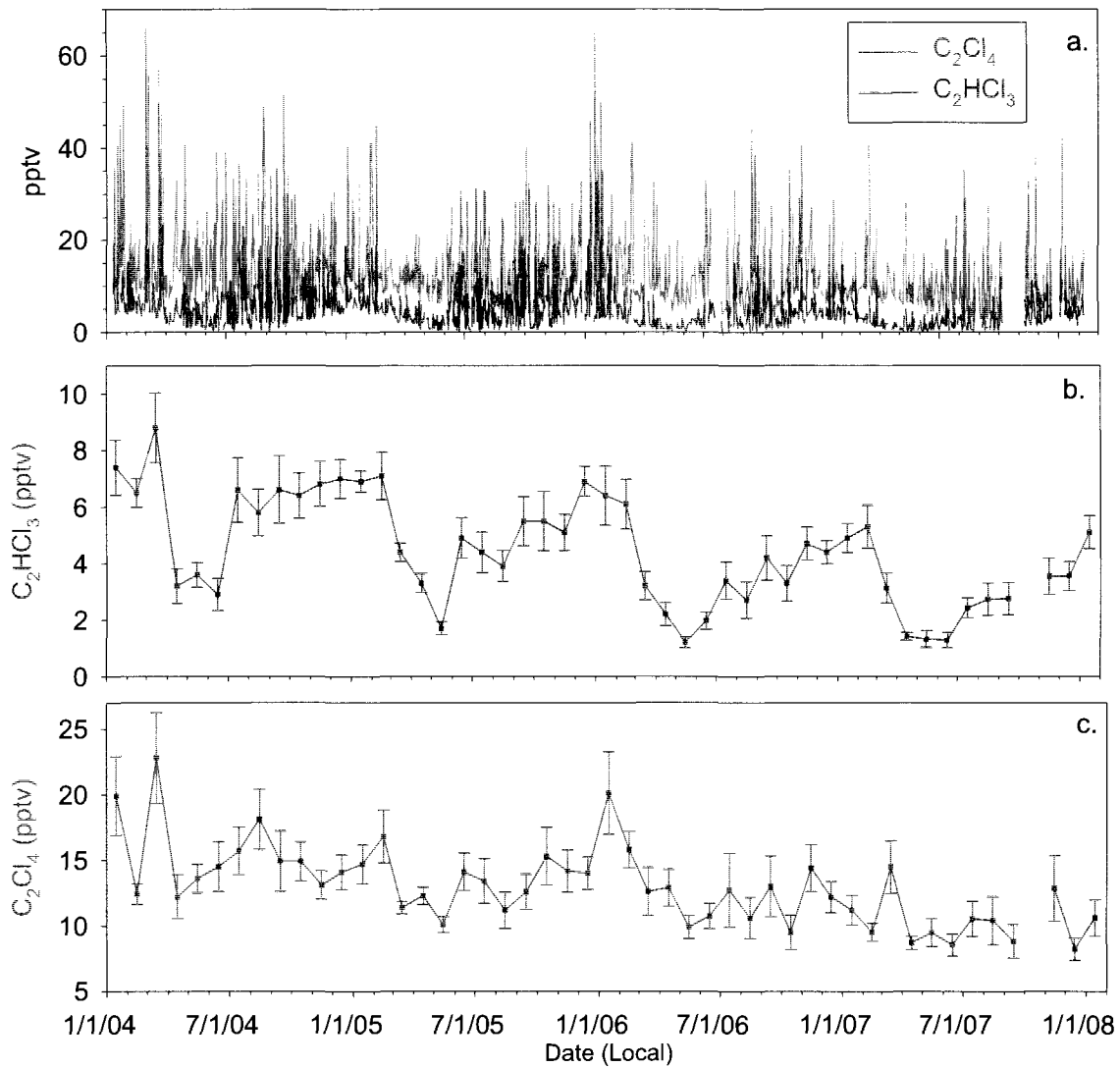


Figure 2.5. (a) Time series of C_2Cl_4 and C_2HCl_3 (pptv) at TF during January 2004-February 2008. Monthly mean \pm standard error mixing ratios of (b) C_2HCl_3 and (c) C_2Cl_4 .

	January	February	March	April	May	June	July	August	September	October	November	December
Ethane												
Mean (SD)	2436 (621)	2395 (443)	2138 (435)	1856 (278)	1423 (205)	1104 (306)	1023 (324)	876 (277)	998 (275)	1238 (367)	1859 (544)	2278 (939)
Median (N)	2248 (125)	2288 (101)	2104 (98)	1835 (86)	1401 (102)	1057 (92)	942 (91)	784 (99)	961 (103)	1099 (86)	1734 (94)	2074 (94)
Range	984-4673	1656-3901	872-3709	947-2604	859-2079	488-2049	453-2655	465-1765	530-1815	720-2567	881-3778	1085-7622
Propane												
Mean (SD)	1498 (612)	1332 (481)	1002 (371)	674 (231)	444 (204)	497 (340)	559 (308)	505 (314)	605 (331)	786 (471)	1217 (527)	1518 (795)
Median (N)	1309 (125)	1161 (101)	933 (98)	622 (86)	387 (102)	380 (92)	522 (91)	399 (99)	532 (103)	666 (86)	1164 (94)	1299 (94)
Range	439-3907	806-3128	358-2419	225-1682	125-1135	103-1488	137-1600	91-1647	134-1766	274-3229	446-2788	608-4549
i-Butane												
Mean (SD)	269 (109)	253 (109)	190 (116)	98 (46)	54 (26)	65 (39)	70 (39)	60 (36)	75 (59)	126 (67)	210 (99)	266 (144)
Median (N)	234 (125)	220 (99)	163 (96)	89 (86)	47 (102)	57 (92)	64 (92)	46 (99)	58 (103)	106 (86)	201 (94)	225 (94)
Range	66-679	140-694	59-655	17-224	13-125	12-172	15-224	6-161	9-276	34-289	64-434	90-866
n-Butane												
Mean (SD)	500 (208)	444 (169)	308 (138)	174 (86)	96 (48)	103 (73)	105 (59)	95 (61)	118 (81)	217 (125)	376 (191)	502 (349)
Median (N)	429 (125)	400 (101)	279 (98)	153 (86)	85 (102)	72 (92)	92 (92)	78 (99)	99 (103)	180 (85)	333 (93)	422 (93)
Range	111-1325	261-1230	108-708	29-423	19-227	16-349	26-350	10-271	21-478	54-577	105-833	171-2160
i-Pentane												
Mean (SD)	202 (112)	163 (74)	125 (93)	74 (47)	67 (46)	105 (77)	115 (60)	110 (75)	109 (80)	127 (90)	177 (104)	211 (140)
Median (N)	170 (125)	151 (100)	95 (98)	63 (86)	59 (102)	79 (92)	106 (92)	88 (99)	92 (103)	100 (86)	150 (94)	176 (93)
Range	55-710	67-427	33-517	13-216	11-265	15-341	30-301	17-377	13-399	23-412	46-467	59-767
n-Pentane												
Mean (SD)	129 (61)	101 (38)	72 (43)	40 (23)	34 (20)	45 (30)	52 (28)	51 (34)	52 (35)	66 (42)	104 (53)	135 (83)
Median (N)	114 (125)	91 (100)	60 (98)	33 (86)	31 (102)	38 (92)	49 (92)	44 (99)	45 (103)	57 (86)	88 (94)	114 (94)
Range	26-374	51-237	21-235	7-124	5-114	7-151	12-140	7-165	10-168	16-179	19-250	49-465
n-Hexane												
Mean (SD)	53 (32)	42 (22)	27 (20)	16 (11)	18 (11)	23 (17)	25 (15)	25 (16)	25 (18)	29 (21)	40 (23)	52 (32)
Median (N)	42 (125)	37 (100)	23 (93)	12 (82)	15 (89)	18 (86)	22 (88)	22 (91)	19 (90)	23 (81)	38 (94)	42 (92)
Range	14-180	17-130	3-116	3-59	2-51	5-90	5-82	4-75	3-83	3-84	6-95	10-144

Table 2.1. Monthly mean, standard deviation (SD), median, number of samples (N), and range of NMHC mixing ratios (pptv) from the daily canister samples collected at TF throughout January 2004- February 2008.

	<u>January</u>	<u>February</u>	<u>March</u>	<u>April</u>	<u>May</u>	<u>June</u>	<u>July</u>	<u>August</u>	<u>September</u>	<u>October</u>	<u>November</u>	<u>December</u>
Ethylene												
Mean (SD)	730 (260)	704 (177)	560 (157)	394 (94)	256 (68)	215 (121)	235 (108)	203 (98)	222 (107)	318 (129)	498 (198)	624 (230)
Median (N)	631 (125)	650 (101)	533 (98)	379 (86)	242 (102)	181 (92)	216 (92)	179 (99)	193 (103)	289 (85)	440 (93)	588 (93)
Range	222-1804	475-1329	251-1146	184-723	118-455	80-643	82-499	56-515	72-614	121-700	247-1331	318-1552
Ethane												
Mean (SD)	579 (387)	437 (259)	346 (291)	337 (335)	216 (185)	216 (169)	192 (104)	184 (136)	192 (118)	240 (154)	437 (284)	679 (412)
Median (N)	455 (125)	364 (101)	257 (98)	162 (86)	158 (102)	165 (92)	177 (91)	155 (99)	158 (103)	209 (86)	380 (93)	534 (93)
Range	168-2552	120-1245	32-1270	41-1181	38-854	31-788	70-717	36-938	41-552	57-758	87-1284	141-2110
Propene												
Mean (SD)	89 (72)	66 (48)	52 (37)	38 (20)	43 (22)	43 (20)	52 (30)	54 (44)	53 (34)	54 (33)	71 (48)	98 (74)
Median (N)	64 (125)	50 (101)	38 (98)	34 (86)	37 (102)	40 (92)	47 (91)	46 (99)	42 (103)	43 (86)	57 (93)	75 (93)
Range	21-427	9-244	11-198	13-95	12-115	10-94	17-214	11-295	13-180	16-164	15-212	21-380
1-Butene												
Mean (SD)	20 (16)	18 (12)	16 (10)	12 (7)	13 (10)	11 (6)	10 (6)	12 (12)	12 (8)	12 (9)	18 (12)	20 (15)
Median (N)	14 (120)	14 (95)	13 (94)	9 (79)	11 (97)	8 (88)	9 (90)	9 (92)	9 (91)	9 (82)	13 (89)	16 (92)
Range	4-26	3-79	4-56	4-38	3-63	3-27	5-47	2-81	3-43	3-43	3-55	4-90
Isoprene												
Mean (SD)	35 (54)	24 (51)	20 (33)	9 (9)	50 (125)	666 (674)	1278 (848)	1078 (657)	464 (420)	86 (116)	16 (15)	93 (150)
Median (N)	17 (40)	10 (34)	9 (23)	5 (31)	15 (84)	376 (92)	1007 (92)	946 (99)	336 (103)	40 (77)	11 (45)	25 (47)
Range	3-303	3-301	3-149	3-49	2-829	13-3131	176-3893	103-3714	26-2486	3-566	2-72	2-551

Table 2.1 continued. Monthly NMHC statistics (pptv) for January 2004-February 2008.

	January	February	March	April	May	June	July	August	September	October	November	December
Benzene												
Mean (SD)	167 (50)	159 (42)	133 (42)	88 (24)	60 (18)	55 (35)	60 (26)	55 (26)	59 (28)	75 (28)	114 (39)	151 (56)
Median (N)	152 (125)	148 (101)	126 (99)	88 (86)	59 (102)	45 (92)	55 (92)	50 (99)	54 (103)	69 (85)	110 (94)	136 (94)
Range	61-364	108-372	72-297	42-182	25-111	18-207	21-123	9-136	15-139	27-147	46-229	57-373
Toluene												
Mean (SD)	136 (91)	126 (102)	125 (215)	67 (53)	73 (48)	109 (74)	106 (68)	91 (63)	102 (80)	99 (80)	122 (87)	131 (85)
Median (N)	104 (125)	96 (101)	61 (99)	49 (86)	56 (100)	92 (92)	87 (91)	74 (98)	78 (103)	77 (85)	101 (94)	111 (93)
Range	48-535	40-621	16-1979	9-235	13-203	16-291	31-379	14-340	6-375	16-352	22-442	33-416
Ethylbenzene												
Mean (SD)	18 (12)	16 (9)	15 (17)	10 (9)	9 (6)	13 (11)	14 (10)	11 (7)	10 (8)	12 (9)	15 (10)	17 (12)
Median (N)	14 (124)	13 (99)	8 (99)	7 (87)	8 (98)	10 (89)	11 (90)	9 (99)	8 (102)	10 (86)	11 (94)	14 (94)
Range	4-68	4-45	3-118	2-62	1-26	0.7-60	3-59	2-40	2-34	2-44	3-44	5-57
m+p-Xylene												
Mean (SD)	23 (19)	18 (13)	17 (20)	11 (10)	11 (8)	18 (24)	19 (22)	12 (12)	12 (10)	15 (13)	20 (15)	24 (18)
Median (N)	15 (124)	15 (99)	8 (99)	8 (87)	8 (98)	10 (89)	12 (90)	8 (99)	8 (102)	12 (86)	16 (94)	19 (93)
Range	4-126	3-64	2-113	1-47	2-47	0.6-150	3-125	2-85	2-47	2-73	2-62	5-107
o-Xylene												
Mean (SD)	13 (11)	10 (7)	9 (10)	7 (5)	6 (4)	11 (13)	12 (11)	9 (9)	8 (6)	9 (7)	11 (8)	13 (10)
Median (N)	9 (123)	9 (97)	5 (98)	5 (86)	5 (98)	7 (88)	9 (90)	6 (99)	6 (102)	7 (86)	9 (94)	11 (93)
Range	2-73	2-33	1-61	2-30	1-22	2-75	2-62	1-61	1-31	2-39	1-36	3-56

Table 2.1 continued. Monthly NMHC statistics (pptv) for January 2004-February 2008.

	<u>C₂HCl₃</u>	<u>C₂Cl₄</u>
	2004	
Mean (SD)	6.0 (4.7)	15.8 (10.5)
Median (N)	4.6 (277)	12.3 (277)
Background	1.30	6.73
Range	0.25-23.4	3.3-65.7
	2005	
Mean (SD)	5.0 (3.7)	13.3 (7.6)
Median (N)	4.5 (323)	11.0 (324)
Background	0.93	6.20
Range	0.16-21.1	3.4-44.7
	2006	
Mean (SD)	4.0 (3.6)	13.1 (9.2)
Median (N)	2.9 (264)	9.6 (270)
Background	0.73	5.70
Range	0.14-20.3	3.3-65.3
	2007	
Mean (SD)	3.0 (2.6)	10.5 (6.5)
Median (N)	2.5 (240)	8.6 (244)
Background	0.46	4.48
Range	0.12-14.6	2.4-40.6
pptv/year±(SD)	-0.27±0.05	-0.73±0.24
r ²	0.99	0.95

Table 2.2. Annual C₂HCl₃ and C₂Cl₄ statistics (pptv) for 2004-2008, and the rate of decrease (pptv/year) in the annual background mixing ratios. SD = standard deviation. N = number of samples. Background = 10th percentile for the year.

2.4 NMHC Source Identification

2.4.1 Comparison with Tracers and Source Signatures

The following source signature information is used to interpret and identify the sources of NMHCs observed at TF. The major sources of ethyne, benzene, carbon monoxide (CO), and alkenes are incomplete combustion of fossil fuels, biomass burning, and vehicle exhaust emissions (e.g., Harley et al., 1992; McLaren et al., 1996; Harley et al., 2001; Choi and Ehrman, 2004). C₂-C₄ alkanes are emitted from natural gas, incomplete combustion, and unburned gasoline. Fuel evaporation emissions (caused by

ambient temperature changes or residual engine heat during vehicle operation, resting, or refueling) are a dominant source of C₄-C₅ alkanes because of their high vapor pressures (Harley et al., 2001; Choi and Ehrman, 2004). The leakage of unburned liquefied petroleum gas (LPG) (during storage, distribution, or refilling) is a significant source of propane, i-butane, and n-butane and a minor source of alkenes (Blake and Rowland, 1995; Chen et al., 2001; Jobson et al., 2004). Aromatics are a major component of liquid gasoline and are often observed in vehicle exhaust because of incomplete combustion or leakage of unburned fuel (e.g., Kirchstetter et al., 1999; Harley et al., 2000, 2001). Toluene, ethylbenzene, m+p-xylene, and o-xylene are also emitted from fuel evaporation and industrial processes (i.e., painting, architectural coating, manufacturing, printing, degreasing solvents) (e.g., Monod et al., 2001).

Ethyne and CO were fairly well correlated at TF ($r^2=0.5-0.9$) demonstrating a year-round impact from combustion emissions (Figure 2.6a). The correlations between alkenes and ethyne showed considerable scatter and were strongest in winter. The alkenes are very reactive (lifetime \leq 1 day to 2 weeks depending on season) and had presumably undergone mixing and oxidative removal during transport resulting in weaker correlations in spring, summer, and fall. Based on the winter measurements, the ethene and propene correlation slopes with ethyne (1.2 and 0.21, respectively) were similar to light duty gasoline and vehicle exhaust emission ratios (0.91-1.7 and 0.1-0.5, respectively) (Conner et al., 1995; Watson et al., 2001; Choi and Ehrman, 2004; McGaughey et al., 2004) suggesting that vehicular emissions, rather than LPG, were the dominant source of these alkenes. Propene and 1-butene were well correlated throughout the majority of the study period reflecting their common source (Figure 2.6b). The

correlation coefficients between ethyne and the alkanes, benzene, and toluene were fairly variable within each season and year ($r^2=0.4-0.9$), but overall suggest that combustion sources were collocated with or were the same as the alkane and aromatic sources.

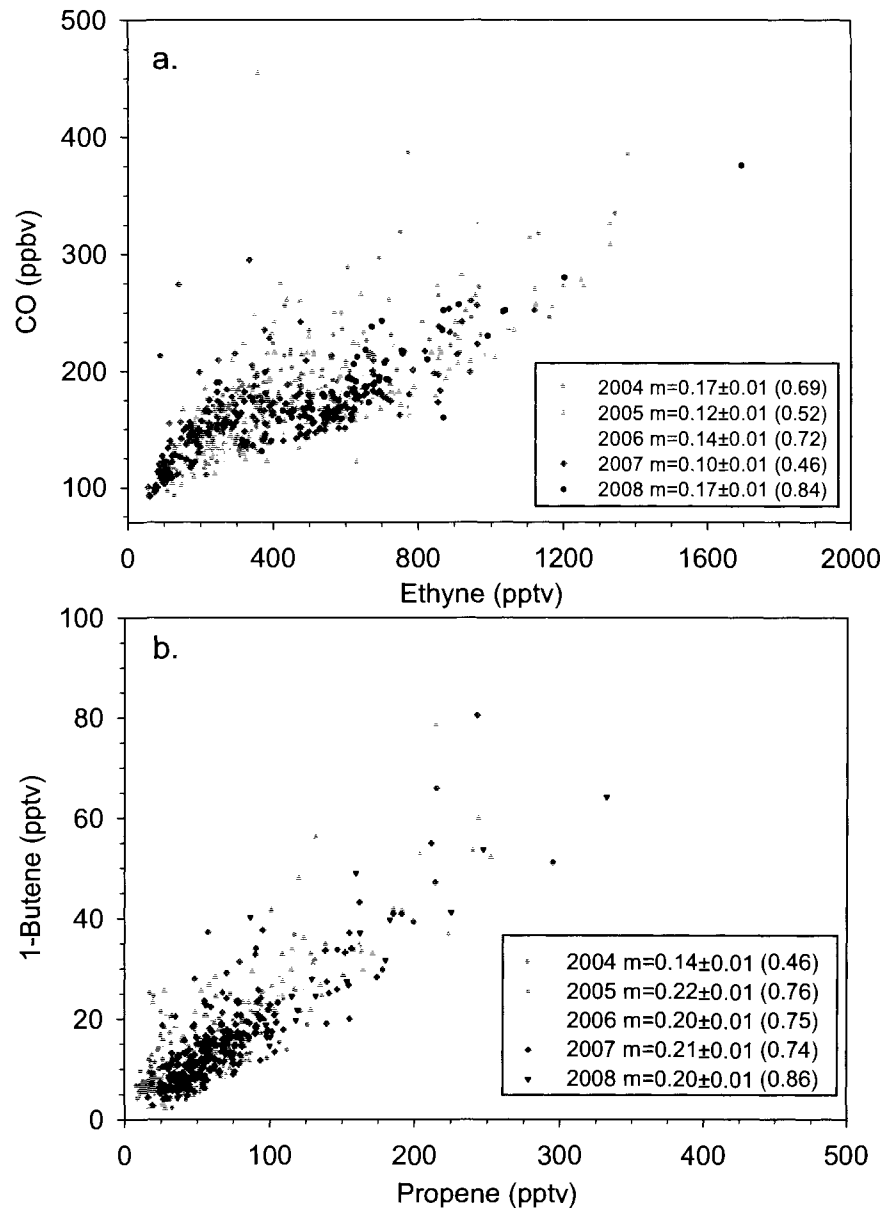


Figure 2.6. Correlations between (a) ethyne and CO (ppbv) and (b) propene and 1-butene for each year (2004, 2005, 2006, 2007, 2008). m =slope \pm standard error (SE) (r^2).

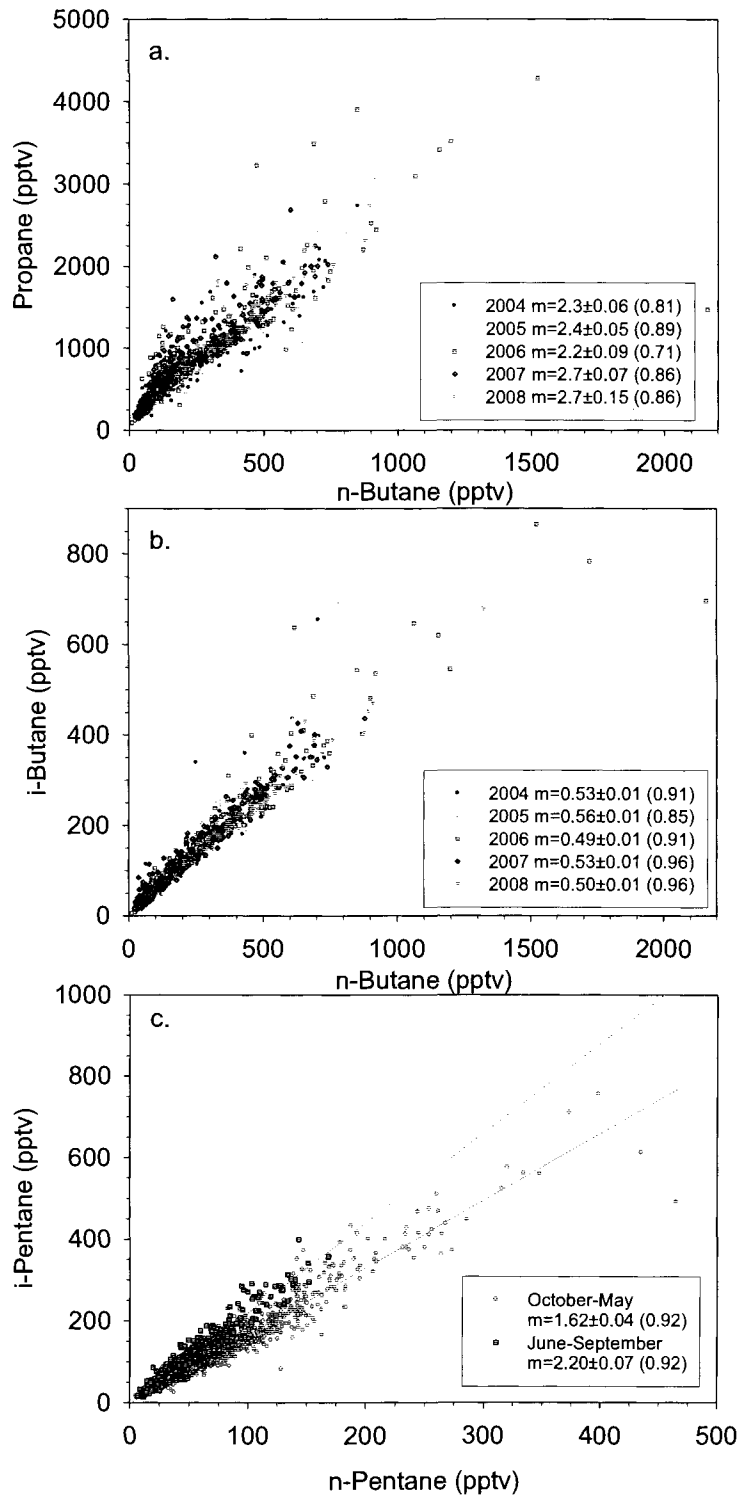


Figure 2.7. Correlations between (a) n-butane and propane and (b) n-butane and i-butane for each year. (c) Correlation between n-pentane and i-pentane. Gray circles are all of the samples collected in October-May of 2004-2008. Red squares are all of the samples collected in June-September of 2004-2007. $m = \text{slope} \pm \text{SE}$ (r^2).

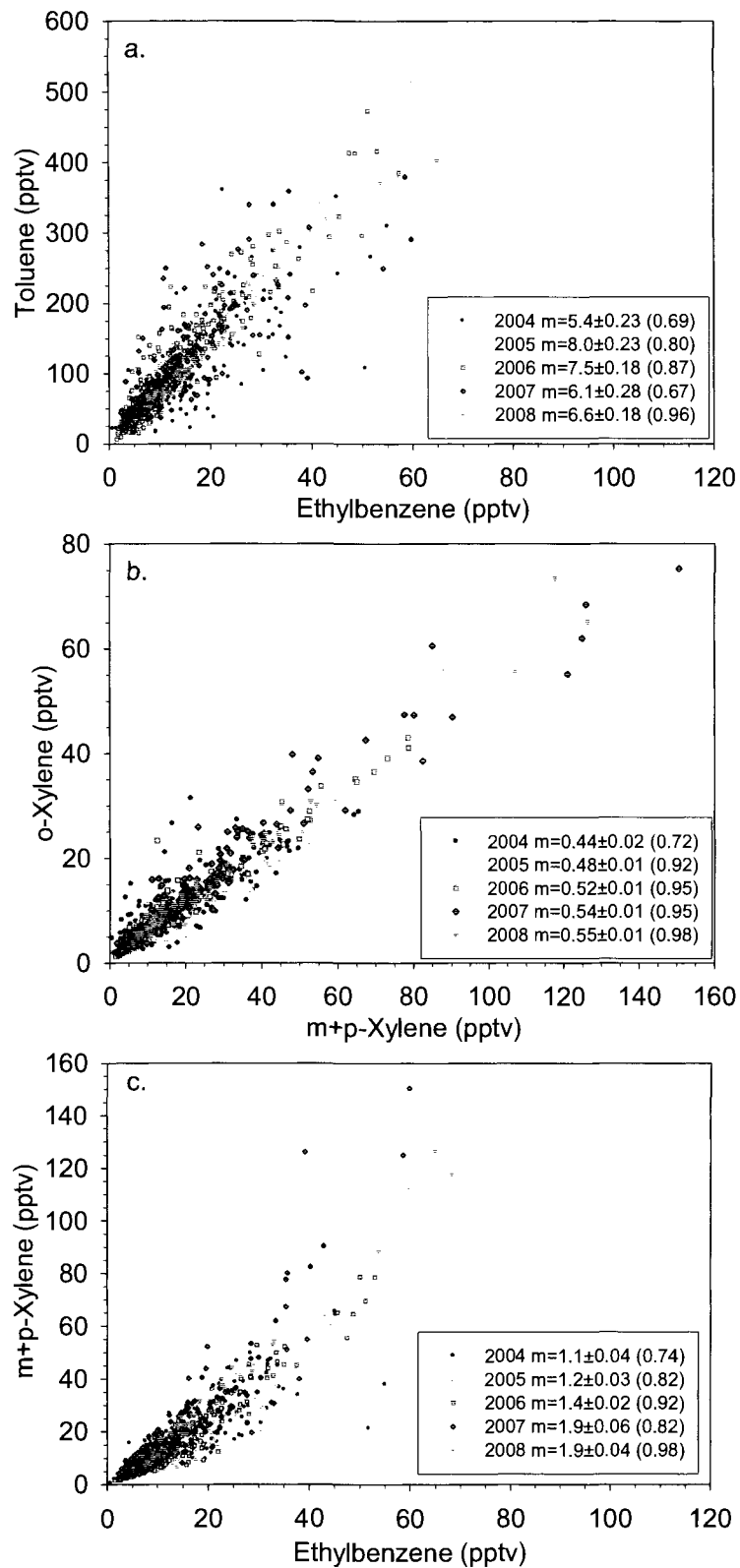


Figure 2.8. Correlations between (a) toluene and ethylbenzene, (b) o-xylene and m+p-xylene, and (c) m+p-xylene and ethylbenzene for each year. $m = \text{slope} \pm \text{SE}$ (r^2).

The C₃-C₆ alkanes were well correlated with each other ($r^2=0.6-0.9$), while correlations between ethane and the C₃-C₆ alkanes were slightly weaker ($r^2=0.3-0.7$). The slopes of the correlation between propane and n-butane (2.2-2.7, Figure 2.7a) and i-butane (3.8-5.5, not shown) agree with LPG emission ratios (2-4 and 3-7, respectively) (e.g., Blake and Rowland, 1995; Chen et al., 2001; Barletta et al., 2008) indicating that LPG emissions are widespread and prevalent in New England. Moreover, the correlation slope between i-butane and n-butane (0.49-0.56, Figure 2.7b) is within the range of reported emission ratios from several sources, including urban (~ 0.3), vehicular exhaust (~ 0.2), petroleum ($> \sim 1$), LPG (0.46), and natural gas ($\sim 0.6-1$) (B. Sive, unpublished data; Blake and Rowland, 1995; Jobson et al., 1998, 2004; Fujita et al., 2001; Watson et al., 2001; Barletta et al., 2002; Choi and Ehrman, 2004; Velasco et al., 2007). This suggests that a uniform mix of emissions from all of these sources is observed at TF.

Similarly, i-pentane and n-pentane were strongly correlated ($r^2=0.92$) (Figure 2.7c), and the slope was within the range of reported emission ratios for vehicle exhaust and tunnel studies ($\sim 2.2-3.8$), liquid gasoline (1.5-3), and fuel evaporation (1.8-4.6) (Conner et al., 1995; Kirchstetter et al., 1996; McLaren et al., 1996; Sagebiel et al., 1996; Rogak et al., 1998; Harley et al., 2001; Watson et al., 2001; Jobson et al., 2004; McCaughey et al., 2004; Lough et al., 2005; Velasco et al., 2007). The correlation slope was noticeably higher in the warmer months (June-September slope=2.2) reflecting enhanced evaporative emissions of i-pentane. Additionally, the correlation slopes between the C₅-C₆ alkanes and butanes were higher in summer. For example, the slope of the correlation between i-pentane with i-butane and n-butane was approximately a factor of two higher in summer (1.6 and 1.0, respectively) compared to winter (0.83 and 0.41,

respectively), while the summer n-pentane (0.72 and 0.46, respectively) and n-hexane (0.32 and 0.19, respectively) slopes were ~40-70% higher than winter. This demonstrates that fuel evaporation and headspace vapor emissions of the C₅-C₆ alkanes were strong enough to counteract OH chemistry throughout the entire summer despite the required use of reformulated gasoline with a lower Reid vapor pressure (RVP) in order to reduce emissions of highly volatile NMHCs (U.S. EPA, 2003, 2008).

The C₇-C₈ aromatics were well correlated illustrating their common sources. The toluene/ethylbenzene correlation slope was in good agreement with vehicular and urban emission ratios (Figure 2.8a) (e.g., Parrish et al., 1998; Monod et al., 2001). The o-xylene/m+p-xylene correlation slope (0.44-0.55, Figure 2.8b) was slightly higher, and the m+p-xylene/ethylbenzene (1.1-1.9, Figure 2.8c) and o-xylene/ethylbenzene (0.53-1.1, not shown) slopes were lower than urban, gasoline, fuel evaporation, and vehicle exhaust emission ratios (~0.36-0.4, 2.2-4.6, and 1.2-1.8, respectively) (Conner et al., 1995; Kirchstetter et al., 1996; Sagebiel et al., 1996; Rogak et al., 1998; Monod et al., 2001; Watson et al., 2001; Choi and Ehrman, 2004; Jobson et al., 2004; Velasco et al., 2007). The differences between the emission and ambient C₈ aromatic ratios likely reflect the preferential loss of the xylenes during transport because of their greater reactivity.

2.4.2 Ambient Ratios: Compounds with Similar Lifetimes

Information on the relative impact of various sources in a region can be obtained by comparing the ambient ratio of two compounds that have similar rates of reaction with OH but different sources (e.g., Klemp et al., 1997; Jobson et al., 1999; Goldan et al., 2000). The ratio should reflect the integration of several factors, such as air mass mixing and dilution, new emission inputs, and oxidative removal, because neither compound will

be removed preferentially during transport. Thus, on average, the ratio can be assumed to remain fairly constant and approximately equal to the emission ratio (Parrish et al., 1998). For example, propane, ethyne, and benzene have similar lifetimes ($<30\%$ difference in k_{OH}) (Atkinson et al., 2006a), but propane is a tracer of gasoline, natural gas, or petroleum while ethyne and benzene are tracers of combustion. The propane/ethyne and propane/benzene vehicular exhaust emission ratios are < 1 while ratios from natural gas and LPG are ≥ 1 (Conner et al., 1995; Fujita et al., 1995; Watson et al., 2001, Choi and Ehrman, 2004; White et al., 2008). In 2004-2008, the propane/ethyne and propane/benzene ratios (correlation slopes) ranged from 1-5 (~ 2) and 3-25 (~ 9), respectively, demonstrating the stronger influence of natural gas or LPG relative to incomplete combustion as a source of propane throughout the entire year. This corroborates previous work at TF and Appledore Island (10 km off the NH coast) during summer 2004 which concluded that LPG was the dominant source of propane throughout the entire day in southern NH (White et al., 2008). The strong correlations between propane and ethyne (Figure 2.9a), propane and benzene ($r^2=0.71-0.76$, not shown), and benzene and ethyne (Figure 2.9b) illustrate that emissions from natural gas or LPG were concurrent and/or collocated with fossil fuel/incomplete combustion. Furthermore, this suggests that non-vehicular exhaust emissions, such as residential use of natural gas or LPG, were important sources of ethyne and benzene.

The slope of the benzene vs. ethyne correlation was the same in each season of every year at TF (slope of all data=0.21, $r^2=0.91$) (Figure 2.9b). This value is consistent with observations of ambient benzene/ethyne ratios measured during several spring-summer field campaigns conducted throughout the U.S. (Fortin et al., 2005; Harley et al.,

2006; Parrish, 2006; Sistla and Aleksic, 2007; Warneke et al., 2007) and in major cities (Parrish et al., 2008). Decreasing ratio values since the mid-1990's have been interpreted as evidence of reduced benzene emissions, rather than an increase in ethyne, because of federal requirements to reduce the benzene content of gasoline (Fortin et al., 2005; Harley et al., 2006; U.S. EPA, 2008). The constant ratio value throughout 2004-2008 suggests that benzene and ethyne emissions have not changed which is supported by the lack of an interannual trend in their mixing ratios (Figure 2.3d). The benzene content in gasoline has remained fairly constant (0.6-0.9%) over the past several years (U.S. EPA, 2008) which may also partly account for the constant benzene/ethyne ratio.

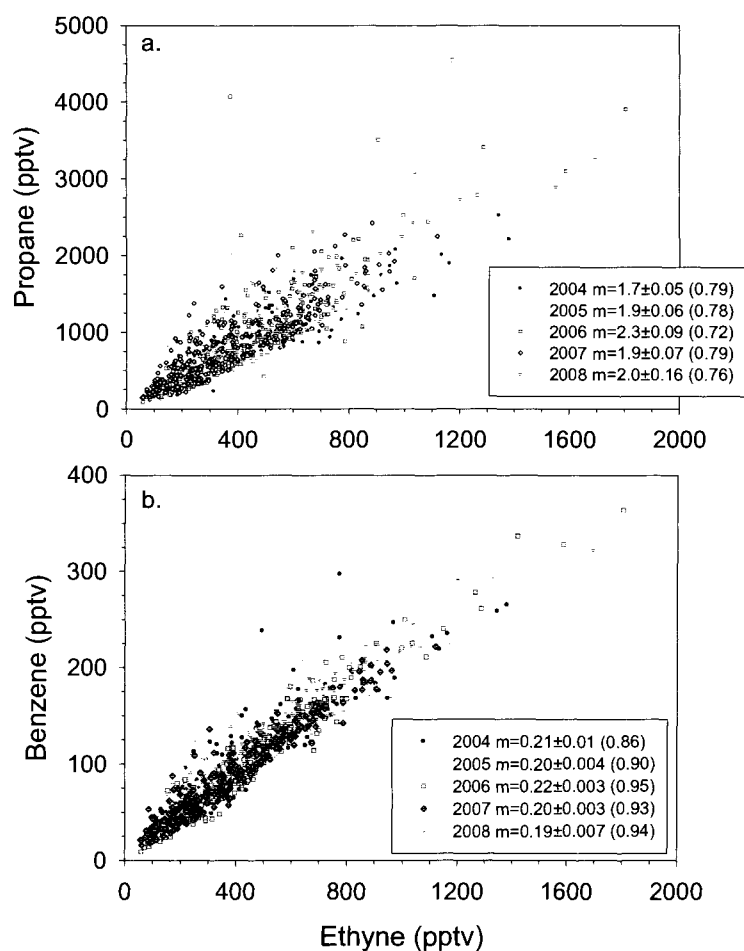


Figure 2.9. Correlations between (a) propane and ethyne, and (b) benzene and ethyne for each year. $m = \text{slope} \pm \text{SE}$ (r^2).

2.4.3 Ambient Ratios: Compounds with Different Lifetimes

The analysis in the previous section was based on the assumption that the ambient ratio between two compounds with similar rates of removal from the atmosphere will remain nearly constant during transport. Additionally, ambient ratios between compounds with different rates of reaction with OH and with well characterized sources and sinks are frequently used to estimate the relative photochemical age of air masses, transport times and distances, or OH concentrations (e.g., Jobson et al., 1994; McKeen et al., 1996; Parrish et al., 1998; Smyth et al., 1999; Dimmer et al., 2001; Kleinman et al., 2003; Russo et al., 2003). A fundamental drawback to estimating air mass processing times using ambient ratios is a lack of information on seasonal variations in sources, especially when analyzing data from short-term field campaigns. Analysis of the long-term measurements from TF provided a unique perspective on the interrelationships between seasonal variations in sources and chemical processing in this region.

Four common ratios with the shorter-lived compound in the numerator are ethyne/CO, propane/ethane, toluene/benzene, and C_2HCl_3/C_2Cl_4 (Figure 2.10). The general behavior of these ratios can be predicted based on the differential removal of the compounds in each ratio. For example, if reaction with OH was the only factor influencing the seasonality in mixing ratios, a decrease in ratio values from winter to summer would be expected to occur concurrently with the increase in atmospheric OH concentrations because the shorter-lived compound is removed preferentially. The ethyne/CO ratio trend reflects the seasonal variation in OH concentrations with higher winter ratios (4-5 pptv/ppbv) indicating less processed emissions and low summer ratios (1-2 pptv/ppbv) reflecting more processed air masses (Figure 2.10a). The propane/ethane

and C_2HCl_3/C_2Cl_4 ratios tracked each other very well, and the temporal variation of both ratios resembled the ethyne/CO ratio with maximum values in winter and minimum values in late spring-summer (Figure 2.10b). However, the propane/ethane and C_2HCl_3/C_2Cl_4 ratios increased throughout summer and fall which reflects the similar lifetimes and seasonal variation of propane and C_2HCl_3 combined with the mid-late summer minimum ethane and C_2Cl_4 mixing ratios.

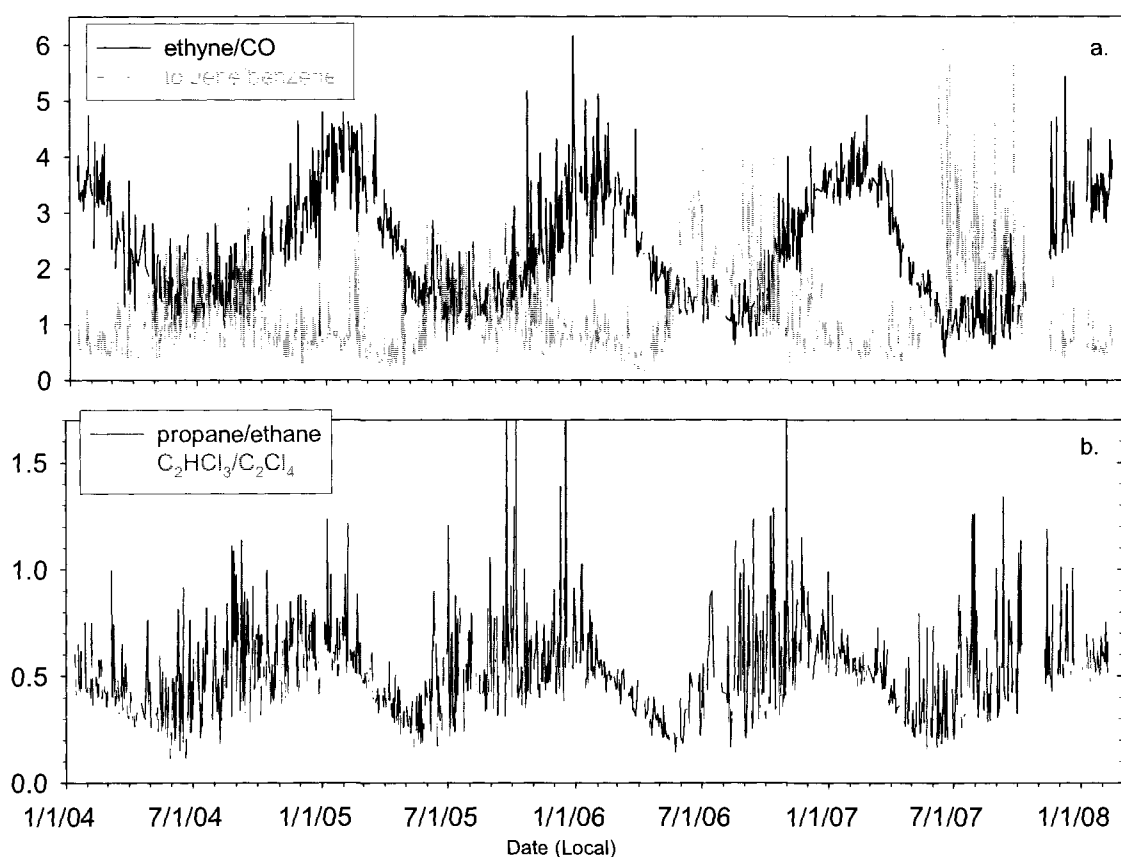


Figure 2.10. Time series of the (a) ethyne/CO (pptv/ppbv) and toluene/benzene ratios and (b) propane/ethane and C_2HCl_3/C_2Cl_4 ratios during January 2004-February 2008.

In contrast, the seasonal variation of the toluene/benzene ratio was opposite of the ethyne/CO, propane/ethane, and C_2HCl_3/C_2Cl_4 ratio behavior, and thus contrary to the expected photochemical trend (Figure 2.10a). The toluene/benzene ratio was lowest in

winter-spring (~0.5-1.5) and highest in summer-fall (0.5-7). These ratio values are comparable to ambient ratios (1-5) observed in numerous continental/urban areas (e.g., Parrish et al., 1998; Monod et al., 2001). However, the fact that the ratio increases in the summer is indicative of an additional source or enhanced emissions of toluene in this region. White et al. (2009) illustrated that the anomalous toluene behavior at TF could not be fully explained by fuel evaporation and industrial emissions. Toluene emissions were observed using dynamic branch enclosure and static chamber flux measurements suggesting that biogenic emissions contributed to the summer toluene enhancements (White et al., 2009). It was also noted that the toluene enhancements were larger with each successive year. This trend continued into 2007 when the highest toluene/benzene ratios (mean = 2.1) were observed.

This analysis provides a good illustration of the necessity of characterizing VOC sources in individual regions. Furthermore, these results have important implications because numerous studies have used the toluene/benzene ratio to estimate photochemical air mass ages (e.g., Roberts et al., 1984; Gong and Demerjian, 1997; Kang et al., 2001; de Gouw et al., 2005; Warneke et al., 2007) or to distinguish between industrial, evaporative, and exhaust emission sources (e.g., Barletta et al., 2008). The TF measurements demonstrate that the toluene/benzene ratio may not be appropriate for estimating relative air mass ages in this region because an initial ratio (e.g., toluene/benzene emission ratio) needs to be assumed. An additional source of toluene will cause the initial toluene/benzene ratio used in the processing time calculations to be erroneously high leading to overestimated photochemical ages and transport distances.

2.5 Regional Emission Rates of NMHCs

Emission rates of VOCs based on ambient measurements are critical values needed for developing regional budgets and emission inventories and as input to air quality models. Unfortunately, estimates of emission rates are extremely limited and are primarily reported on global scales (e.g., Boissard et al., 1996; Gupta et al., 1998) or in urban areas (e.g., Blake and Rowland, 1995; Chen et al., 2001). Major reasons for the lack of information on regional VOC emissions are the complications involved with differentiating between local, regional, and distant sources and the scarcity of long-term continuous measurements. Thus it is optimal to use measurements made when these complications are minimized. One possibility is to use data collected when long-range and regional transport to a site is minimal. For example, low wind speeds facilitate radiative cooling of the surface at night leading to the formation of an inversion layer which isolates the air near the surface from the air above the inversion layer (e.g., Hastie et al., 1993; Gusten et al., 1998; Talbot et al., 2005). The stable and calm conditions under this nocturnal boundary layer (NBL) inhibit vertical and horizontal mixing (Talbot et al., 2005). Therefore, an increase in VOC mixing ratios under these stable conditions can be attributed to emissions from local sources.

The daily canister samples were collected after the NBL dissipated and are representative of daytime conditions when mixing and transport may be occurring. Consequently, emission rates of NMHCs were calculated by two different methods. First, emission rates were estimated using the measurements made once per hour by the automated GC system at TF during December 2005-January 2006. Both the mixing ratios and temporal variation of the automated GC and canister sample measurements agreed

very well (Figure 2.11). This demonstrates that the daily samples captured a wide range of air mass types and compositions including background air masses and significant winter pollution events with enhanced NMHC mixing ratios lasting longer than one day.

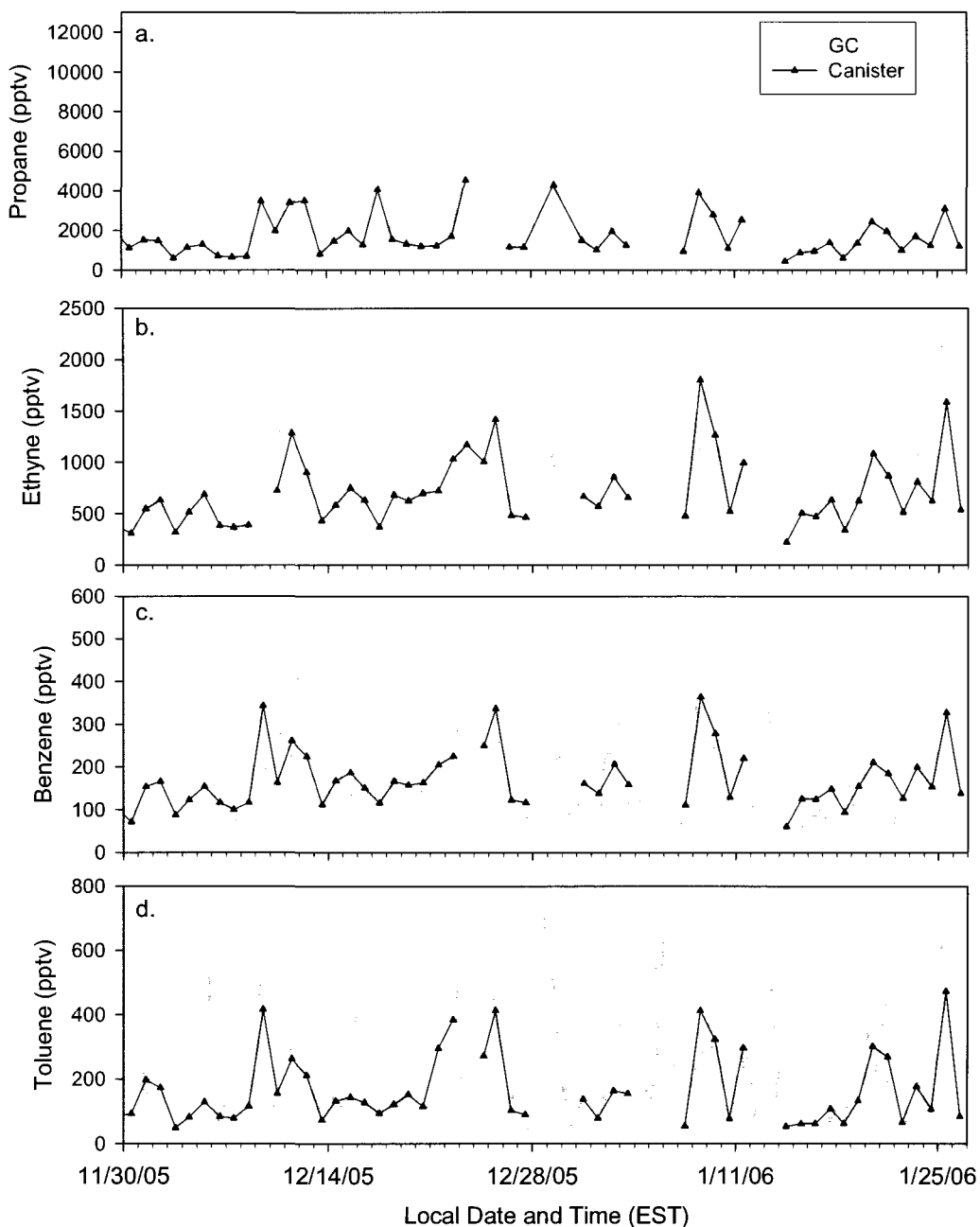


Figure 2.11. Comparison between (a) propane, (b) ethyne, (c) benzene, and (d) toluene measurements made by the automated TF GC system during December 2005-January 2006 and the daily canister samples collected during the same time period. Note: the canister samples with mixing ratios $>95^{\text{th}}$ percentile for each month have been removed.

Two criteria were used for identifying nights when a stable inversion layer developed: (1) wind speeds < 1 m/s and (2) O₃ ≤ 5 ppbv. The two criteria conditions were met on several nights between approximately midnight and 05:00 with concurrent increases in NMHC mixing ratios. Emission rates were calculated by multiplying the slope of the linear regression between the change in hourly average concentrations (dC in molecules cm⁻³) per unit time (dt = 5 hours) by the boundary layer height (H):

$$\text{Emission Rate} = \left[\frac{dC}{dt} \right] \times H$$

A boundary layer height of 125 m was used because it is a representative value for this area (e.g., Talbot et al., 2005; Zhou et al., 2005; Mao et al., 2008; White et al., 2008).

The emission rate of propane (4.2 x 10¹⁰ molecules cm⁻² s⁻¹) was 1-2 orders of magnitude larger than the other NMHCs (range 0.5-7 x 10⁹ molecules cm⁻² s⁻¹) (Table 2.3). The high propane emission rate is another illustration of the persistent impact of leakage from LPG tanks or refilling stations throughout the region (section 2.4.1). Additionally, assuming the TF results are representative of the state and region, the NMHC emission rates extrapolated to the state of New Hampshire and New England are ~2-61 Mg/day and ~12-430 Mg/day, respectively (Table 2.3). The emission rates of propane, i-butane, and n-butane in New Hampshire were 20-90% lower than observed from LPG leakage in Mexico City, Mexico (Elliott et al., 1997) and in Santiago, Chile (Chen et al., 2001). These results suggest that potential emissions of NMHCs from the northeast U.S. are comparable to emission rates that have been observed in densely populated urban areas. Furthermore, the subsequently high levels of precursor compounds in air masses transported to and across the North Atlantic may contribute to O₃ and SOA production, thus influencing the air quality of downwind regions.

	Winter 2006 TF GC		Winter 2006 Daily Can		Winter 2006 Daily Can		New	
	Emission Rate	r^2	NMHC/Ethylene	Emission Ratio	Emission Rate	Emission Rate	Hampshire	England
	$\times 10^9 \pm \text{SE}$				$\times 10^9 \pm \text{SE}$		Mg/day	Mg/day
Ethylene	7.4 ± 2.0	0.78					6.4	45
Propane	42 ± 4.0	0.96	2.30	0.57	17.1		61	427
Propene	3.2 ± 0.7	0.86	0.25	0.75	1.9		4.5	32
i-Butane	3.2 ± 0.6	0.89	0.44	0.60	3.3		6.1	43
n-Butane	3.6 ± 0.8	0.83	0.85	0.40	6.3		6.9	48
i-Pentane	2.4 ± 0.3	0.94	0.43	0.68	3.2		5.8	41
n-Pentane	1.4 ± 0.1	0.96	0.22	0.46	1.6		3.3	23
n-Hexane	0.6 ± 0.1	0.87	0.09	0.61	0.67		1.7	12
Benzene	1.6 ± 0.4	0.81	0.19	0.94	1.4		4.3	30
Toluene	2.7 ± 0.6	0.82	0.30	0.79	2.2		8.2	58
Ethylbenzene	0.5 ± 0.1	0.86	0.04	0.69	0.30		1.8	13
m+p-Xylene	1.3 ± 0.3	0.80	0.04	0.61	0.30		4.4	31
o-Xylene	0.5 ± 0.1	0.88	0.02	0.65	0.15		1.8	13

Table 2.3. Emission rates \pm standard error (SE) (molecules $\text{cm}^{-2} \text{s}^{-1}$) of $\text{C}_3\text{-C}_8$ NMHCs calculated using nighttime measurements (00:00-05:00 local time) made by the automated TF GC when a stable nocturnal inversion layer developed. The winter 2006 daily canister emission ratio was calculated from the slope of the correlation between a NMHC and ethylene. The winter 2006 daily can emission rate (molecules $\text{cm}^{-2} \text{s}^{-1}$) was calculated by multiplying the daily can emission ratios by the winter 2006 TF GC ethylene emission rate. The emission rates (Mg/day) from New Hampshire and New England were extrapolated from the winter TF GC emission rates.

The second method examined the utility of using the daytime canister samples to calculate emission rates. Emission rates were estimated by multiplying the emission ratios for each compound by the emission rate of ethyne estimated from the nighttime TF GC measurements (Table 2.3, 7.4×10^9 molecules $\text{cm}^{-2} \text{s}^{-1}$). Emission ratios using the winter 2006 daily can data were determined from the slope of the correlation between a specific NMHC and ethyne (NMHC/ethyne). Ethyne is frequently used as a reference compound because of its relatively long lifetime (weeks-months) and because its major source (combustion) is well known (e.g., Conner et al., 1995; Goldstein et al., 1995; de Gouw et al., 2005; Lee et al., 2006).

The emission rates of the NMHCs calculated using the daily canister emission ratios were within ~5-75% of the automated GC estimates (Table 2.3). The daily canister emission rates of several compounds (i-butane, n-pentane, n-hexane, benzene, toluene) were within the uncertainty range estimated using the nighttime GC measurements. The largest difference was the factor of 2-4 lower emission rates of m+p-xylene and o-xylene based on the emission ratio method. However, this result is not unexpected because the xylenes have short lifetimes (≤ 2 days in winter) and the samples were collected during the day when photochemistry was active. Additionally, emission rates determined using emission ratios from winters 2004, 2005, 2007, or 2008 were within ~10-50% of the winter 2006 values. Furthermore, the winter 2006 emissions rates of propane, i-butane, n-butane, i-pentane, and propene agreed (within factors of 0.2-4) with estimates made using nighttime measurements from the automated TF GC during summers 2003 and 2004 (White et al., 2008). The consistency between the estimates for different winters and for winter and summer suggests that emission rates do not vary significantly with season or

year. Overall, these results suggest that the daytime canister samples provide reasonable estimates of emission rates for this region and may be used if the emission rate of a reference compound is available.

2.6 Comparison with the 2002 EPA National Emissions Inventory

A fundamental shortcoming of emission inventories is the lack of speciated VOC emission estimates. The utility of the long-term speciated VOC data from TF as an evaluation method of the 2002 EPA National Emissions Inventory (NEI) (www.epa.gov/ttn/chief/net/index) was investigated by comparing emission rates of benzene, toluene, ethylbenzene, m+p+o-xylene, and ethyne from the NEI to the estimates from TF (section 2.5). The NEI provides speciated emission rates for a subset of toxic compounds, including benzene, toluene, ethylbenzene, and m+p+o-xylene. Emission rates of ethyne were estimated using the EPA recommended composite source profiles for vehicle exhaust (gasoline and diesel), recreational equipment, lawn and garden equipment, and fireplace wood combustion. The results are constrained by the accuracy and completeness of emission reporting and are dependent upon the speciation profiles which are often dated composites of several similar sources from various locations throughout the country. In addition, the TF measurements reflect air masses that have undergone mixing and dilution and thus are not representative of direct emissions. Despite these limitations, an effective method for inventory validation is to compare the inventory emission rates to ambient emission rates.

Overall, the TF and NEI emission rates agree fairly well (Table 2.4). The NEI slightly overestimated (by ~5-50%) the ambient benzene, toluene, xylenes, and ethyne emission rates. These results suggest that the ethyne (or another compound) emission rate

from the NEI could be used to estimate emission rates of other VOCs by using their emission ratios relative to ethyne from the daily canister samples. This may be a valuable tool for modeling or predicting ambient VOC concentrations. The agreement between our results and the inventory may be fortuitous or it may indicate that VOC emissions are more accurately represented in the 2002 NEI than in earlier versions. In contrast to our results, Parrish (2006) concluded that the 1996 and 1999 NEIs overestimated VOC emissions by up to factors of 3-4 based on comparing inventory emissions and ambient measurements of benzene and ethyne. Possible reasons for the contrasting results are different methods used to estimate benzene and ethyne inventory emissions or the use of different versions of the NEI. The on-road benzene/ethyne ratio (0.35) is similar to the value from the 1999 on-road NEI (0.32) (Parrish, 2006). The total inventory ratio value (0.21) (Table 2.4) is in excellent agreement with the ambient ratio at TF discussed in section 2.4.2 and supports the continued downward trend of the benzene/ethyne ratio in the 1996 to 1999 NEI reported by Parrish (2006). Similarly, the inventory total and TF toluene/benzene ratios agree, and the range of NEI ratio values is consistent with the range of ambient ratios observed at TF (Figure 2.10a).

	Mobile						Point	NEI Total	TF
	Onroad		Nonroad		Nonpoint	TF			
	Exhaust	Evaporation							
Benzene	540	25	730	520	10	1830	1555		
Toluene	1400	160	1660	480	100	3801	3000		
Ethylbenzene	200	30	365	25	30	655	660		
Xylenes	790	100	1120	195	120	2330	2260		
Ethyne	520		1055	1360		2940	2350		
				<i>New Hampshire</i>					
Benzene	4745	230	3060	3350	110	11500	10890		
Toluene	12000	1545	11060	4950	2060	31640	21000		
Ethylbenzene	1700	340	1700	360	100	4200	4640		
Xylenes	6790	1000	8700	3280	400	20170	15870		
Ethyne	4610		8380	7125		20120	16460		
				<i>New England</i>					
Toluene/Benzene	2.2	5.5	1.9	0.78	8.6	1.8	1.6		
Benzene/Ethyne	0.35		0.23	0.13		0.21	0.22		

Table 2.4. Emission rates (Mg/year) of benzene, toluene, ethylbenzene, xylenes, and ethyne from the 2002 EPA National Emissions Inventory for New Hampshire and New England. The TF column lists the emission rates (converted from Mg/day to Mg/year) estimated from the winter 2006 TF GC nighttime measurements in Table 2.3.

2.7 Summary

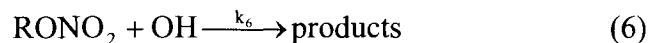
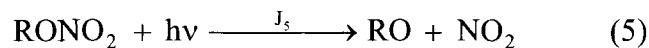
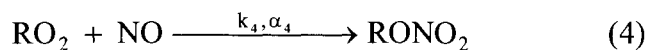
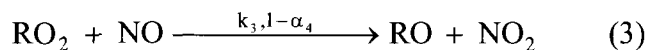
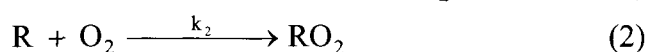
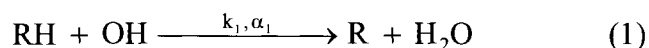
This work characterized the mixing ratios, seasonal to interannual variability, and sources of C₂-C₈ NMHCs, C₂HCl₃, and C₂Cl₄ from samples collected during January 2004-February 2008 at Thompson Farm in Durham, NH. The midday canister samples provided a comprehensive and representative picture of the day-to-day and interannual VOC trends and captured a wide range of mixing ratios and various sources. For example, separate estimates of NMHC emission rates using the daily canister sample and automated GC measurements agreed within 5-75% (range = 10⁹-10¹⁰ molecules cm⁻² s⁻¹). Additionally, benzene, toluene, ethylbenzene, xylene, and ethyne emission rates from the 2002 EPA National Emissions Inventory were within 5-50% of the TF emission rates. Other than small differences in actual mixing ratios, the alkanes, ethyne, benzene, and halocarbons exhibited consistent and reproducible seasonal trends each year. In contrast, the alkenes, toluene, ethylbenzene, and xylenes (m+p and o) illustrated greater interannual variability reflecting their shorter lifetimes and/or varying sources or emission ratios. A persistent mix of emissions from several sources (fossil fuel combustion, gasoline, LPG, fuel or solvent evaporation, industry, biogenic) was observed each season and year.

CHAPTER 3

TEMPORAL VARIABILITY, SOURCES, AND SINKS OF C₁-C₅ ALKYL NITRATES IN COASTAL NEW ENGLAND

3.1 Introduction

Alkyl nitrates are secondary products of the photooxidation of volatile organic compounds (VOCs) in the presence of nitrogen oxides (NO_x=NO+NO₂) and represent a link between the atmospheric carbon and nitrogen cycles. Alkyl nitrate production (reactions 1-4) is initiated by the oxidation of a hydrocarbon (RH). The resulting alkyl radical (R) quickly reacts with O₂ to form an alkyl peroxy radical (RO₂). Further reaction with nitric oxide (NO) yields an alkoxy radical (RO) and nitrogen dioxide (NO₂) or an alkyl nitrate (RONO₂):



where k_1 , k_2 , k_3 , k_4 , and k_6 are reaction rate constants, J_5 is the photolysis rate constant, and α_1 and α_4 are the reaction branching ratios. The primary removal mechanisms from the atmosphere are photolysis and reaction with the hydroxyl radical (OH) (reactions 5 and 6). Photolysis is dominant for the shorter-chain (C₁-C₃) alkyl nitrates while OH oxidation becomes a more important loss process for the larger alkyl nitrates (Roberts,

1990; Clemitshaw et al., 1997; Talukdar et al., 1997; Flocke et al., 1998). Reactions (1-4) demonstrate that alkyl nitrates share a common photochemical production mechanism with ozone (O_3), as O_3 formation follows the photolysis of the NO_2 formed in reaction (3). The formation of alkyl nitrates serves as a sink for NO_x and for the RO and RO_2 radicals, and therefore, impacts the O_3 production efficiency (Atkinson et al., 1982; Ranschaert et al., 2000). Alkyl nitrates may be transported long distances because of their long lifetimes and serve as a temporary reservoir for NO_x ultimately leading to O_3 production in remote regions (Clemitshaw et al., 1997; Flocke et al., 1998; Roberts et al., 1998). In addition, alkyl nitrates are a component of total reactive nitrogen ($NO_y = NO_x + HNO_3 + NO_3 + N_2O_5 +$ organic nitrates), and their relative contribution to NO_y varies with location. For example in continental regions, alkyl nitrates typically comprise less than 10% of NO_y because of the close proximity to primary NO_x emissions (e.g., Shepson et al., 1993; Flocke et al., 1998; Thornberry et al., 2001; Simpson et al., 2006). In contrast, they may constitute a much larger proportion of NO_y in remote regions, such as the equatorial marine boundary layer (20-80%) (Talbot et al., 2000; Blake et al., 2003a) or the Arctic (~10-20%) (Muthuramu et al., 1994).

Characterizing alkyl nitrates may help explain imbalances in the atmospheric NO_y budget. Discrepancies between surface deposition rates determined from the sum of the individual NO_y compounds compared to the measured total NO_y deposition suggests that all the species contributing to the total deposition are not being accounted for (e.g., Nielsen et al., 1995; Lefer et al., 1999; Horii et al., 2006). The shortfall is often largest in photochemically processed air masses and is usually attributed to unidentified alkyl and multifunctional organic nitrates (e.g., Nielsen et al., 1995; Munger, et al., 1998; Horii et

al., 2006). Consequently, research on the contribution of organic nitrogen to atmospheric nitrogen deposition and the impact on ecosystem functioning has been gaining importance (Cornell et al., 2003).

In addition to their secondary photochemical source, primary emissions of light alkyl nitrates from the ocean (Atlas et al., 1993; Chuck et al., 2002; Moore and Blough, 2002; Blake et al., 2003a) and biomass burning have been observed (Simpson et al., 2002). However, information on the relative influence of primary marine and secondary anthropogenic sources of alkyl nitrates in coastal regions is limited (e.g., Roberts et al., 1998; Chuck et al., 2002; Simpson et al., 2006). Recent modeling results suggest that the photolysis of alkyl nitrates emitted from the tropical Pacific Ocean, and the subsequent production of NO_2 , may increase O_3 production by up to 20% (Neu et al., 2008). This demonstrates the importance of identifying alkyl nitrate sources and quantifying their mixing ratios in marine environments.

The seacoast region of New Hampshire is downwind of the heavily populated and urban northeastern U. S. corridor and is in an excellent location for studying the chemical composition of air masses transported from the continental U.S. to the North Atlantic. Previous research has shown that this area is influenced by marine, vegetative, and anthropogenic sources of nonmethane hydrocarbons (NMHCs) and halocarbons (Sive et al., 2007; Varner et al., 2008; White et al., 2008; Zhou et al., 2005, 2008) and is strongly impacted by boundary layer dynamics (Mao and Talbot, 2004a; Talbot et al., 2005). In this work, we characterize the seasonal and diurnal variability, sources, and sinks of alkyl nitrates in southeastern NH and coastal New England. A portion of the alkyl nitrate data was obtained as a component of the 2002 New England Air Quality Study (NEAQS). The

objectives of NEAQS were to examine the transport, formation, and distribution of air pollutants in New England and the Gulf of Maine. Additionally, we incorporate data from a one day intensive study throughout the Great Bay estuary in August 2003 and from daily canister samples collected during 2004-2008 in order to further describe the temporal variability and atmospheric distribution of alkyl nitrates.

3.2 Experimental

3.2.1 NEAQS 2002

3.2.1.1 Thompson Farm GC System. Measurements of C₂-C₁₀ NMHCs, C₁-C₂ halocarbons, and C₁-C₅ alkyl nitrates were made during winter (January 11-March 1) and summer (June 1-August 31) 2002 at the University of New Hampshire Atmospheric Observing Station at Thompson Farm (TF) (43.11°N, 70.95°W, elevation 24 m) in Durham, New Hampshire (Figure 2.1). TF is surrounded by a mixed forest and is located ~20 km inland from the Gulf of Maine, 5 km northwest of the Great Bay estuary, and ~100 km north of Boston, MA. Samples were analyzed onsite by an automated gas chromatography (GC) system equipped with two flame ionization detectors (FID) for detecting NMHCs and two electron capture detectors (ECD) for measuring halocarbons and alkyl nitrates (described in detail by Zhou et al., 2005; 2008). Briefly, air was drawn continuously through a PFA Teflon lined manifold from the top of a 15 m tower. Once per hour, a 1000 cc aliquot of this air was collected through a dual stage trap for water management and sample concentration. Following enrichment, the sample was rapidly heated to 100°C and injected. Helium carrier gas flushed the sample to the GC where the stream was split into four channels for analysis. A 1000 cc aliquot from one of two working standards was analyzed every fifth sample. The measurement precision for each

of the hydrocarbons, halocarbons, and alkyl nitrates ranged from 0.3-15%. Specifically, the alkyl nitrate measurement precision is conservatively 5% for mixing ratios above 5 pptv and 10% for mixing ratios below 5 pptv. The accuracy of the alkyl nitrate measurements is 10–20%, and their detection limit is 0.01 pptv. The alkyl nitrates discussed in this work are methyl nitrate (MeONO₂), ethyl nitrate (EtONO₂), 2-propyl nitrate (2-PrONO₂), 1-propyl nitrate (1-PrONO₂), 2-butyl nitrate (2-BuONO₂), 2-pentyl nitrate (2-PenONO₂), and 3-pentyl nitrate (3-PenONO₂).

3.2.1.2 GC System on the NOAA R/V *Ronald H. Brown*. During July 30-August 6, 2002, ambient air and surface seawater samples were collected onboard the NOAA Research Vessel *Ronald H. Brown* off the coasts of New Hampshire and Boston, MA. An automated GC measured MeONO₂, 2-PrONO₂, and 2-BuONO₂ in addition to several hydrocarbons and halocarbons. Ambient air was sampled from ~15 m above the sea surface and traveled approximately 80 m to the GC located near the back of the ship. A portion of this air flow was drawn by the sample concentrator and a 1000 cc sample was cryogenically trapped. Water from the ship's clean seawater system flowed to a Weiss type equilibrator. Air was drawn from the equilibrator at 200 ccm for determining concentrations of the stripped gases from the surface seawater. After the ambient air or equilibrator sample was concentrated, it was injected on to a two gas chromatograph system. One GC quantified halocarbons and alkyl nitrates with an ECD, and the other GC measured C₂-C₆ hydrocarbons by FID (Zhou et al., 2005).

3.2.2 Canister Samples

3.2.2.1 Great Bay Experiment. In addition to the routine measurements at TF (section 3.2.1.1), an intensive study was conducted from 18:00 on August 18 to 19:00 on

August 19, 2003 (local time) to examine the influence of marine derived halocarbons from the Great Bay estuary throughout southeast NH. The Great Bay is a 2140 hectare estuary located ~16 km inland from the coast of NH. The study area consisted of TF and 4 sites located in southern NH: Downtown Boat Launch, Exeter (42.98°N, 70.95°W); Fort Constitution (FC), Newcastle (43.07°N, 70.71°W); Pease Weather Station, Portsmouth (43.08°N, 70.82°W); and Wagon Hill Farm (WHF), Durham (43.13°N, 70.87°W) (Figure 2.1 inset). At each of the four sites, a two-liter electropolished stainless steel canister was filled to ambient pressure each hour. The samples were returned to the laboratory at UNH for analysis on a three GC system equipped with 2 FIDs, 2 ECDs, and a mass spectrometer (MS). The lab GC system has been previously described in Sive et al. (2005), White et al. (2008), and Zhou et al. (2005; 2008). Briefly, the samples were analyzed by cryotrapping 1000 cc of air on a glass bead filled loop immersed in liquid nitrogen. The loop was then isolated, warmed to ~80°C with hot water, and then the sample was injected. Helium carrier gas flushed the contents of the loop and the stream was split into five, with each sub-stream feeding a separate GC column. The FIDs were used for detecting C₂-C₁₀ NMHCs, and the ECDs measured C₁-C₅ alkyl nitrates and C₁-C₂ halocarbons. Oxygenated VOCs, sulfur compounds, halocarbons, and several NMHCs were detected by the MS. A 1000 cc aliquot from one of two working standards was assayed every fifth analysis. The measurement precision for each of the hydrocarbons, halocarbons, and alkyl nitrates ranged from 0.1-12%. The alkyl nitrate measurement precision for the canister samples is conservatively 3-4% for mixing ratios above 5 pptv and <10% for mixing ratios below 5 pptv. The accuracy of the alkyl nitrate canister measurements is 10–20%, and the detection limit is 0.01 pptv.

3.2.2.2 Thompson Farm Daily Canister Samples. Measurements of C₁-C₅ alkyl nitrates from daily canister samples collected throughout January 12, 2004 to February 8, 2008 are also presented. The four year data set was separated into four seasons which are defined as winter: December, January, February; spring: March, April, May; summer: June, July, August; fall: September, October, November. Note that the data includes five winter seasons (2004-2008) and four spring, summer, and fall seasons (2004-2007). Details of the sample collection and analysis are given in Russo et al. (2009). Briefly, the ambient air samples were collected at approximately noon (local time) from the top of the 15 m tower at TF. The samples were analyzed in the lab at UNH every 1-3 months for a large suite of volatile organic compounds (C₂-C₁₀ NMHCs, C₁-C₅ alkyl nitrates, C₁-C₂ halocarbons, and selected oxygenated and sulfur compounds) using the same three GC system described in section 2.2.1. The primary working standards for the canister analysis system were two calibrated whole air samples contained in 36 liter electropolished low pressure pontoons (~350 psi). Due to overlapping periods when different working standards were being used throughout the four years, mixing ratios were verified and recalibrated, if/when necessary, and were cross referenced with other calibrated whole air and synthetic standards maintained by our lab. Furthermore, we have conducted several instrument intercomparison studies to ensure that the measurements from the in situ TF GC and canister samples made over multiple years are comparable (see Sive et al., 2005; 2007; Zhou et al., 2008; Russo et al., 2009 for additional information).

3.2.3 Measurement Intercomparison

It is also necessary to intercompare our standards and calibration scales with other laboratories conducting VOC measurements. In summer 2004, an informal VOC intercomparison experiment was conducted by D. Blake at UCI to evaluate the comparability of measurements made by different investigators during the summer 2004 ICARTT campaign. The intercomparison data presented here was provided by D. Blake (personal communication, UCI, 2005). Four pressurized canisters filled with whole air collected by UCI were sent to each laboratory for analysis. The mixing ratios in each canister as well as the mean of the four samples were reported. In total, UNH reported mixing ratios for 99 compounds, including C₂-C₁₀ NMHCs, C₁-C₅ alkyl nitrates, and C₁-C₂ halocarbons (e.g., Varner et al., 2008; Zhou et al., 2008). The UNH alkyl nitrate measurements were in good agreement with UCI (Figure 3.1). The mean mixing ratios (in pptv) of each alkyl nitrate in the four canister samples were: (UNH/UCI) MeONO₂ 8.2/8.4, EtONO₂ 8.4/8.5, 2-PrONO₂ 24.2/27.3, 1-PrONO₂ 4.4/3.7, 2-BuONO₂ 30.2/29.5, 3-PenONO₂ 7.6/8.8, and 2-PenONO₂ 12.4/12.8. Furthermore, the percent difference between the UNH and UCI C₂-C₄ alkane measurements was ≤ 2%, and the C₅ alkanes agreed within 7-8%. These results demonstrate that the alkyl nitrate and NMHC mixing ratios reported by these various laboratories were based on similar calibration scales, and thus the measurements can be meaningfully compared.

3.2.4 Ancillary Measurements

Hourly average measurements of O₃, carbon monoxide (CO), carbon dioxide (CO₂), and NO_y made at TF during winter and summer 2002 and August 18-19, 2003 were also used in this analysis. The instruments used were a Thermo Environmental

Instruments (TEI) model 49C-PS using ultraviolet spectroscopy at 254 nm for O₃, a custom modified TEI model 48CTL using absorption of infrared radiation at 4600 nm for CO, a Licor model 7000 differential infrared absorption instrument for CO₂, and a TEI model 42C using chemiluminescence measured NO_y (Mao and Talbot, 2004a, b; Talbot et al., 2005). Meteorological parameters (wind speed, wind direction, temperature) were measured with a Met One model 014A anemometer.

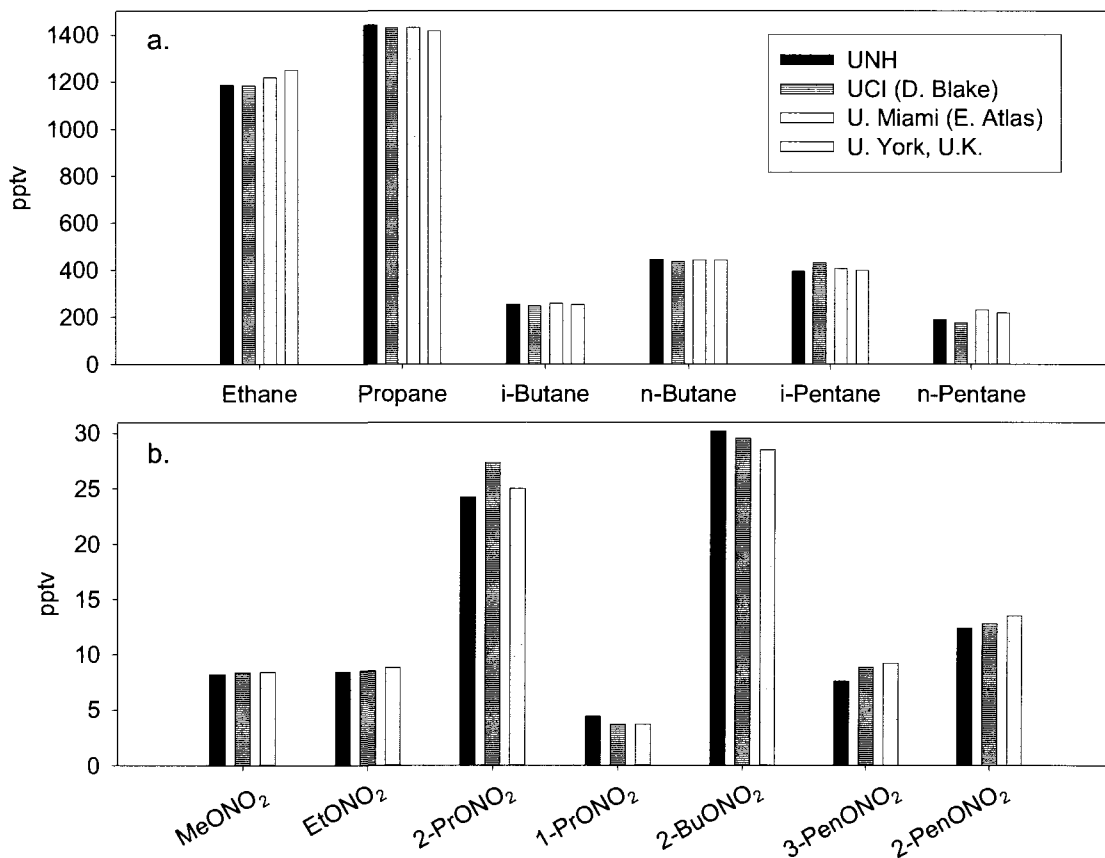


Figure 3.1. (a) NMHC and (b) alkyl nitrate measurement intercomparison between the UNH, UCI, U Miami and U. York (NMHCs only) laboratories. Each bar is the average mixing ratio (pptv) of four canister samples analyzed by each lab.

3.3 Temporal Variation of Alkyl Nitrates at Thompson Farm

Two distinct data sets are combined to provide a robust characterization of the temporal variation of alkyl nitrates in rural New England. The continuous in situ measurements made at TF during winter and summer 2002 and the four years (2004-2008) of daily canister samples allow both the short (diurnal to seasonal) and long (seasonal to interannual) term trends to be described (Figures 3.2 and 3.3).

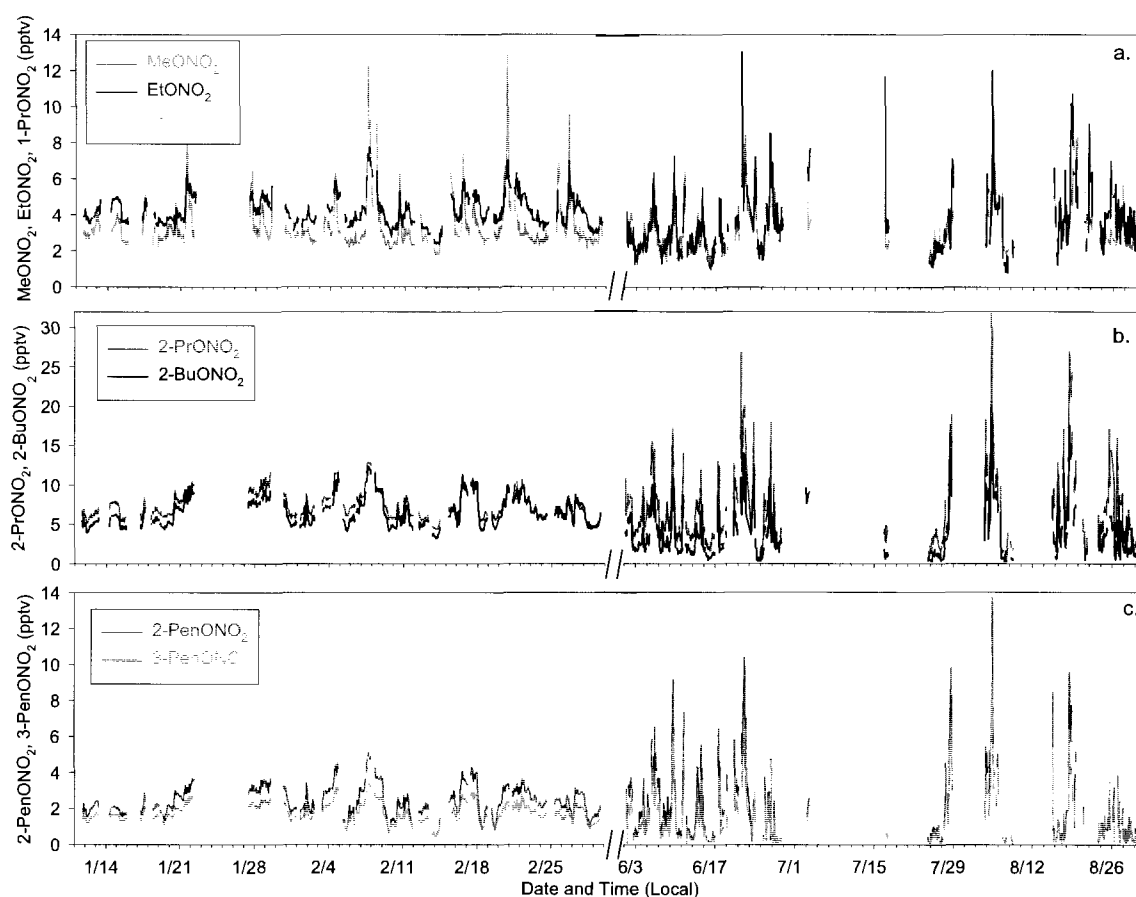


Figure 3.2. Time series of (a) MeONO₂, EtONO₂, 1-PrONO₂, (b) 2-PrONO₂, 2-BuONO₂, and (c) 2-PenONO₂, 3-PenONO₂ (pptv) from measurements made by the automated GC system at TF during Winter (January 11-March 1) and Summer (June 1-August 31) 2002. Note: there is a break in the x-axis during March-May 2002.

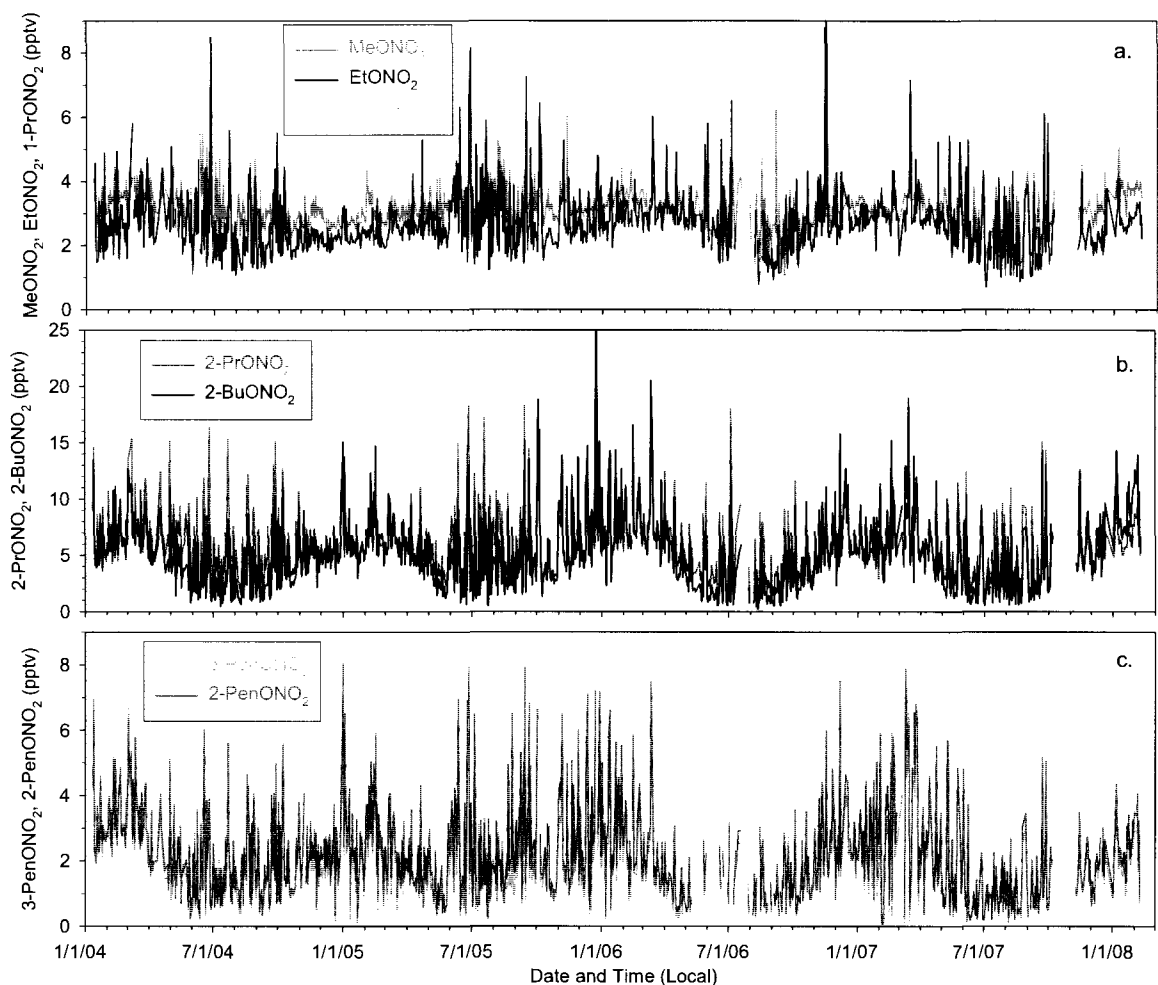


Figure 3.3. Time series of (a) MeONO₂, EtONO₂, 1-PrONO₂, (b) 2-PrONO₂, 2-BuONO₂, and (c) 2-PenONO₂, 3-PenONO₂ (pptv) from daily canister samples collected at TF during January 12, 2004 to February 8, 2008.

3.3.1 Seasonal Variation

The median (\pm standard deviation) total alkyl nitrate mixing ratio (Σ RONO₂ = sum of individual C₁-C₅ alkyl nitrates) in winter and summer 2002 was 25 (\pm 7) and 16 (\pm 14) pptv, respectively (Table 3.1). Similar median (\pm standard deviation) mixing ratios of 23 (\pm 8) and 14 (\pm 10) pptv were observed in the winter and summer daily canister samples, respectively (Table 3.2). The nearly 60% lower Σ RONO₂ mixing ratio in summer was driven by the reduced levels of C₃-C₅ alkyl nitrates which were typically highest in late

winter-early spring (February-March) and exhibited a broad minimum from May-October (Figure 3.3, Table 3.2). In contrast, monthly mean and median MeONO₂ and EtONO₂ mixing ratios were fairly constant (~2-4 pptv) all year, and both compounds exhibited low day-to-day variability in late fall-winter (Figure 3.3a). This behavior may reflect their longer lifetimes resulting in a more homogeneous distribution throughout the year.

	Mean	Median	Max	Min	St. Dev.	N	% ΣRONO ₂
Winter							
MeONO ₂	3.4	3.0	12.8	1.8	1.3	735	12
EtONO ₂	4.2	4.0	7.7	2.3	0.8	720	16
2-PrONO ₂	7.4	6.9	12.9	4.3	1.7	731	27
1-PrONO ₂	1.4	1.3	2.7	0.7	0.3	716	5
2-BuONO ₂	6.5	6.1	12.3	3.2	1.8	739	24
3-PenONO ₂	1.8	1.7	3.4	0.5	0.5	738	7
2-PenONO ₂	2.4	2.2	5.1	0.5	0.8	735	9
ΣRONO ₂	26.3	24.9	52.9	7.9	6.9	748	
%NO _y	0.30	0.20	2.80	0.03	0.40	649	
Summer							
MeONO ₂	3.1	2.7	8.4	1.2	1.3	775	17
EtONO ₂	3.4	3.0	13.0	0.8	1.6	773	19
2-PrONO ₂	6.5	4.9	31.7	0.4	4.7	771	30
1-PrONO ₂	1.2	1.1	5.5	0.1	0.8	783	6
2-BuONO ₂	3.6	2.6	18.1	0.2	3.1	768	16
3-PenONO ₂	1.4	0.9	9.0	0.04	1.4	697	5
2-PenONO ₂	2.0	1.2	13.7	0.04	2.1	671	7
ΣRONO ₂	20.2	15.9	92.4	0.1	13.6	797	
%NO _y	0.70	0.60	5.50	0.002	0.50	759	

Table 3.1. Seasonal mean, median, maximum (Max), and minimum (Min) mixing ratios, standard deviation (SD), and number of samples (*N*) of alkyl nitrates at Thompson Farm during winter and summer 2002 (pptv). % ΣRONO₂ is the median contribution of each alkyl nitrate to the ΣRONO₂ mixing ratio in both seasons. % NO_y is the median contribution of ΣRONO₂ to NO_y in both seasons (i.e., seasonal median value of ΣRONO₂/NO_y).

	January	February	March	April	May	June	July	August	September	October	November	December
MeONO₂												
Mean (SD)	3.0 (0.5)	3.4 (0.4)	3.4 (0.5)	3.2 (0.4)	3.2 (0.4)	3.1 (0.9)	3.0 (0.9)	3.0 (0.9)	3.0 (0.9)	3.0 (0.6)	3.2 (0.5)	3.1 (0.4)
Median (N)	3.3 (135)	3.4 (109)	3.4 (107)	3.2 (95)	3.2 (103)	3.0 (99)	2.9 (98)	2.9 (107)	2.9 (106)	2.9 (91)	3.1 (101)	3.1 (100)
% ΣRONO ₂	14	13	13	16	20	21	19	20	19	19	15	14
EtONO₂												
Mean (SD)	2.7 (0.6)	2.8 (0.6)	3.2 (0.9)	2.9 (0.7)	2.7 (0.8)	2.9 (1.5)	2.6 (1.2)	2.2 (1.0)	2.3 (1.1)	2.5 (0.8)	2.8 (1.2)	2.6 (0.6)
Median (N)	2.7 (136)	2.7 (108)	3.0 (107)	2.8 (95)	2.6 (103)	2.5 (99)	2.4 (92)	1.9 (105)	2.0 (111)	2.2 (92)	2.5 (102)	2.4 (102)
% ΣRONO ₂	11	11	12	14	16	17	15	14	14	14	12	11
1-PrONO₂												
Mean (SD)	0.8 (0.3)	0.9 (0.3)	0.9 (0.3)	0.8 (0.3)	0.7 (0.5)	0.7 (0.5)	0.7 (0.4)	0.6 (0.3)	0.6 (0.4)	0.7 (0.4)	0.7 (0.3)	0.8 (0.4)
Median (N)	0.8 (137)	0.8 (108)	0.8 (108)	0.7 (94)	0.6 (105)	0.6 (101)	0.6 (98)	0.5 (107)	0.5 (109)	0.5 (92)	0.6 (102)	0.7 (102)
% ΣRONO ₂	3	3	3	4	4	4	4	4	4	3	3	3
2-PrONO₂												
Mean (SD)	6.2 (2.0)	6.8 (1.8)	7.7 (2.8)	6.2 (2.1)	4.9 (2.3)	5.0 (3.7)	5.4 (3.4)	4.6 (2.8)	4.9 (3.2)	5.1 (2.8)	5.9 (2.0)	6.3 (2.8)
Median (N)	5.8 (137)	6.4 (108)	6.8 (108)	5.6 (95)	4.1 (105)	3.6 (101)	4.6 (98)	3.7 (107)	4.0 (111)	4.0 (92)	5.4 (102)	5.4 (102)
% ΣRONO ₂	24	25	27	28	27	25	29	27	27	26	26	25
2-BuONO₂												
Mean (SD)	7.2 (2.7)	7.5 (2.6)	7.7 (3.0)	5.2 (2.0)	3.2 (1.8)	3.2 (2.7)	3.1 (2.2)	2.9 (2.1)	3.6 (2.8)	4.5 (3.1)	6.1 (2.6)	7.0 (4.1)
Median (N)	6.8 (135)	6.8 (108)	6.9 (106)	4.7 (95)	2.8 (105)	2.1 (101)	2.7 (98)	2.3 (107)	2.7 (111)	3.2 (92)	5.1 (102)	5.7 (102)
% ΣRONO ₂	28	26	27	23	18	15	17	17	18	21	25	26
3-PenONO₂												
Mean (SD)	2.4 (1.1)	2.8 (1.2)	2.7 (1.6)	1.7 (0.9)	1.4 (1.0)	1.7 (1.5)	1.5 (1.0)	1.5 (1.0)	1.6 (1.2)	1.7 (1.0)	2.1 (0.9)	2.2 (1.2)
Median (N)	2.3 (132)	2.8 (105)	2.2 (105)	1.5 (95)	1.1 (96)	1.2 (83)	1.2 (96)	1.2 (103)	1.4 (105)	1.4 (89)	1.9 (101)	1.9 (98)
% ΣRONO ₂	9	11	9	8	7	8	8	8	9	9	9	9
2-PenONO₂												
Mean (SD)	2.8 (1.3)	3.0 (1.3)	3.0 (1.7)	1.9 (1.0)	1.5 (1.1)	2.1 (1.8)	1.6 (1.1)	1.7 (1.2)	1.9 (1.4)	1.8 (1.2)	2.5 (1.2)	2.6 (1.5)
Median (N)	2.6 (132)	3.0 (106)	2.6 (104)	1.7 (95)	1.3 (96)	1.4 (83)	1.3 (95)	1.5 (103)	1.5 (106)	1.4 (89)	2.2 (101)	2.3 (98)
% ΣRONO ₂	11	12	10	8	8	10	8	11	10	9	10	11
ΣRONO₂												
Mean (SD)	25.1 (7.6)	26.8 (7.3)	28.2 (10.0)	22.0 (6.5)	17.3 (7.2)	18.0 (11.7)	17.6 (9.4)	16.2 (8.7)	17.6 (10.5)	19.1 (8.9)	23.2 (7.8)	24.1 (9.4)
Median (N)	23.3 (134)	25.1 (109)	24.2 (108)	20.5 (95)	15.2 (105)	13.6 (101)	16.2 (98)	14.3 (107)	15.3 (111)	15.5 (92)	20.7 (102)	21.5 (101)
% NO _y	0.6	0.8	1.0	0.9	0.7	0.6	0.6	0.6	0.7	0.6	0.5	0.5

Table 3.2. Monthly mean (pptv), standard deviation (SD), median, and number of samples (N) from the daily canister samples collected at TF throughout January 12, 2004-February 8, 2008. % ΣRONO₂ is the median contribution of each alkyl nitrate to the ΣRONO₂ mixing ratio each month. % NO_y is the median contribution of ΣRONO₂ to NO_y in each month.

The relative contributions of the individual C₁-C₅ alkyl nitrates to ΣRONO₂ were nearly the same in the continuous measurements and in the daily samples (Tables 3.1 and 3.2). 2-propyl nitrate was generally the most abundant (~4-7 pptv), and 2-BuONO₂ was at comparable to slightly higher levels in winter-early spring. In all study years, 2-BuONO₂ exhibited the most pronounced seasonal variation with approximately a factor of 2-3 higher median mixing ratio in winter than in summer. While the relative contribution of 2-BuONO₂ to ΣRONO₂ decreased from winter to summer, the contributions from MeONO₂ and EtONO₂ increased. As a result, MeONO₂, EtONO₂, and 2-BuONO₂ made nearly equal contributions to ΣRONO₂ in summer (15-20%). The pentyl nitrates and 1-PrONO₂ were the least abundant components of ΣRONO₂ all year (<1-3 pptv). Overall, the alkyl nitrate mixing ratios and distributions at TF were comparable to levels observed at other North American sites, such as Michigan (Ostling et al., 2001), Colorado and the eastern U. S. (Stroud et al., 2001), the southeastern U. S. (Bertman et al., 1995), Summit, Greenland (Swanson et al., 2003), Ontario, Canada (Shepson et al., 1993), Alert NW Territories, Canada (Muthuramu et al., 1994), and Chebogue Point, Nova Scotia (Roberts et al., 1998).

One possible explanation for the seasonal variation of alkyl nitrates at TF is their different tropospheric lifetimes throughout the year reflecting changes in photochemical production and/or destruction (OH oxidation and photolysis) rates. Lifetimes are shorter in summer than in winter (Table 3.3) because of higher OH concentrations and faster photolysis rates which may explain the lower C₃-C₅ alkyl nitrate mixing ratios. In addition, weaker photochemical activity may contribute to the low MeONO₂ and EtONO₂ variability in winter (Figures 3.2, 3.3; Tables 3.1, 3.2). Another possible explanation for

the seasonal trend is changes in the dominant source regions and regional scale transport pathways. Previous research has documented that the chemical composition of air masses transported to New England strongly depends on both the season and source region. For example, north-northwesterly winds typically transport clean, Canadian air masses to New England that contain low O₃, CO, NO_y, and hydrocarbon mixing ratios and that are representative of background conditions (Munger et al., 1996; Moody et al., 1998; Shipham et al., 1998). This transport pattern is more frequent during the winter and often occurs behind a cold front. Air masses containing enhanced levels of anthropogenic emissions are primarily observed during transport from the south and west which occurs most frequently in summer and when New England is on the western side of a high pressure system after it has moved offshore or in the warm sector of an approaching low pressure system (Moody et al., 1998; Fischer et al., 2004; Mao and Talbot, 2004b). Consequently, the greater frequency of northwesterly winds in winter and southerly winds in summer may also contribute to the seasonal trends by influencing the dominant source region(s) of alkyl nitrates and their precursors transported to TF.

3.3.2 Diurnal Variation

The chemical and physical processes controlling the atmospheric distribution of alkyl nitrates can be elucidated through examination of their diurnal trends. During both winter and summer 2002, the hourly average alkyl nitrate mixing ratios steadily decreased overnight, reached minimum levels at ~05:00-07:00 (local time), increased throughout the morning, and reached peak levels at approximately noon (Figure 3.4). The morning increase likely reflects a combination of vertical mixing, advection, and photochemical production. This is supported by comparison to the O₃, wind speed, and

J_{NO_2} diurnal cycles (Figure 3.4). Following sunrise, surface heating causes the nocturnal boundary layer (NBL) to dissipate and air masses from the residual layer above the NBL are mixed toward the surface resulting in increased O_3 and alkyl nitrate mixing ratios.

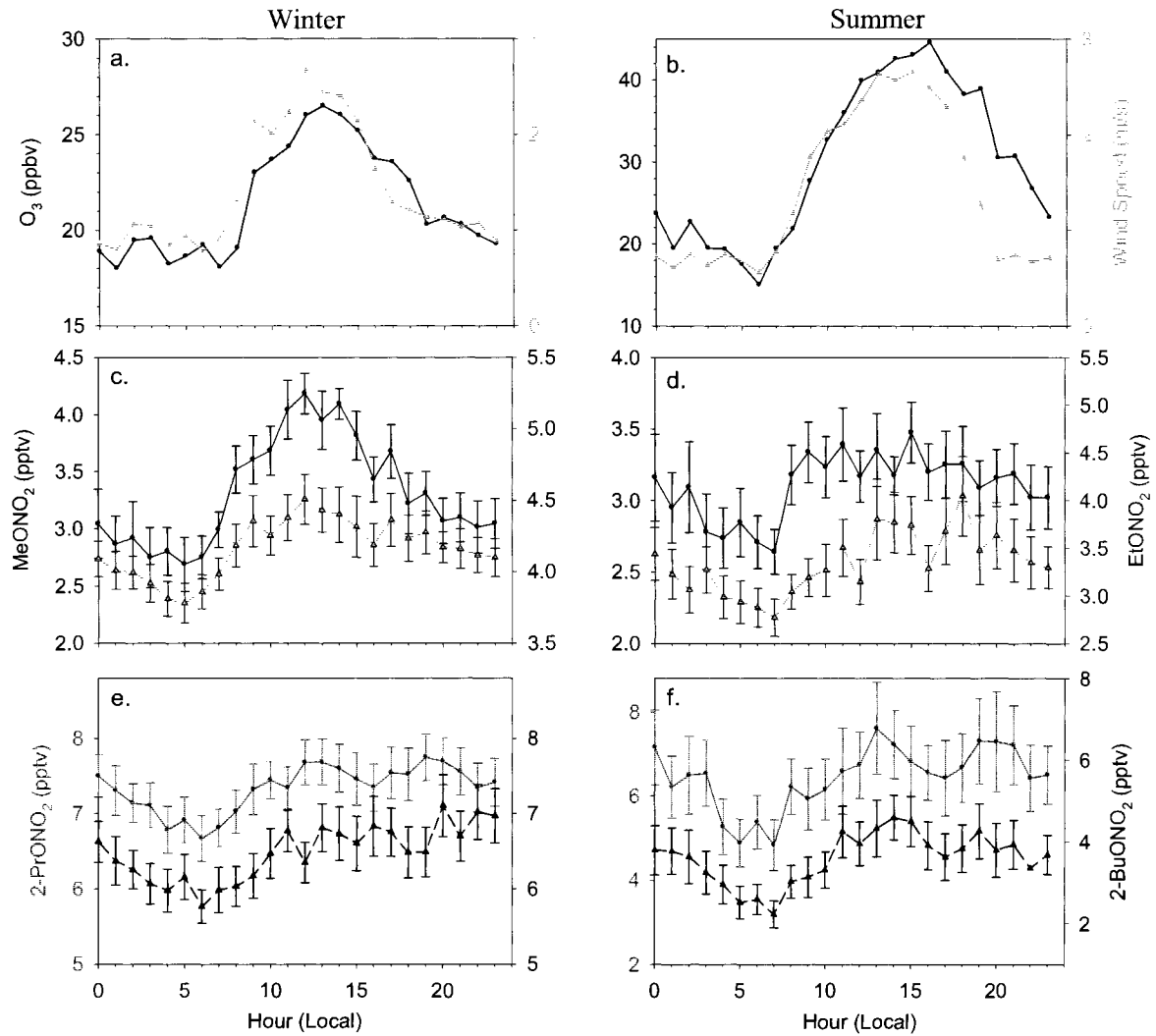


Figure 3.4. Hourly average (local time) (a) and (b) O_3 (ppbv), wind speed (m/s), and J_{NO_2} (yellow shaded curve), (c) and (d) MeONO_2 (black left axes) and EtONO_2 (pink right axes) (ppbv), (e) and (f) 2-PrONO_2 (green left axes) and 2-BuONO_2 (blue right axes) (ppbv) in winter (left column) and summer (right column) 2002 at Thompson Farm. Error bars in 3.4c-f are the standard error.

The lifetimes of the C₁-C₅ alkyl nitrates due to the known removal mechanisms (photolysis and reaction with OH) are longer than one day, which suggests that their mixing ratios should be relatively constant over the course of a day (Table 3.3). However, the decrease in mixing ratios throughout the night indicates that removal processes occurring on a time scale ≤ 1 day were dominant. Processes potentially contributing to the early morning minima include losses from chemistry, deposition, decomposition, or mixing with air masses having lower mixing ratios. The rates of reaction with oxidants potentially available at night, such as O₃ and the nitrate radical (NO₃), are insignificant for alkyl nitrates (Becker and Wirtz, 1989; Atkinson, 1990); thus chemical reactions can be neglected. Decomposition can be ignored because alkyl nitrates are thermally stable at tropospheric temperatures (Roberts, 1990). Additionally, it is typically thought that alkyl nitrates do not undergo wet and dry deposition because of their low solubility (e.g., Roberts, 1990, Shepson et al., 1996). However, wet deposition of alkyl nitrates has been reported in some studies (e.g., Hauff et al., 1998). Moreover, Henry's Law constants of the C₁-C₅ alkyl nitrates (~ 0.5 - 2.6 M/atm) (Luke et al., 1989; Kames and Schurath, 1992) are similar to peroxyacyl nitrates (1-5 M/atm) and higher than O₃ (~ 0.01 M/atm) (Kames and Schurath, 1992; Sander, 1999). Both PAN and O₃ are well known to undergo surface deposition (e.g., Schrimpf et al., 1996; Finkelstein et al., 2000; Sparks et al., 2003). Transport or mixing may play a role in regulating nighttime ambient mixing ratios. However, the observation of decreasing alkyl nitrate mixing ratios on nights with calm winds and stable inversion layers is indicative of a process besides advection or vertical mixing of different air masses (see below). Therefore, it seems likely that deposition contributed to the alkyl nitrate diurnal behavior at TF.

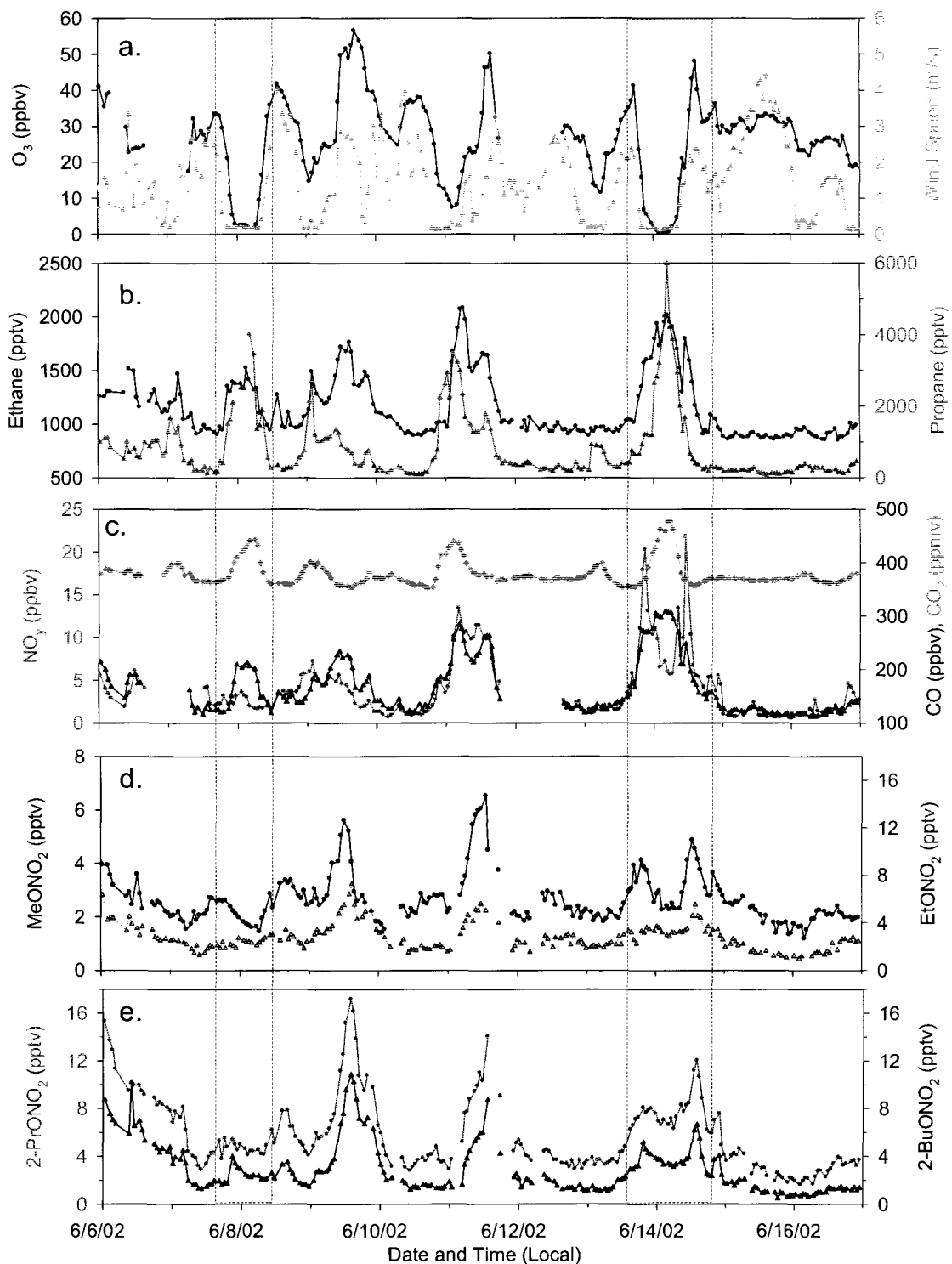


Figure 3.5. Time series of (a) O_3 (ppbv) and wind speed (m/s), (b) ethane and propane (pptv), (c) NO_y (ppbv), CO (ppbv), and CO_2 (ppmv), (d) MeONO₂ and EtONO₂, and (e) 2-PrONO₂ and 2-BuONO₂ (pptv) at TF during June 6-16, 2002. Dry deposition of alkyl nitrates was observed on the nights of June 8 and 14 (between the dashed lines).

Detailed analysis of two nights during June 2002 provides evidence for the surface deposition of alkyl nitrates. On the evenings of June 7 and 13, 2002, O₃ decreased to ≤ 3 ppbv and the wind speed was near zero (Figure 3.5a). Ozone and wind speed remained at these levels through ~07:00 on June 8 and 14 indicating that a stable nocturnal inversion layer had developed. Under these stable and calm conditions, the surface air is isolated from the air in the remnant boundary layer aloft which inhibits vertical mixing and advection (e.g., Hastie et al., 1993; Gusten et al., 1998; Talbot et al., 2005). Therefore, variations in trace gas mixing ratios reflect local sources or sinks. This is illustrated by the large increase in carbon monoxide (CO), carbon dioxide (CO₂), and NMHC mixing ratios on both nights resulting from local liquefied petroleum, natural gas, vehicular, or combustion emissions (e.g., Talbot et al., 2005; White et al., 2008) (plant respiration also contributes to the increase in CO₂) (Figures 3.5b,c). Additionally, NO_y decreased (Figure 3.5c) mainly due to wet and dry deposition of HNO₃ and NO₂ (e.g., Munger et al., 1998). Furthermore, on both nights, each of the C₁-C₅ alkyl nitrates decreased, maintained nearly constant mixing ratios for several hours, and increased in the morning concurrently with O₃ and wind speed (Figures 3.5d, e).

The diurnal variation of the light alkyl nitrates at TF provides evidence for a previously unaccounted for removal mechanism from the atmosphere and for a potential additional source of organic nitrogen to the surface. The flux from the atmosphere to the surface and the dry deposition velocities (V_d) of the alkyl nitrates were estimated as follows:

$$\text{Flux} = \left[\frac{dC}{dt} \right] \times H = -C \times V_d \quad (7)$$

where C is the mean alkyl nitrate concentration (molecules cm^{-3}) between 00:00-06:00, H is the nocturnal boundary layer height, and $[dC/dt]$ is the change in alkyl nitrate concentration between 0:00-06:00. The resulting dry deposition flux and velocity estimates strongly depend on the value chosen for the boundary layer height which varies with meteorological conditions and season. In these calculations, we used $H=125$ m because it is a typical nocturnal boundary layer height for this site (e.g., Talbot et al., 2005; Sive et al., 2007; Mao et al., 2008; White et al., 2008; Zhou et al., 2008; Russo et al., 2009).

The deposition rates of the individual alkyl nitrates were estimated to range from -0.1 to $-1.8 \text{ nmol m}^{-2} \text{ hr}^{-1}$, and the dry deposition velocities were 0.04 to 0.26 cm s^{-1} (Table 3.3). The dry deposition rates and velocities were slightly higher in summer than in winter. These dry deposition flux and velocity values are at the lower end of estimates compared to other organic nitrogen compounds at North American sites. For example, dry deposition velocities were estimated to be 0.65 cm s^{-1} for isoprene nitrates (Giacopelli et al., 2005), 0.4 cm s^{-1} for hydroxyalkyl nitrates (Shepson et al., 1996), and 0.1 to 0.6 cm s^{-1} for PAN (Shepson et al., 1992; Schrimpf et al., 1996; Sparks et al., 2003; Doskey et al., 2004; Turnipseed et al., 2006; Wolfe et al., 2009). Nighttime V_d values for MPAN and PPN ranging from ~ 0.1 to 0.7 cm s^{-1} and fluxes of ~ 10 to $50 \text{ nmol m}^{-2} \text{ hr}^{-1}$ have been observed over pine forests (Turnipseed et al., 2006; Wolfe et al., 2009). Furthermore, the lifetimes ($\tau_d = H/V_d$) of each alkyl nitrate due to dry deposition at TF were estimated to range from 0.6 to 3 days (Table 3.3). These lifetimes are shorter than the ones derived from OH oxidation and photolysis combined.

	Winter					Summer				
	Flux	r^2	V_d	τ_d	$\tau_{OH+IRONO_2}$	Flux	r^2	V_d	τ_d	$\tau_{OH+IRONO_2}$
MeONO ₂	-0.27 ± 0.07	0.74	0.06 ± 0.02	2.4	38	-0.38 ± 0.11	0.70	0.08 ± 0.03	1.8	5
EtONO ₂	-0.27 ± 0.06	0.82	0.04 ± 0.01	3.4	28	-0.47 ± 0.11	0.78	0.09 ± 0.03	1.5	6
2-PrONO ₂	-0.72 ± 0.10	0.92	0.06 ± 0.01	2.3	16	-1.8 ± 0.48	0.74	0.19 ± 0.09	0.8	4
1-PrONO ₂	-0.14 ± 0.03	0.78	0.07 ± 0.02	2.2	16	-0.30 ± 0.09	0.67	0.16 ± 0.07	0.9	4
2-BuONO ₂	-0.37 ± 0.05	0.91	0.09 ± 0.02	1.6	13	-1.4 ± 0.16	0.93	0.26 ± 0.13	0.6	4
3-PenONO ₂	-0.27 ± 0.04	0.91	0.10 ± 0.02	1.5	8	-0.46 ± 0.16	0.62	0.23 ± 0.16	0.6	3
2-PenONO ₂	-0.41 ± 0.05	0.93	0.11 ± 0.03	1.3	11	-0.70 ± 0.21	0.69	0.24 ± 0.16	0.6	2
Σ RONO ₂	-2.9 ± 0.37	0.93	0.09 ± 0.01	1.7		-5.3 ± 1.0	0.85	0.18 ± 0.07	0.8	

Table 3.3. Dry deposition fluxes ± standard error ($\text{nmol m}^{-2} \text{hr}^{-1}$), velocities ± standard error (V_d) (cm s^{-1}), and lifetimes (days) ($\tau_d = H/V_d$) of alkyl nitrates during winter and summer 2002 at TF. Fluxes were calculated from the linear regression between the change in hourly average alkyl nitrate mixing ratios versus time (00:00-06:00, EDT). r^2 is the correlation coefficient of this regression. Values used for calculating the photolysis and oxidation lifetimes ($\tau_{OH+IRONO_2}$) are given in Table 3.5.

The TF results support previous research conducted at Harvard Forest (HF) (a temperate deciduous forest ~110 km southwest of TF) which concluded that the deposition of unmeasured organic nitrogen compounds could explain discrepancies between total NO_y and the sum of speciated NO_y compound measurements (Munger et al., 1996, 1998; Lefter et al., 1999; Horii et al., 2004, 2006). Additionally, studies conducted at several sites throughout Canada found that “Other-NO_y” compounds (i.e., excluding HNO₃, NO₂, pNO₃⁻, PAN, PPN) contributed 9-38% to NO_y dry deposition (Zhang et al., 2009). Based on the summer flux estimates for TF, ΣRONO₂ (~5 nmol m⁻² hr⁻¹ ~ 0.16 g N m⁻² yr⁻¹) constituted a non-negligible amount (~1-6%) of the “Other-NO_y” deposition rates at the two Canadian sites closest to TF (Frelighsburg, Quebec ~400 km northwest and Kejimikujik, Nova Scotia ~500 km northeast) (Zhang et al., 2009). While these results suggest that the dry deposition of C₁-C₅ alkyl nitrates is not necessarily a major source of nitrogen to the surface, they do provide evidence that unaccounted for reactive nitrogen compounds contribute to NO_y deposition, and this may be an important loss process at night when photolysis and oxidation are not occurring.

3.4 Sources of Alkyl Nitrates in Coastal New England

The following discussion uses a combination of four separate VOC data sets, which are representative of three different environments, in order to identify the major source(s) of alkyl nitrates in southeastern New Hampshire by comparing their temporal and/or spatial distributions to characteristic source signatures and to NMHC and halocarbon trends.

3.4.1 Inland/Coastal Environment: Thompson Farm

The predominant source region and regional transport pathway of air masses to TF varies with season as discussed in section 3.3.1. In order to determine whether the alkyl nitrate mixing ratios observed at TF depend upon the source region, the hourly average wind direction data from winter and summer 2002 was separated into four sectors (northeast (0-90°), southeast (90-180°), southwest (180-270°), and northwest (270-360°)). In winter, mixing ratios were fairly uniform in the SW, NW, and NE sectors but were significantly higher ($p < 0.05$) in the SE sector, while in summer, the mean mixing ratios in both the SE and SW sectors were significantly higher ($p < 0.001$) than in the northern sectors (Table 3.4). It is not unexpected that enhanced mixing ratios would be observed during transport from the SE. Previous studies have shown that air masses that passed over east coast metropolitan areas and over the Atlantic Ocean can be transported inland to TF from the south-southeast by the sea breeze (Miller et al., 2003; Angevine et al., 2004; Mao and Talbot, 2004a; Zhou et al., 2008). Furthermore, in both seasons, the highest and lowest mean parent hydrocarbon (ethane, propane, n-butane, n-pentane) mixing ratios were observed in the southern and northern transport sectors, respectively (not shown). This suggests that a major source region of NMHCs was the urban/industrial regions to the west-southwest of New England. In addition, this points toward a continental source of alkyl nitrates which was most likely secondary production following the oxidation of hydrocarbons. Moreover, the highest mixing ratios of alkyl nitrates corresponded to events with enhanced mixing ratios of NMHCs and carbon monoxide. For example, the highest C₂-C₅ alkyl nitrate mixing ratios during winter 2002 were observed on February 7 under west-southwesterly winds (Figure 3.2). Concurrent

with the high alkyl nitrates were enhanced (above 90th percentile for winter) mixing ratios of CO (370-750 ppbv), ethane (4-7.2 ppbv), propane (5.7-11 ppbv), n-butane (1-3.7 ppbv), and n-pentane (0.3-0.5 ppbv).

	Winter			
	NE	SE	SW	NW
MeONO ₂	3.6 ± 0.2	4.2 ± 0.2	3.2 ± 0.1	2.9 ± 0.1
EtONO ₂	4.2 ± 0.1	4.7 ± 0.1	4.0 ± 0.04	4.0 ± 0.1
2-PrONO ₂	7.3 ± 0.2	7.9 ± 0.1	7.1 ± 0.1	7.4 ± 0.1
1-PrONO ₂	1.5 ± 0.05	1.5 ± 0.03	1.3 ± 0.02	1.4 ± 0.02
2-BuONO ₂	6.4 ± 0.3	7.0 ± 0.1	6.3 ± 0.1	6.5 ± 0.1
3-PenONO ₂	1.8 ± 0.1	1.9 ± 0.04	1.7 ± 0.03	2.3 ± 0.05
2-PenONO ₂	2.4 ± 0.1	2.6 ± 0.1	2.3 ± 0.1	2.3 ± 0.1
ΣRONO ₂	26.2 ± 1.0	29.0 ± 0.6	25.5 ± 0.4	25.8 ± 0.5

	Summer			
	NE	SE	SW	NW
MeONO ₂	2.4 ± 0.1	3.2 ± 0.1	3.4 ± 0.1	2.7 ± 0.1
EtONO ₂	2.6 ± 0.1	3.5 ± 0.1	3.6 ± 0.1	2.9 ± 0.1
2-PrONO ₂	4.2 ± 0.3	6.9 ± 0.4	7.3 ± 0.3	5.1 ± 0.3
1-PrONO ₂	1.0 ± 0.1	1.3 ± 0.1	1.4 ± 0.1	1.0 ± 0.1
2-BuONO ₂	2.1 ± 0.2	3.9 ± 0.2	4.2 ± 0.2	2.8 ± 0.2
3-PenONO ₂	0.7 ± 0.1	1.5 ± 0.1	1.6 ± 0.1	1.0 ± 0.1
2-PenONO ₂	0.9 ± 0.1	2.2 ± 0.2	2.5 ± 0.1	1.4 ± 0.1
ΣRONO ₂	13.3 ± 0.7	21.6 ± 1.0	22.6 ± 0.8	16.1 ± 0.9

Table 3.4. Mean (± standard error) mixing ratios of alkyl nitrates (pptv) in the northeast (NE, 0-90°), southeast (SE, 90-180°), southwest (SW, 180-270°), and northwest (NW, 270-360°) transport sectors during winter (top) and summer (bottom) 2002.

The dominant and consistent contribution of 2-PrONO₂ and 2-BuONO₂ to ΣRONO₂ at TF over various years and time scales further corroborates that their major source was photochemical production from propane and n-butane (Tables 3.1 and 3.2). Both 2-PrONO₂ and 2-BuONO₂ have been found to be the most abundant alkyl nitrates at numerous continental locations (Ridley et al., 1990; Shepson et al., 1993; Ostling et al., 2001; Stroud et al., 2001; Blake et al., 2003b; Swanson et al., 2003; Simpson et al., 2003; 2006). This characteristic continental source signature reflects a balance between the increasing alkyl nitrate yield and the decreasing lifetimes of both the parent alkane and alkyl nitrate with increasing carbon number (Atkinson et al., 1982; Flocke et al., 1991; 1998; Arey et al., 2001). In contrast, in remote oceanic regions, the C₁-C₃ alkyl nitrates have been found to be supersaturated (Chuck et al., 2002; Dahl et al., 2005) and positively correlated with marine halocarbons (Atlas et al., 1993; Blake et al., 1999, 2003a). Additionally, oceanic emissions of MeONO₂ were estimated to be a factor of ~3-4 larger than EtONO₂ in the Pacific (Blake et al., 2003a; Dahl et al., 2007) and Atlantic Oceans (Chuck et al., 2002). Although TF is often influenced by marine air masses originating from the SE and NE (Zhou et al., 2005; 2008), MeONO₂ and EtONO₂ were not correlated with marine halocarbons, and the year-round MeONO₂/EtONO₂ ratio averaged ~1. This suggests that the MeONO₂ and EtONO₂ levels observed in seacoast New Hampshire were controlled by anthropogenic precursor source(s).

Furthermore, the C₃-C₅ alkyl nitrates were strongly correlated with each other in both winter and summer 2002 ($r^2 \sim 0.7-0.9$), and in all seasons throughout 2004-2008 ($r^2 \sim 0.60-0.96$). Ethyl nitrate exhibited slightly weaker correlations with the C₃-C₅ alkyl nitrates ($r^2 \sim 0.4-0.8$). In winter, MeONO₂ was poorly correlated with the other alkyl

nitrates, whereas in summer 2002 and spring-fall 2004-2008, MeONO₂ was moderately correlated with the C₂-C₅ compounds ($r^2 \sim 0.3-0.6$). The weaker MeONO₂ and EtONO₂ correlations may be a consequence of their longer lifetimes or different sources. In addition, the C₁-C₅ alkyl nitrates tracked each other extremely well (Figures 3.2 and 3.3) reflecting their similar and/or collocated precursor sources.

3.4.2 Marine Environment: Measurements onboard the NOAA R/V *Ronald H. Brown*

Measurements of MeONO₂, 2-PrONO₂, and 2-BuONO₂ were made from ambient air and surface seawater samples collected onboard the NOAA R/V *Ronald H. Brown* during July 30-August 6, 2002 as a component of the NEAQS 2002 campaign. Sampling occurred in Boston Harbor on 30-31 July and off the coast of New Hampshire from 1-6 August. 2-Propyl and 2-butyl nitrate were well correlated in air ($r^2 = 0.97$) and were positively, but weakly ($r^2 \sim 0.34$), correlated with MeONO₂ indicating that the alkyl nitrates shared a common source. In the air samples, MeONO₂, 2-PrONO₂, and 2-BuONO₂ ranged from 2-8, 4-30, and 2-16 pptv, respectively (Figures 3.6a, c; 2-BuONO₂ not shown). In contrast, 2-PrONO₂ and 2-BuONO₂ mixing ratios in the surface seawater were lower and more uniform (9-13 pptv $\sim 0.008-0.017$ nmol L⁻¹ and 2-5 pptv $\sim 0.002-0.006$ nmol L⁻¹, respectively) (Figure 3.6d). Methyl nitrate was more variable in the seawater but exhibited a similar range of mixing ratios (1-6 pptv $\sim 0.007-0.051$ nmol L⁻¹) as in the air samples (Figure 3.6b). These results suggest that the New England coastal waters were undersaturated in 2-PrONO₂ and 2-BuONO₂ and that MeONO₂ was near equilibrium with respect to the overlying atmosphere. These results are consistent with Chuck et al. (2002) and Reeves et al. (2007) who proposed that alkyl nitrates in northern hemisphere temperate waters were near equilibrium with the atmosphere. Similar to the

TF results (section 3.4.1), this limited data set from the Gulf of Maine during NEAQS 2002 does not provide conclusive evidence for a marine source of light alkyl nitrates in this region.

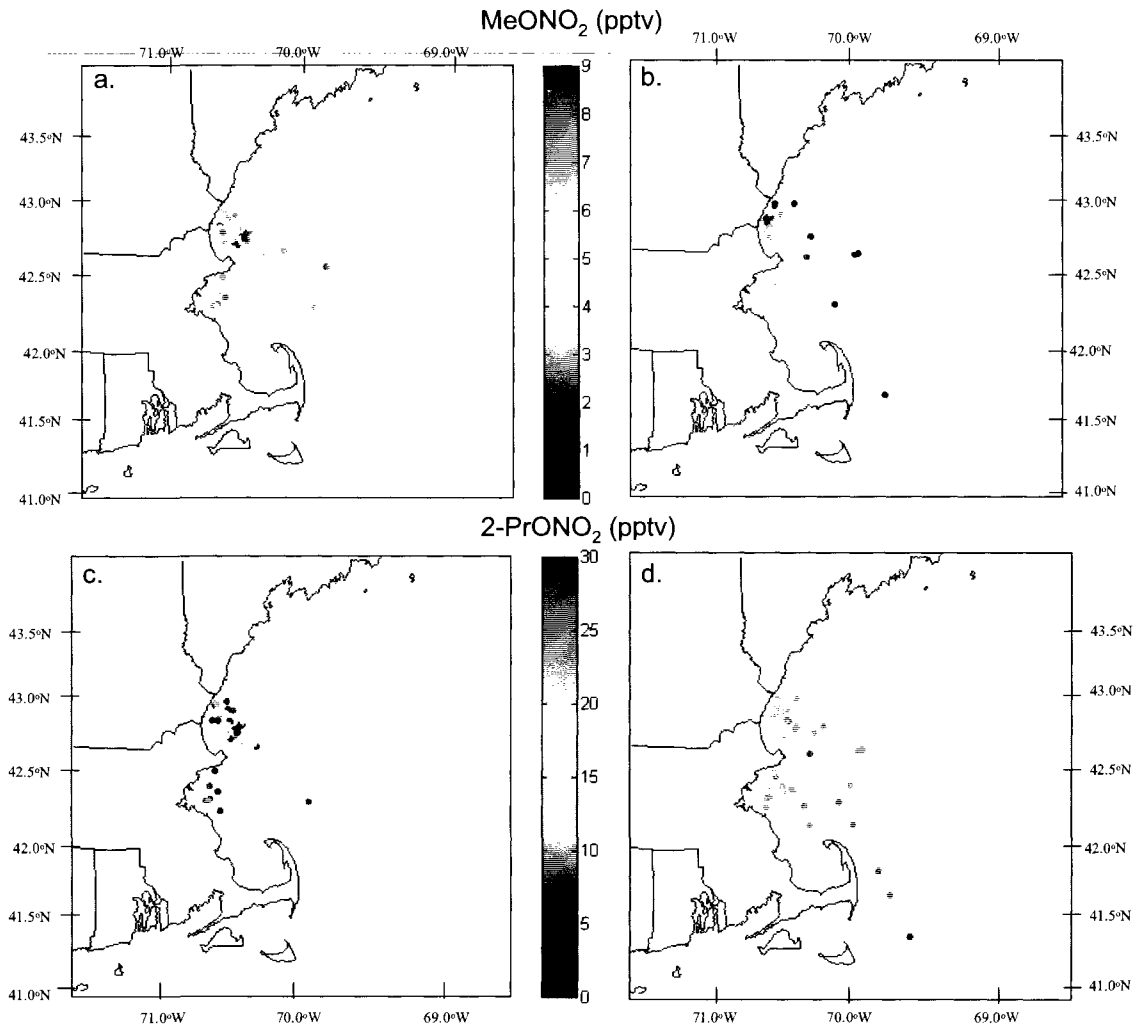


Figure 3.6. (a) Ambient air and (b) surface seawater mixing ratios of MeONO₂ (pptv), and (c) ambient air and (d) surface seawater mixing ratios of 2-PrONO₂ from samples collected in the Gulf of Maine throughout July 30-August 6, 2002 onboard the NOAA R/V *Ronald H. Brown* during NEAQS 2002

3.4.3 Estuarine Environment: Great Bay Experiment

An intensive study focused on examining the spatial variability and sources of VOCs throughout the Great Bay estuary in seacoast New Hampshire was conducted from 18:00 August 18 to 19:00 August 19, 2003 (local time) (Figure 2.1 inset). At TF, winds were from the south-southeast from noon on August 18 until early morning on August 19 when they shifted to the west-northwest (Figure 3.7b). Three day back trajectories obtained from the NOAA HYSPLIT model (Draxler and Rolph, 2003) showed that air masses originated in eastern Canada and traveled along the Maine coastline before reaching NH from the east on the evening of August 18. Furthermore, a strong nocturnal inversion layer developed between midnight and 07:00 on August 19 as demonstrated by decreases in O₃ and wind speed and by an increase in carbon dioxide (Figures 3.7a, b).

The mixing ratios of each alkyl nitrate were remarkably uniform across the five sampling locations (Figures 3.7c-i). The standard deviation of the mixing ratios at all five sites each hour was ≤ 0.2 pptv for MeONO₂, EtONO₂, 1-PrONO₂, 2-PenONO₂, and 3-PenONO₂ and ≤ 0.5 pptv for 2-PrONO₂ and 2-BuONO₂. The lack of a spatial variation in mixing ratios and a correlation with marine derived compounds suggests that the source(s) of the alkyl nitrates was not associated with coastal emissions. In contrast, the marine halocarbons (bromoform (CHBr₃), dibromomethane (CH₂Br₂), methyl iodide (CH₃I), and ethyl iodide (C₂H₅I)) exhibited a distinct spatial variation with higher mixing ratios at coastal sites (FC, WHF) compared to inland sites (TF, Pease, Exeter) (Zhou et al., 2005). For example, the elevated mixing ratios of CHBr₃ (>10 pptv) reflect the influence of local coastal and estuarine emissions on the evening of August 18 (Figure 3.7j). Additionally, NMHC mixing ratios increased significantly under the nocturnal

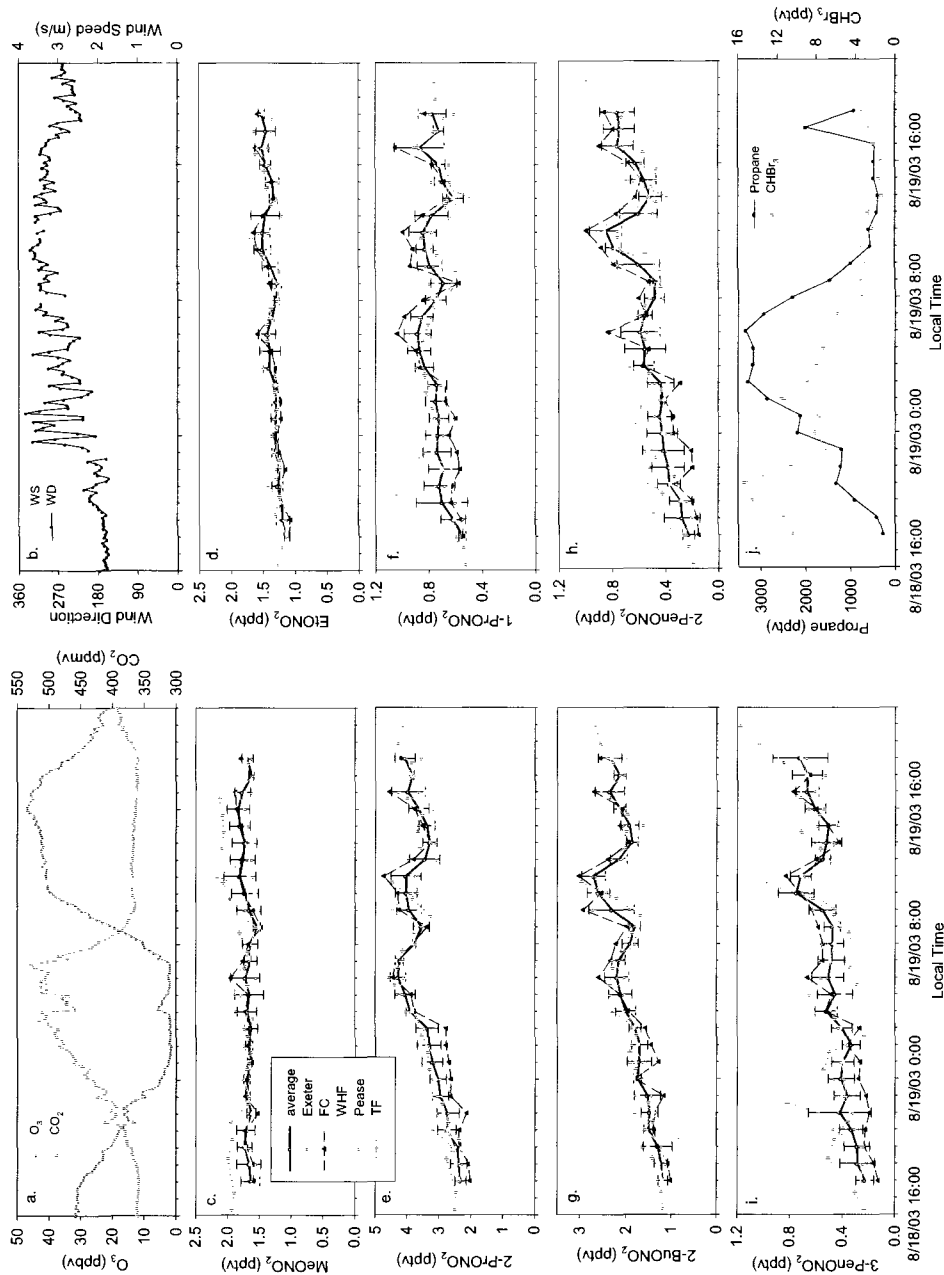
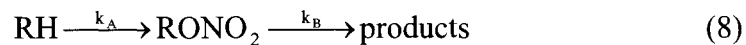


Figure 3.7. (a) 10 minute average O_3 (ppbv) and CO_2 (ppmv) mixing ratios and (b) wind speed (m/s), wind direction, and J_{NO_2} (yellow shaded curve) at Thompson Farm from August 18 at 16:00 to August 19, 2003 at 22:00 (local time). Alkyl nitrate mixing ratios (pptv) at four sites throughout the Great Bay estuary and at Thompson Farm: (c) $MeONO_2$, (d) $EtONO_2$, (e) $2-PrONO_2$, (f) $1-PrONO_2$, (g) $2-BuONO_2$, (h) $2-PeONO_2$, (i) $3-PeONO_2$, and (j) hourly average propane and $CHBr_3$ mixing ratios (pptv) for the five sampling sites. (c)-(i) The black line is the average \pm standard deviation mixing ratio of all 5 sites each hour.

boundary layer at each sampling location and decreased rapidly following the breakup of the inversion layer in the morning (White et al., 2008) (Figure 3.7j). The slightly increasing alkyl nitrate mixing ratios on August 19 likely reflect processed continental emissions and/or the downward mixing of air from above the inversion layer in the morning. Overall, the different temporal and spatial distributions of the alkyl nitrates throughout the Great Bay estuary compared to tracers of anthropogenic and marine emissions is further evidence for their dominant secondary source.

3.5 Alkyl Nitrate/Parent Hydrocarbon Ratio Relationships

In the previous section, the analysis of four distinct data sets indicated that the dominant source of alkyl nitrates in the seacoast region of New Hampshire was photochemical production from hydrocarbons. Accordingly, the relationships with the parent hydrocarbons were further examined using a sequential reaction scheme. The production and loss reactions of alkyl nitrates summarized in equations (1)-(6) can be simplified as follows by assuming that reaction (1) between the parent hydrocarbon and OH is the rate-limiting step:



The simplified kinetic equations lead to a differential equation, whose solution is a function only of time, and can thus be integrated to yield equation (9) (see Bertman et al., 1995 for details on the derivation of equation (9)):

$$\frac{[\text{RONO}_2]}{[\text{RH}]} = \frac{\beta k_A}{(k_B - k_A)} (1 - e^{(k_A - k_B)t}) + \frac{[\text{RONO}_2]_o}{[\text{RH}]_o} e^{(k_A - k_B)t} \quad (9)$$

where $k_A = k_1[\text{OH}]$, $k_B = k_6[\text{OH}] + J_5$, $\beta = \alpha_1 \alpha_4$, and $[\text{RONO}_2]_o / [\text{RH}]_o$ is the initial alkyl nitrate/parent hydrocarbon ratio (see Tables 3.3 and 3.5 for parameter values). If

$[\text{RONO}_2]_0/[\text{RH}]_0=0$, the solution to the equation describes the time evolution of the alkyl nitrate/parent hydrocarbon (RONO_2/RH) ratio based solely on gas phase hydrocarbon chemistry (Bertman et al., 1995). Previous studies typically assumed that the initial alkyl nitrate mixing ratio is zero (Bertman et al., 1995; Roberts et al., 1998; Stroud et al., 2001; Simpson et al., 2003), while more recent studies included analyses using non-zero initial ratios (Reeves et al., 2007). Some studies have also attempted to quantify the influence of additional hydrocarbon precursors (e.g., Sommariva et al., 2008).

In order to examine the relationships between alkyl nitrates and their parent hydrocarbons, we compared the observed RONO_2/RH ratios to the values calculated when the initial $[\text{RONO}_2]_0/[\text{RH}]_0$ ratio equaled zero (pure photochemistry curve), the mean, and the background (10th percentile) ratio values at TF during winter and summer 2002 (Figure 3.8, Table 3.5). Also included in Figure 3.8 are the mean RONO_2/RH ratios from samples collected at several remote sites along the U.S. west coast (34-47°N) during December 2001 and June 2002 (unpublished data, D. Blake, UCI). These samples are representative of background air masses and generally agree with the highest TF RONO_2/RH ratios (i.e., more aged air masses) in winter. The lower summer ratios at TF, compared to the west coast, likely reflect the influence of more recent emissions and higher parent hydrocarbon mixing ratios because of the closer proximity to anthropogenic sources. In fact, the samples collected on nights with a stable NBL, and thus representing local NMHC emissions and low RONO_2/RH ratios, largely correspond to the points on the lower left of the plots at the most recent processing times. In both winter and summer, air mass ages ranging from several hours to 5 days were observed at TF.

	k_1^a	α_1^b	α_4	$k_6^{f,g}$	J_5		$[\text{RONO}_2]_0/[\text{RH}]_0$	
					Winter	Summer	Winter	Summer
MeONO ₂	0.0064			0.23	0.29 ^l	2.2 ^j		
EtONO ₂	0.24	1	0.006 ^c	1.8	0.33 ^h	1.5 ⁱ	0.002 (0.001)	0.003 (0.002)
2-PrONO ₂	1.1	0.7	0.039 ^d	2.9	0.43 ^h	1.6 ⁱ	0.004 (0.002)	0.012 (0.002)
1-PrONO ₂	1.1	0.3	0.02 ^e	5.8	0.58 ^h	2.2 ⁱ	0.0004 (0.0002)	0.003 (0.0004)
2-BuONO ₂	2.3	0.86	0.084 ^d	8.6	0.48 ⁱ	1.1 ^k	0.013 (0.005)	0.039 (0.01)
3-PenONO ₂	3.8	0.35	0.126 ^d	11	0.47 ⁱ	1.2 ^k	0.008 (0.004)	0.016 (0.003)
2-PenONO ₂	3.8	0.55	0.106 ^d	19	0.45 ⁱ	1.2 ^k	0.011 (0.006)	0.023 (0.003)

References: ^aAtkinson et al. (2006a); ^bKwok and Atkinson (1995); ^cRanschaert et al. (2000); ^dArey et al. (2001); ^eAtkinson et al. (1987); ^fAtkinson, 2003; ^gAtkinson, 1990; ^hClemmishaw et al. (1997); ⁱSimpson et al. (2003); ^jRoberts, (1990); ^kBertman et al. (1995); ^lMeONO₂ winter photolysis rate from http://cprm.acd.ucar.edu/Models/TUV/Interactive_TUV.

Table 3.5. Values used in equation (9) to produce the predicted photochemical evolution curves in Figure 3.8. k_1 ($\times 10^{-12}$) and k_6 ($\times 10^{-13}$) are the rate constants ($\text{cm}^3 \text{ molecule}^{-1} \text{ s}^{-1}$) for the reactions between the parent hydrocarbon (1) and alkyl nitrate (6) with OH, respectively. α_1 and α_4 are the branching ratios of reactions (1) and (4) producing the alkyl peroxy radical and alkyl nitrate, respectively. J_5 ($\times 10^{-6} \text{ s}^{-1}$) is the alkyl nitrate photolysis rate constant. $[\text{RONO}_2]_0/[\text{RH}]_0$ is the initial alkyl nitrate/parent hydrocarbon ratio used in (9) and is equal to the seasonal mean (seasonal background) ambient ratios at TF. In Figures 3.8a-f, $[2\text{-BuONO}_2]_0/[\text{n-butane}]_0 =$ background ratio. In Figures 3.8g-j, $[2\text{-BuONO}_2]_0/[\text{n-butane}]_0 =$ mean ratios. $[\text{OH}] = 6 \times 10^5$ (winter) and 2×10^6 (summer) molecules cm^{-3} (Spivakovsky et al., 2000).

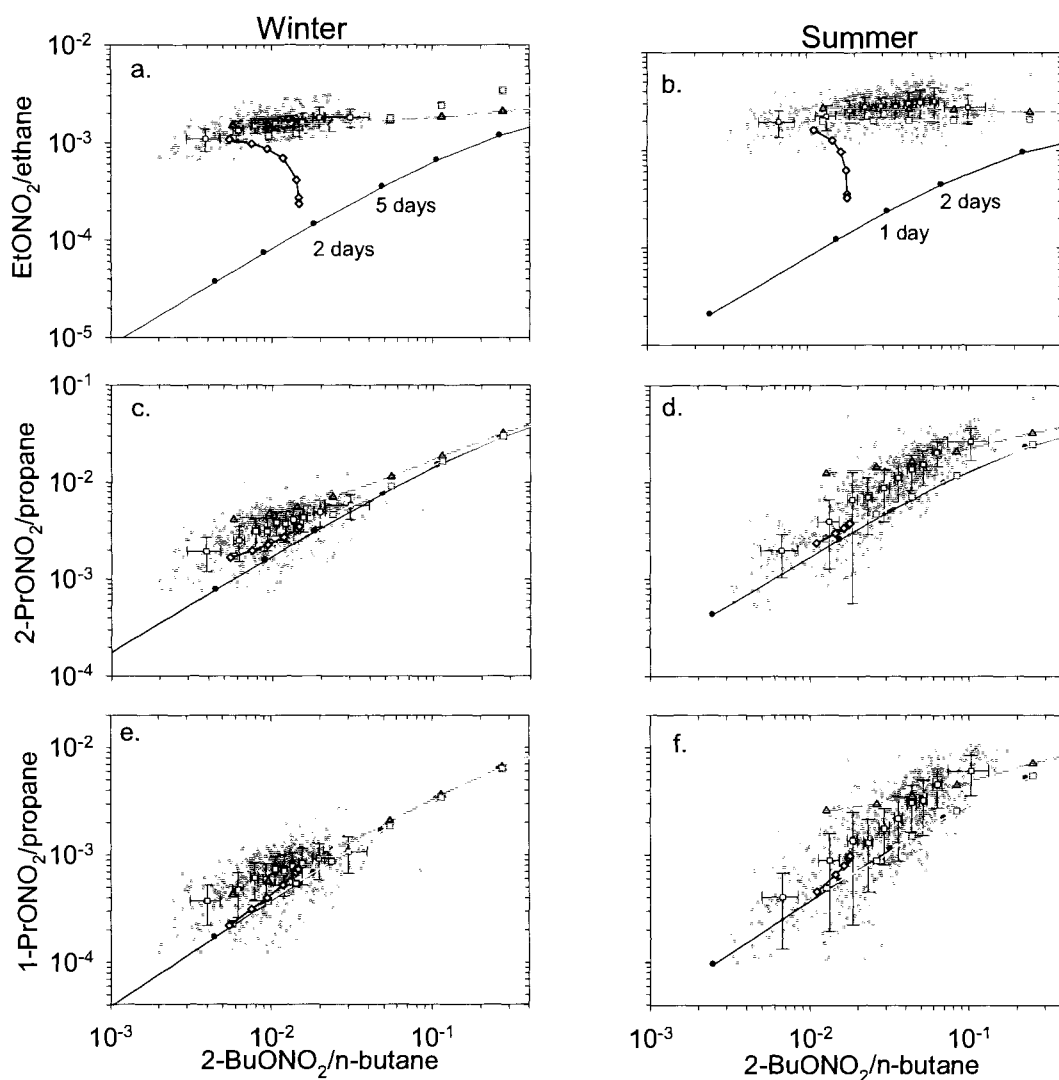


Figure 3.8. Alkyl nitrate/parent hydrocarbon ratios versus 2-BuONO₂/n-butane for winter (left) and summer (right) 2002: (a) and (b) EtONO₂/ethane, (c) and (d) 2-PrONO₂/propane, (e) and (f) 1-PrONO₂/propane, (g) and (h) 3-PenONO₂/n-pentane, and (i) and (j) 2-PenONO₂/n-pentane. The white squares are averages each containing 10% of the data. Error bars represent ± 1 standard deviation of the 2-BuONO₂/n-butane ratio in the x-direction and ± 1 standard deviation of the RONO₂/RH ratio in the y-direction. Solid black line and circles: $[\text{RONO}_2]_o/[\text{RH}]_o = 0$, the black dots correspond to the number of days since the parent alkane was emitted; (a-f) red dashed line with triangles: $[\text{RONO}_2]_o/[\text{RH}]_o = \text{seasonal mean}$ and $[\text{2-BuONO}_2]_o/[\text{n-butane}]_o = \text{seasonal background}$; green lines with squares: $[\text{RONO}_2]_o/[\text{RH}]_o$ and $[\text{2-BuONO}_2]_o/[\text{n-butane}]_o = \text{seasonal background}$; (g-j) pink dashed lines with diamonds: $[\text{PenONO}_2]_o/[\text{n-pentane}]_o = \text{seasonal background}$ and $[\text{2-BuONO}_2]_o/[\text{n-butane}]_o = \text{seasonal mean}$; blue lines with diamonds are curves calculated including background initial ratios and a dry deposition term. See Table 3.5 for initial ratio values. The yellow diamonds are RONO₂/RH ratios from samples collected at remote sites along the U. S. west coast in December 2001 and June 2002.

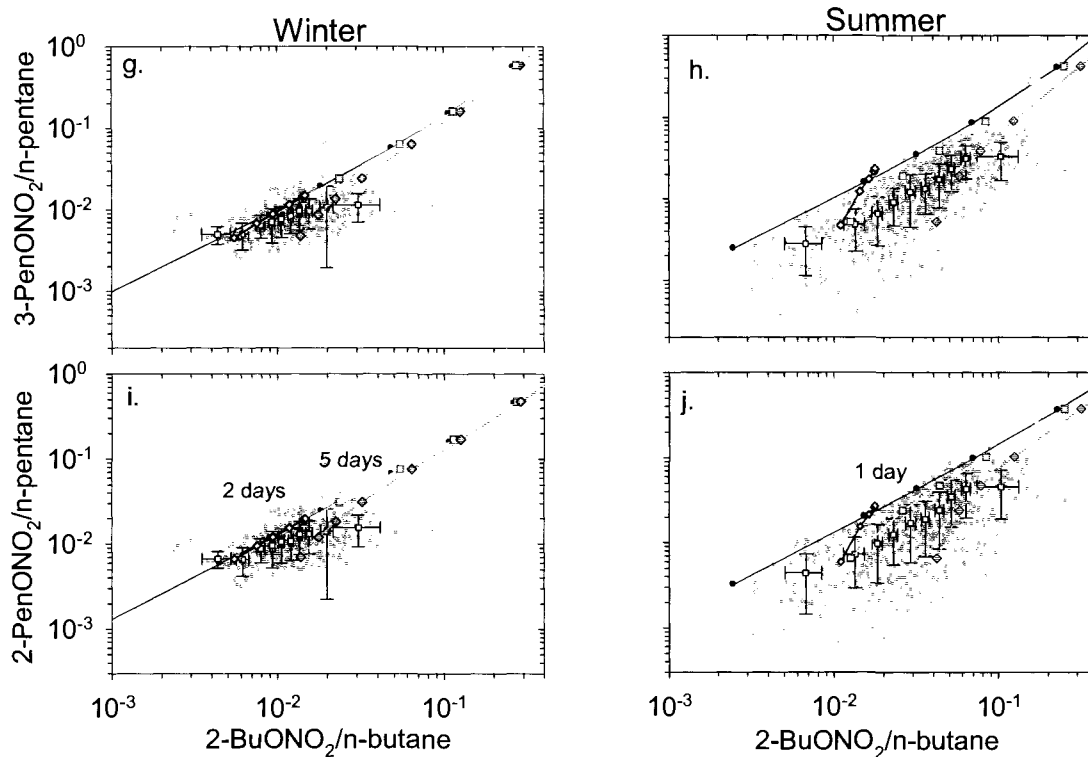


Figure 3.8 continued.

In both seasons, the $\text{EtONO}_2/\text{ethane}$ ratios were factors of ~ 5 - 10 above the pure photochemistry curve (Figures 3.8a,b). The trend toward the curve at the longest processing times is indicative of mixing with aged air masses containing lower ratios. Previous studies have also observed large deviations between predicted and observed $\text{EtONO}_2/\text{ethane}$ ratios (Bertman et al., 1995; Roberts et al., 1998; Simpson et al., 2003). The deviation has typically been interpreted as evidence of a primary source of EtONO_2 or of an additional source of the precursor ethyl peroxy radical from the decomposition of larger organic compounds, specifically alkoxy radicals (Bertman et al., 1995; Flocke et al., 1998). Interestingly, the mean and background initial ratio curves agreed with the TF observations very well in both the winter and summer over the entire range of measured

ratios (Figures 3.8a,b). Thus, the deviation from the zero initial ratio curve may reflect background EtONO₂/ethane ratios in the atmosphere because of the sufficiently long lifetimes of EtONO₂ and ethane (~1 month and several months, respectively, in winter and ~1 week and 1-2 months, respectively, in summer). Bertman et al. (1995) and Reeves et al. (2007) also found better agreement between observed and predicted EtONO₂/ethane ratios at short processing times when an initial ratio was used. It should be noted that these results do not rule out a potential contribution from direct emissions or additional precursor sources of EtONO₂. Rather, these results provide an additional explanation for the discrepancy between observed and predicted ratios.

The 2-PrONO₂/propane and 1-PrONO₂/propane ratios were factors of 2-3 higher than the pure photochemistry curve at the shortest processing times in winter and trended toward the curve at longer times (Figures 3.8c,e). In contrast, in summer, the propyl nitrate/propane ratios were factors of 0.5-0.9 above the pure photochemistry curve at all air mass ages (Figures 3.8d,f). The small offsets above the curve at TF were much lower than observed by other studies conducted in North America (Bertman et al., 1995; Roberts et al., 1998; Stroud et al., 2001). The close agreement between the measured and predicted ratios and the similar behavior exhibited by both propyl nitrate/propane ratios indicates that 1-PrONO₂ and 2-PrONO₂ share a similar production mechanism following the oxidation of propane. This is in contrast to observations over the Atlantic Ocean (Reeves et al., 2007) and at Chebogue Point, Nova Scotia (Roberts et al., 1998) where the 2-PrONO₂/propane and 1-PrONO₂/propane ratios displayed different behavior which was attributed to the influence of different precursor compounds. Furthermore, the lifetimes of propane (weeks-months), 2-PrONO₂, and 1-PrONO₂ (days-weeks) are sufficiently

long to sustain background propyl nitrate/propane ratios which may contribute to the deviations between ambient and predicted ratios. Overall, a significant amount of the data in both seasons falls between the mean, background, and zero initial ratios curves further suggesting that precursor sources other than propane may not contribute to the propyl nitrate distribution observed at TF. Additionally, in Figures 3.8a-f, the initial 2-BuONO₂/n-butane ratio was equal to its background values (Table 3.5) in order to highlight how well the predicted C₂-C₃ RONO₂/RH ratio curves encompass the observations.

The pentyl nitrate/n-pentane ratios were slightly (factors of 0.3-0.4) below the pure photochemistry curves except at the shortest reaction times in winter (Figures 3.8g-j). Previous studies have also found the pentyl nitrate/n-pentane ratios to lie slightly below the predicted curve, but the cause of this unexpected behavior has remained unknown (Roberts et al., 1998; Stroud et al., 2001; Simpson et al., 2003). One possible explanation suggested by Reeves et al. (2007) was the fragmentation of n-pentane to alkyl radicals other than the 2-pentyl and 3-pentyl radicals. At TF, the slopes of the pentyl nitrate/n-pentane ratios were consistent with the zero initial ratio curves, especially in summer, suggesting that photochemical production from n-pentane was the main source of both 2- and 3-PenONO₂. In contrast to the C₂-C₃ RONO₂/RH ratios, the mean initial ratio curves overestimated the observations in both seasons (not shown). In this case, plotting the mean initial 2-BuONO₂/n-butane ratio with the background pentyl nitrate/n-pentane curves resulted in better agreement with the observations (pink lines in Figures 3.8g-j). This result is not unexpected when the different lifetimes of the C₄ and C₅ alkyl nitrates are considered. 2-butyl nitrate and n-butane have longer lifetimes and

higher background mixing ratios than the pentyl nitrates and n-pentane, respectively, suggesting that the initial pentyl nitrate/n-pentane ratio would be lower than the 2-BuONO₂/n-butane ratio near a source region. This is corroborated by the TF measurements in which the mean and background pentyl nitrate/n-pentane ratios were lower than the 2-BuONO₂/n-butane ratios (with the exception of the winter background 2-PenONO₂/n-pentane ratio) (Table 3.5).

The influence of alkyl nitrate dry deposition on the interpretation of RONO₂/RH vs. 2-BuONO₂/n-butane relationships was also investigated. A term representing the first order removal rate due to dry deposition ($k_D = V_d/H = 1/\tau_d$; Table 3.3) was added to the alkyl nitrate removal rate constant term ($k_B = k_6[\text{OH}] + J_5 + k_D$) in equation (9). The calculated curves agreed with the observations but quickly reached a constant value and did not extend beyond processing times of ~1-2 days on the pure photochemistry curve (Figure 3.8). This reflects the shortened lifetimes when dry deposition is considered (Table 3.3). The pronounced decrease in EtONO₂/ethane ratios is caused by the decrease in ratios with increased processing time (discussed above) and the larger k_D for 2-BuONO₂ (Figures 3.8a,b). Considering that the observed RONO₂/RH ratios extend to longer processing times, the significant influence of atmospheric mixing is apparent. Additional research is needed to quantify the seasonal variation, if any, in dry deposition rates and velocities of alkyl nitrates and is being conducted using the long-term and continuous measurements currently being made at Thompson Farm.

3.6 Summary

Measurements of C₁-C₅ alkyl nitrates made at various locations throughout seacoast New Hampshire and spanning several years (2002-2008) were presented. The

total alkyl nitrate mixing ratio was generally ~20-30 pptv and constituted only a small component ($\leq 1\%$) of ambient NO_y at TF. This suggests that alkyl nitrates are not likely to have a significant influence on the local O_3 or NO_y budget. However, owing to the high mixing ratios of precursor compounds (NO_x and NMHCs) emitted from the urban northeast U.S. corridor, production of alkyl nitrates during trans-Atlantic transport is likely to occur and has been observed (e.g., Reeves et al., 2007). This may ultimately influence the NO_x and O_3 distributions of downwind regions, such as Europe, making it necessary to accurately quantify the distributions of precursors and secondary species originating in the northeastern U.S. Furthermore, while the alkyl nitrate deposition rates (-0.1 to $-1.8 \text{ nmol m}^{-2} \text{ hr}^{-1}$) at TF were much lower than for other nitrogen species, the observation that alkyl nitrates may undergo dry deposition provides evidence that unaccounted for reactive nitrogen compounds contribute to NO_y deposition.

CHAPTER 4

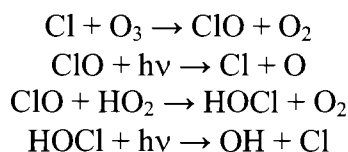
CHLORINE ATOM CONCENTRATIONS AND CONTRIBUTIONS TO VOC OXIDATION DURING SUMMER 2004 AND 2005 AT INLAND AND OFFSHORE COASTAL NEW ENGLAND SITES

4.1 Introduction

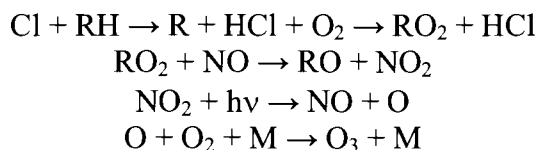
Atomic chlorine (Cl) in the atmosphere originates from natural and anthropogenic sources. The largest source of both particulate and inorganic Cl in the troposphere is dechlorination of sea-salt aerosol emitted by breaking waves over the ocean (e.g., Graedel and Keene, 1995; Erickson et al., 1999; Keene et al., 1999). Several mechanisms have been proposed to explain how the inorganic gaseous chlorine is released following the oxidation of sea-salt aerosol (e.g., Keene et al., 1990; Finlayson-Pitts, 1993, 2003; Platt and Honninger, 2003). One mechanism involves the volatilization of hydrochloric acid (HCl) following displacement reactions with less volatile and stronger acids, such as sulfuric (H₂SO₄) and nitric (HNO₃) acid. A second mechanism is the oxidation of sea-salt halides to reactive halogen molecules, such as Br₂, BrCl, ICl, Cl₂, which are released to the atmosphere. Third, oxidized nitrogen species, such as dinitrogen pentoxide (N₂O₅), HNO₃, nitrogen dioxide (NO₂), chlorine nitrate (ClONO₂), or nitrate (NO₃), react with bromide or chloride in sea-salt to release hydrogen halides (HBr, HCl), nitryl chloride (ClNO₂), or nitryl bromide (BrNO₂). Once in the atmosphere, reactive halogen species are rapidly photolyzed to halogen atoms. Compared to the natural sources, anthropogenic emissions (fossil fuel combustion, waste incineration, water treatment, chemical

manufacturing, cooling towers, paper mills) make a minor contribution to the flux of Cl into the troposphere (Graedel and Keene, 1995; Erickson et al., 1999; Keene et al., 1999). However, the variations in aerosol acidity resulting from reactions with nitrogen and sulfur species (from anthropogenic and natural sources), will have a significant influence on acid-displacement reactions, the oxidation capacity, climate, and ocean productivity in coastal regions.

Atomic chlorine is removed from the atmosphere by reaction with organic compounds or with ozone (O₃) depending on the relative concentrations of organics and nitrogen oxides (NO_x). At low NO_x mixing ratios, the presence of Cl initiates a catalytic O₃ destruction cycle:



This cycle may be important in remote oceanic regions, the Arctic, or in the stratosphere. In continental regions, Cl predominantly reacts with organic compounds, specifically hydrocarbons (RH). The rates of reaction of alkanes, as well as several alkenes and aromatics, with Cl are 1-2 orders of magnitude faster than with the hydroxyl radical (OH). Similar to the OH initiated oxidation of hydrocarbons, the reaction between RH and Cl in the presence of sufficient levels of NO_x can ultimately lead to O₃ production:



The additional supply of radicals resulting from reaction between RH and Cl will significantly influence the cycling of NO_x, HO_x, and sulfur species in the atmosphere.

Unfortunately, techniques are not currently available to measure ambient concentrations of atomic chlorine. Consequently, all estimates of Cl concentrations to date are based on indirect methods and modeling.

Several modeling studies have linked the increased rates of hydrocarbon oxidation by Cl to the subsequent enhancements (~5-15 ppbv) observed in ambient O₃ mixing ratios. However, these studies have been focused on heavily populated areas in southeastern Texas (Tanaka et al., 2003; Chang and Allen, 2006) and southern California (Knipping and Dabdub, 2003; Cohan et al., 2008). Southern New England, including the seacoast region of New Hampshire, is classified as an O₃ nonattainment area, but has only recently been the focus of large-scale air quality campaigns (e.g., Fehsenfeld et al., 2006). The chemical composition of the troposphere over New England is influenced by a complex mixture of primary biogenic (i.e., vegetation, crops) and anthropogenic (i.e., industry, combustion, fuel and gasoline usage) emissions, as well as secondary photochemical species, originating from local and more distant sources regions, such as the Midwest and urban East Coast corridor, (e.g., de Gouw et al., 2005; Lee et al., 2006; Russo et al., 2009a, b; Talbot et al., 2005; White et al., 2008, 2009). Additionally, halocarbons emitted from surface seawater or coastal macroalgae, such as bromoform (CHBr₃), dibromomethane (CH₂Br₂), chloriodomethane (CH₂ClI), methyl iodide (CH₃I), and ethyl iodide (C₂H₅I), are frequently observed at the UNH Observing Station at Thompson Farm (Sive et al., 2007; Varner et al., 2008; Zhou et al., 2005, 2008). The short photolytic lifetime of CH₂ClI (~2 hours) indicates persistent and efficient transport of emissions from local marine and estuarine sources to Thompson Farm (~20 km inland) (Varner et al., 2008).

During a campaign conducted at Appledore Island, ME (July-August 2004), halogen species, including Cl* (primarily Cl₂+HOCl) and HCl (Keene et al., 2007), IO and OIO (Stutz et al., 2007), CH₂ClI (Varner et al., 2008), and CHBr₃ and CH₂Br₂ (Zhou et al., 2008), were observed. The modeling study of Pechtl and von Glasow (2007) demonstrated that the processing of continental outflow from the northeast U. S. can be significantly enhanced by interactions with Cl during transport over the ocean. In addition, Pszenny et al. (2007) estimated chlorine atom concentrations by using the lifetime-variability relationship of selected NMHCs observed at Appledore Island. This work expands upon the analysis of Pszenny et al. (2007) by including data for an inland site, additional compounds, and summer 2005. The objectives of this work are to (1) identify any evidence of Cl chemistry by analyzing and contrasting the VOC trends at an inland and offshore site, (2) estimate [Cl] and [OH]/[Cl] ratios using NMHC measurements during two summers, (3) examine the potential influence of chlorine chemistry on hydrocarbon, DMS, and OVOC removal rates and kinetic reactivity, and (4) assess the relative contribution of OH and Cl chemistry to the oxidation capacity of the troposphere in this region.

4.2 Experimental

4.2.1 Sampling Sites

Measurements of volatile organic compounds were made at the University of New Hampshire Atmospheric Observing Stations at Thompson Farm (TF) (43.11°N, 70.45°W) in Durham, NH and at Appledore Island, ME (AI) (42.67°N, 70.62°W) during July 1-August 15, 2004 and July 7-August 5, 2005 (Figure 4.1). The two sampling sites are approximately 30 km apart. TF is ~20 km inland from the coast of New Hampshire,

~5 km northwest of the Great Bay estuary, and is surrounded by agricultural fields and a mixed deciduous and coniferous forest. Ambient air is sampled from the top of a 15 m tower into a trailer housing the instruments at TF. AI is a 95 acre island located ~10 km offshore of the Maine/New Hampshire coast. Ambient air was sampled from the top of a 40 m WWII surveillance tower located on the island.

4.2.2 Sample Collection and Analysis at Thompson Farm: July-August 2004 and 2005

Approximately every 40 minutes, measurements of C₂-C₁₀ NMHCs, C₁-C₅ alkyl nitrates, and C₁-C₂ halocarbons were made by an automated gas chromatography system. The GC system is equipped with two flame ionization detectors (FID) for detecting NMHCs and two electron capture detectors (ECD) for measuring halocarbons and alkyl nitrates. The system is described in greater detail in Chapters 2 and 3 and in Zhou et al. (2005, 2008).

4.2.3 Appledore Island Canister Samples: July-August 2004 and 2005

4.2.3.1 Canister Sample Collection. Prior to being transported to AI, the 2-liter electropolished stainless steel canisters were prepared by flushing with UHP helium and then evacuating to $\sim 1 \times 10^{-2}$ torr. Canister samples were collected at the top of each hour (00:00, 01:00, 02:00....23:00) during both the 2004 and 2005 campaigns. The air sample passed through ~100 feet of ¼” stainless steel tubing (from the top of the tower to the location of the sampling manifold on the second floor) to the metal bellows pump. The pump was running continuously throughout the campaigns to keep the sampling line clean. The procedure for filling the canisters was: (1) flush the sampling line by quickly opening and closing the outlet valve several times, (2) close the outlet, slowly open the canister, and fill to 25-30 psig, (3) open the outlet valve and empty the canister to ~10

psig, (4) repeat steps 2 and 3 four times, and (5) fill the canister to 30 psig, quickly close the canister valve, open the outlet valve, and disconnect the canister from the sampling manifold.

4.2.3.2 Laboratory Analysis of Canister Samples. The canisters were analyzed in the lab at UNH typically within 1 week of collection for C₂-C₁₀ NMHCs, C₁-C₅ alkyl nitrates, C₁-C₂ halocarbons, several oxygenated volatile organic compounds, and selected sulfur compounds. A three gas chromatograph system in conjunction with flame ionization detection (FID), electron capture detection (ECD), and mass spectrometry (MS) was used for sample analysis. Details of the system configuration are given in Chapters 2 and 3, Sive et al. (2005), and Zhou et al. (2005, 2008).

The mixing ratios of C₂-C₆ and C₆-C₁₀ NMHCs were obtained using the PLOT-FID and DB-1-FID column-detector combinations. The final mixing ratios of C₈-C₉ aromatics and monoterpenes for the AI 2005 samples were obtained using both the FID and MS measurements. The response factors for NMHCs measured by the FID have remained nearly constant throughout 2004-present (see Chapter 2). We are thus confident that the mixing ratios obtained from this channel are accurate. However, several C₈-C₁₀ NMHCs elute within a short time period resulting in considerable peak overlap. These compounds are resolved better by the MS because compounds are identified by both retention time and mass to charge ratio. Therefore, the final mixing ratios were determined by normalizing the mixing ratios obtained for the MS to the median mixing ratios based on the FID: Final MR = (MS MR)*(median FID MR/median MS MR).

4.2.4 Proton Transfer Reaction-Mass Spectrometer

Measurements of oxygenated volatile organic compounds (OVOCs, including methanol, acetone, acetaldehyde, methyl ethyl ketone (MEK), methyl vinyl ketone + methacrolein (MVK + MACR), acetic acid), acetonitrile, and dimethyl sulfide (DMS) were made with a proton transfer reaction-mass spectrometer (PTRMS) during July 1-August 15, 2004 and July 7-August 5, 2005 at both TF and AI. The measurement cycle of the PTRMS was ~4 minutes. Half-hour averages of the PTRMS data were used in this analysis. Additional details of the PTRMS operation can be found in Sive et al. (2005), Ambrose et al. (2007), and Jordan et al. (2009).

4.2.5 Data

This analysis includes several of the most abundant compounds in the different NMHC classes (alkanes, alkenes, aromatics, alkynes, monoterpenes), as well as carbon monoxide (CO), methane (CH₄), DMS, and OVOCs. The following compounds were not included in Pszenny et al. (2007) but are included in the AI 2004 results discussed here: ethylbenzene, m+p-xylene, o-xylene, DMS, and OVOCs. For the most part, the same compounds were measured at TF and AI in both 2004 and 2005. A few exceptions are: (1) o-xylene and n-nonane coeluted in the TF GC during 2004 and are not included, (2) final mixing ratios of 1,3,5-trimethylbenzene from TF in 2005 are not available yet, but will be added later, (3) measurements of 2 and 3-methylpentane and 2,4-dimethylpentane are only available for AI, (4) β-pinene was measured at TF in 2004, but not in 2005; however, measurements of 3-carene are available for 2005, and (5) a constant CH₄ mixing ratio of 1.8 ppmv was used in the AI 2005 analysis.

4.3 Comparison of Source Regions, Meteorology, and Trace Gases at TF and AI during July-August 2004 and 2005

4.3.1 Source Regions

Five source regions (northwest (NW), north-northeast (NNE), marine, southwest (SW), south coastal (SC)) were identified based on visual inspection of 48 hour HYSPLIT backward trajectories created using the EDAS 40 km archived meteorological dataset (Figure 4.1a). Individual trajectories were initialized from both TF and AI in 2004 and 2005 at 16:00 UTC (12:00 local time) at starting heights of 200 and/or 500 m with a new trajectory initialized every six hours (Figure 4.1b). Each measurement from TF and AI in 2004 and 2005 was separated into the appropriate source region corresponding to the time the samples were collected (Figure 4.2).

A few interannual variations in the transport pathways influencing TF and AI are worth noting. The most frequent transport pathways encountered at TF were from the NW and NNE during both summers (20-40%), and the marine sector was sampled the least frequently (8-14%). The SC and SW sectors were consistently observed ~12-18% of the time. In contrast, at AI in 2004, transport from the SC sector was observed a similar amount of the time as the NW and NNE sectors (20-30%). This is not surprising given the offshore location of AI. Transport from the SC sector was observed less often at AI in 2005 (12-15%) while transport from the SW occurred marginally more frequently (17-19% compared to 12-13% in 2004). Overall, the source region frequency distribution was comparable at both sites during 2005.

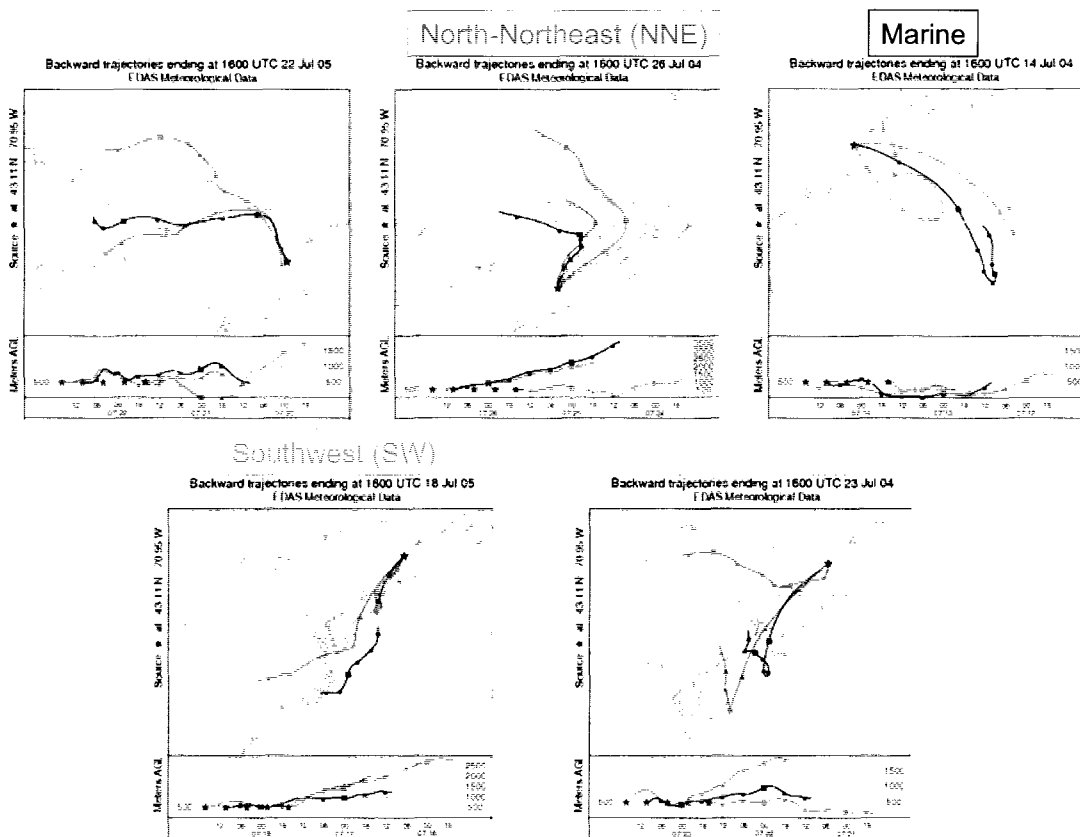
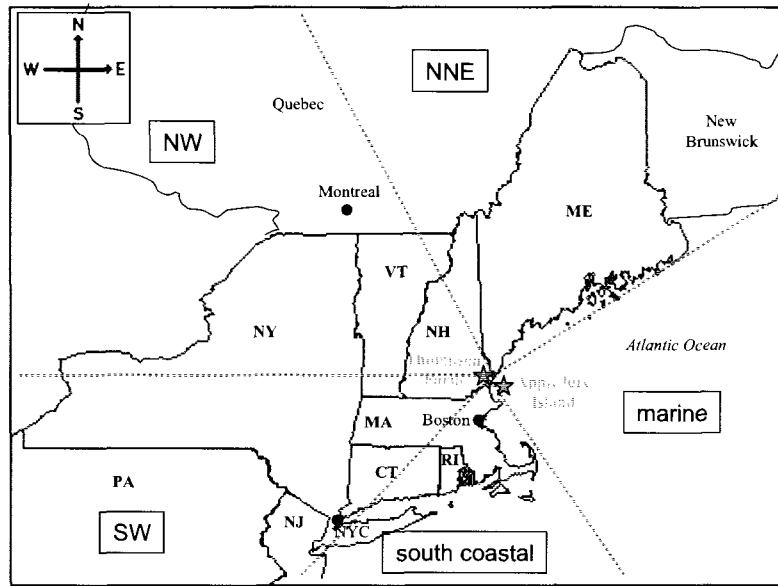


Figure 4.1. (a, top) Location of the UNH Atmospheric Observing Stations at Thompson Farm (TF) (Durham, NH) and Appledore Island (AI), ME. The five major source regions of air masses encountered at TF and AI are also shown. (b, bottom) Examples of HYSPLIT backward trajectories for each of the five source regions.

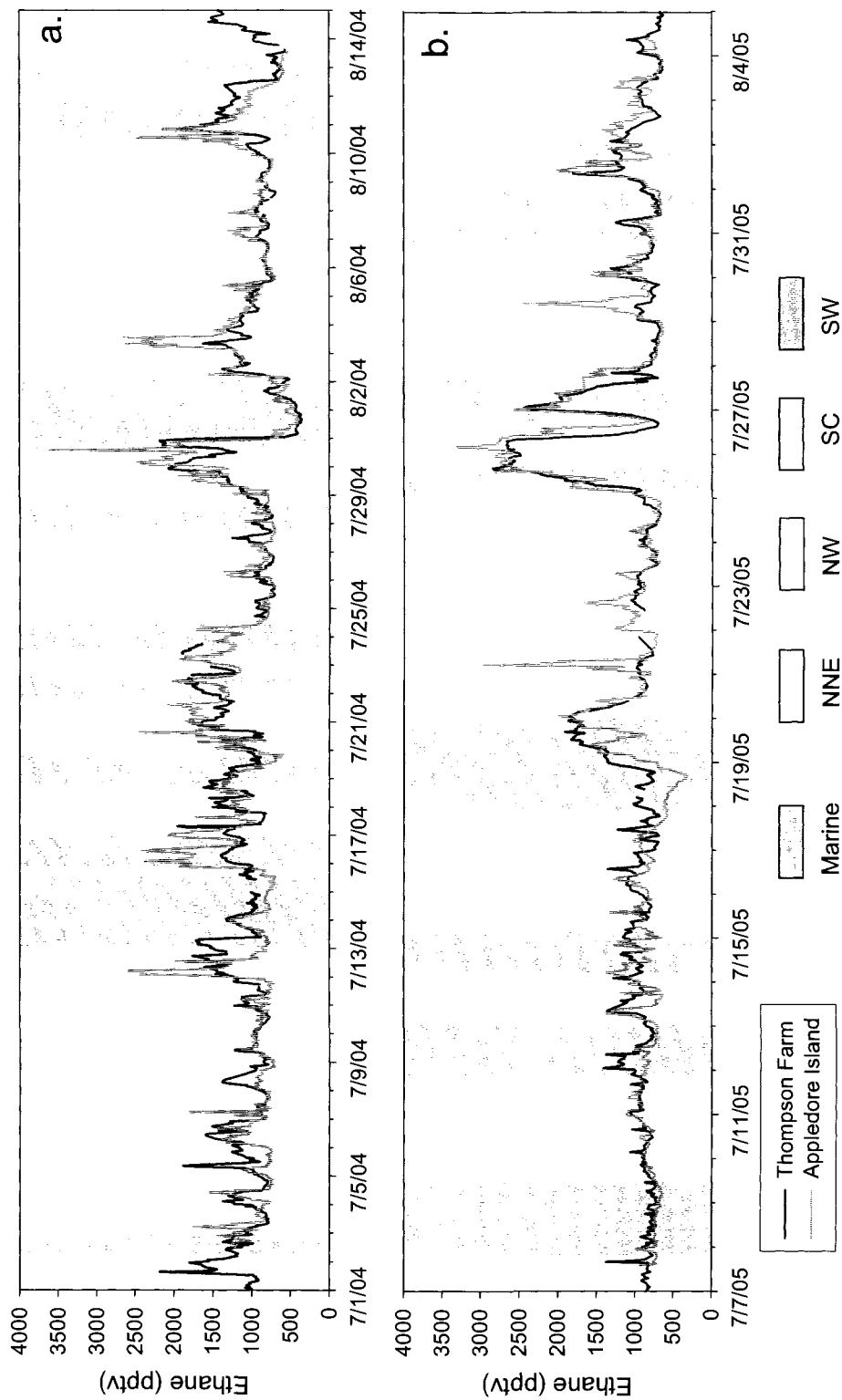


Figure 4.2. Time series of ethane (pptv) at TF and AI in (a) 2004 and (b) 2005. The color coding corresponds to the time series of the specific source regions.

4.3.2 Interannual Variability in Meteorological Conditions

The meteorological conditions in 2004 and 2005 were significantly different which likely influenced regional air quality. The summer of 2004 was cooler and wetter than normal (normal is the 1971-2000 mean) (White et al., 2007; NCDC Climatological Data Summary, 2004, 2005). In contrast, the summer of 2005 was the second warmest on record in the northeast U.S. with temperatures $\sim 3^{\circ}\text{C}$ above normal. The hourly average temperature was $\sim 0.8\text{-}2.3^{\circ}\text{C}$ and $1.4\text{-}4.8^{\circ}\text{C}$ higher at TF and AI, respectively, in 2005 than in 2004 (Figure 4.3a). Daytime temperatures were $\sim 1\text{-}7^{\circ}\text{C}$ higher at TF compared to the offshore sampling site. In addition, J_{NO_2} values at TF were lower in 2004 than in 2005 indicating that less sunlight was available for initiating photochemical processes (Figure 4.3b). The wind speed was also higher throughout the entire day at AI in 2005. Additionally, 7.25" of rain fell at TF during July 1-August 15, 2004 compared to 2.9" between July 7-August 5, 2005 (NCDC Climatological Data Summary, 2004, 2005).

The meteorological differences, as well as the lower O_3 mixing ratios in 2004 (Figure 4.3d), can be explained by variations in the frequency and location of the dominant high and low pressure systems which influence the northeast U. S. during the summer. Summer 2004 (compared to summers 2000-2003) was characterized by a more active storm track along the U. S. east coast with more oceanic cyclones (Hegarty et al., 2007). In addition, the enhanced intensity of the Canadian high pressure system and the lower 500 mbar geopotential height anomaly resulted in more frequent transport of aged Canadian and marine air masses to New England (Hegarty et al., 2007; Yorks et al., 2009). Furthermore, the above average 500 mbar geopotential height anomaly during summer 2005 facilitated the development of stagnant high pressure systems which are

conductive to photochemical O₃ production (Yorks et al., 2009). The more frequent occurrence of oceanic storms and air masses likely explains the higher percentage of time associated with transport from the SC sector at AI during 2004. This meteorological variability resulted in unique opportunities to study the influence of chlorine chemistry during two contrasting summers.

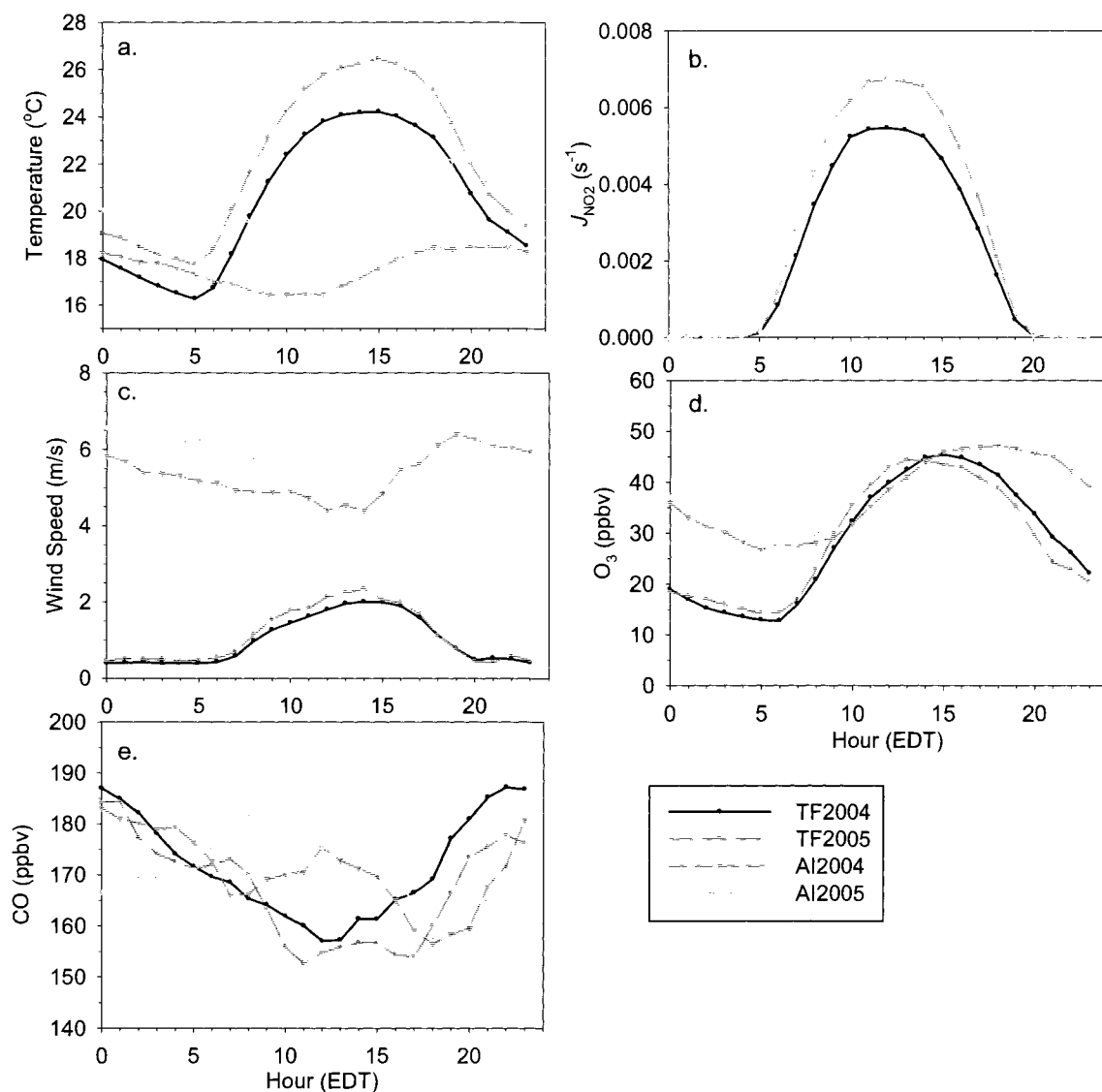


Figure 4.3. Hourly average (a) temperature (°C), (b) J_{NO_2} (s^{-1}), (c) wind speed (m/s), (d) O₃ (ppbv), and (e) CO (ppbv) at TF and AI in 2004 and 2005.

4.3.3 Interannual Variability in VOC Distributions at TF and AI

The median mixing ratios of all of the VOCs included in this analysis in each transport sector, as well as CO and CH₄, are given in Table 4.1. The time series of ethane is shown in Figure 4.2 as a representative example of the similarities and differences in the NMHC distributions at TF and AI. The ethane mixing ratios were within a comparable range (~500-3500 pptv) and track one another very well illustrating that the same or portions of the same air mass were typically encountered at both sites. Rapidly changing mixing ratios and clean and polluted episodes ranging in duration from hours to days were observed. The relatively low and invariant mixing ratios throughout July 7-13, 2005 were associated with Hurricane Cindy traveling up the east coast and Hurricane Dennis passing to the west of New England (July 13-18, 2005).

The estimates of chlorine atom concentrations made in this analysis are derived from the variability trends of eight specific NMHCs (C₃-C₅ alkanes, ethyne, benzene, toluene). The general distribution and diurnal trends of these compounds at TF and AI are discussed here. In 2004, the median C₃-C₄ alkane, n-pentane, ethyne, benzene, and toluene mixing ratios were higher in the NW and SW sectors at AI than at TF (Table 4.1). Moreover, the median mixing ratios of ethene and propene were factors of 1.5-7 higher in the different transport sectors at AI in both 2004 and 2005 compared to TF. This suggests that AI was more directly influenced by anthropogenic emissions and/or by more recent emissions from upwind source regions to the west-southwest of New England and provides an explanation for the higher peak mixing ratios observed at AI (Figure 4.2). The observation of enhanced trace gas mixing ratios, such as O₃, at AI compared to TF has been attributed to shallow layer transport from southern New England and weak

ventilation caused by the lower marine boundary layer height (Mao and Talbot, 2004b). The median NMHC mixing ratios were higher in the marine, NNE, and SC sectors at TF in 2004 which presumably reflects the influence of local sources and the closer proximity to anthropogenic emissions which may reach TF even when air masses are transported from the east or northeast. An important exception to these trends was that i-pentane had higher median mixing ratios in all five sectors at TF. Enhanced emissions from headspace vapor and fuel evaporation caused by the warmer temperatures result in elevated mixing ratios of i-pentane every summer (at least since 2002) at TF (Russo et al., 2009 in preparation; White et al., 2008, 2009).

An important distinction between the 2004 and 2005 NMHC trends at AI is that the median mixing ratios of the C₃-C₅ alkanes, ethyne, benzene, and toluene were higher in the SC and NNE sectors in 2005 (Table 4.1). Additionally, the median levels in the SC sector were comparable to the NW and SW sectors. This likely reflects the more frequent transport from coastal New England and the weaker influence of marine air masses compared to 2004.

The NMHCs mixing ratios exhibit different diurnal variations at the inland and offshore sites (Figure 4.4). The amplitude of the NMHC diurnal cycle at TF is larger because of the development of the deeper continental boundary layer during the day and an inversion layer at night (Talbot et al., 2005; White et al., 2008). The cooler temperatures and low wind speeds at night (Figure 4.3) facilitate development of a stable nocturnal inversion layer, which inhibits vertical mixing and advection of air masses, thus allowing local emissions of NMHCs to build up to maximum levels at ~04:00-06:00. As

the inversion layer dissipates in the morning, mixing ratios decrease rapidly and reach their lowest levels from late morning through the afternoon.

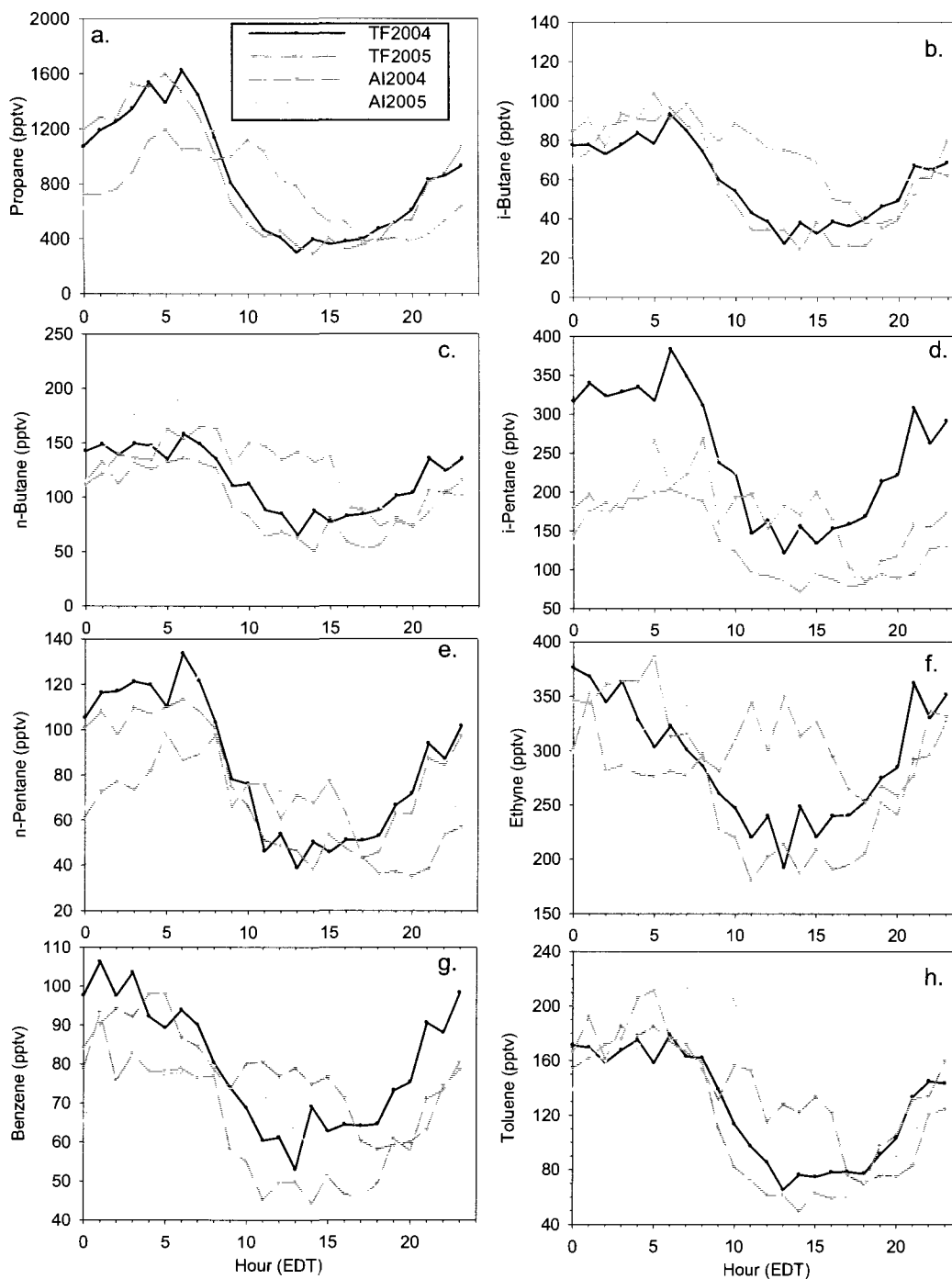


Figure 4.4. Hourly average (a) propane, (b) i-butane, (c) n-butane, (d) i-pentane, (e) n-pentane, (f) ethyne, (g) benzene, and (h) toluene mixing ratios (pptv) at TF and AI in 2004 and 2005.

	TF 2004					AI 2004				
	marine	NNE	NW	SC	SW	marine	NNE	NW	SC	SW
ethane	977.1	883.6	1098.4	1164.0	1250.0	843.6	793.4	1050.8	921.9	1343.7
propane	285.7	514.5	706.3	698.8	555.4	174.9	406.6	797.1	481.0	635.3
i-butane	23.0	33.1	51.8	56.3	47.8	15.2	32.6	81.1	45.5	82.2
n-butane	45.5	72.5	112.4	116.9	104.0	23.6	63.4	141.7	74.7	138.8
i-pentane	89.9	152.1	228.3	255.3	180.9	10.2	83.6	207.5	78.1	166.2
n-pentane	26.0	50.3	75.8	82.8	62.7	7.1	32.7	81.3	32.3	72.6
cyclohexane	8.3	10.6	13.2	13.8	9.6	4.4	8.4	13.7	7.2	12.9
n-hexane	19.1	26.9	37.3	47.6	38.4	5.3	13.6	41.3	17.6	36.7
mecychexane	9.2	11.7	13.7	15.2	12.0	6.4	6.9	12.1	8.4	9.6
n-heptane	11.6	11.9	17.8	21.2	16.5	3.8	9.5	20.0	9.4	18.6
n-octane	6.7	6.8	9.1	9.3	7.4	7.0	7.1	9.1	6.1	7.8
n-nonane						3.4	5.0	8.9	6.6	8.4
n-decane	7.2	9.6	10.2	10.4	9.7	5.8	7.6	14.6	6.8	12.3
2,2,4-tmp	14.5	21.7	35.8	33.1	32.1	7.8	18.5	44.9	19.3	27.0
2,4-dmp						4.4	6.9	12.3	6.1	9.5
2-mepentane						9.7	21.2	57.2	21.0	45.0
3-mepentane						6.2	22.7	46.4	23.2	31.4
ethyne	181.1	212.1	262.0	297.7	275.1	152.9	179.0	379.0	250.8	379.2
ethene	19.8	71.3	71.9	34.1	30.2	52.6	110.9	277.3	120.3	218.8
propene	13.4	37.2	31.6	12.3	12.3	15.6	26.6	63.8	30.8	52.8
trans-2-butene	3.3	6.4	6.0	3.1	4.1	2.4	4.3	3.8	2.7	3.0
1-butene	6.4	8.1	9.8	5.5	6.1	4.1	5.4	10.1	5.8	8.1
cis-2-butene	5.3	7.2	7.6	4.5	4.6	2.6	4.1	4.2	3.7	3.4
2-me-2-butene	5.2	5.9	7.3	4.7	6.4	4.5	4.6	4.3	3.5	4.2
1-pentene	6.2	7.3	8.1	6.4	6.7	4.1	4.9	7.7	5.6	5.2
benzene	59.1	64.1	74.2	78.0	72.8	43.3	42.0	93.6	58.7	91.3
toluene	53.6	85.2	114.0	121.9	94.0	11.5	65.3	188.6	69.3	150.5
ethylbenzene	11.9	16.4	20.9	25.1	17.7	5.9	10.1	23.2	13.2	18.7
m+p-xylene	35.5	51.7	55.0	68.8	49.2	44.7	65.8	98.3	67.6	80.8
o-xylene						14.9	18.7	32.2	24.2	26.6
1,3,5-tmb	6.5	8.0	9.9	8.4	7.6	3.6	4.7	6.4	5.2	5.5
isoprene	108.4	294.8	508.7	186.5	316.4	6.9	20.7	54.0	15.4	20.2
α-pinene	13.8	55.8	73.8	19.2	29.0	4.0	13.3	27.0	7.7	9.6
β-pinene	10.8	43.5	50.6	21.1	23.8	7.2	31.4	36.6	8.9	8.9
camphene	21.2	44.2	75.3	32.7	30.7	5.9	29.1	27.9	4.6	7.0
limonene	6.2	10.5	19.1	12.1	5.3		10.3	6.2	4.6	7.2
DMS	37	16	17	31	22	106	29	27	56	45
methanol	1557	2229	2515	3009	2657	699	1991	3005	1400	2493
acetaldehyde	66	205	272	493	212	168	320	531	323	551
acetone	1050	1562	2097	2678	1954	663	1225	1797	1064	1863
MEK	89	130	218	331	210	44	101	227	129	228
MVK+MACR	89	179	364	284	471	18	73	204	58	195
acetonitrile	127	119	114	137	117	90	80	100	81	124
acetic acid	107	297	286	307	423	279	408	488	378	566
CO	149.0	147.0	171.0	173.0	175.0	132.0	143.0	185.5	151.5	199.5
CH ₄	1.83	1.87	1.87	1.88	1.84	1.73	1.75	1.77	1.77	1.79

Table 4.1a. Median mixing ratios of VOCs (pptv), CO (ppbv), and CH₄ (ppmv) in the five transport sectors at TF and AI in 2004.

	TF 2005					AI 2005				
	marine	NNE	NW	SC	SW	marine	NNE	NW	SC	SW
ethane	806.7	846.9	933.5	934.3	1166.6	747.4	842.5	951.2	907.1	1085.0
propane	337.2	327.6	616.8	745.0	1046.4	206.7	459.4	844.1	617.2	740.2
i-butane	27.4	27.3	38.9	51.8	77.4	25.8	51.4	85.5	60.7	98.5
n-butane	49.5	45.8	77.0	99.5	141.7	37.5	83.8	150.2	109.4	148.1
i-pentane	65.6	66.0	107.5	156.2	188.4	23.5	95.5	168.2	138.2	158.5
n-pentane	34.5	36.8	62.8	89.0	106.2	12.2	40.0	75.8	66.1	76.2
cyclohexane	9.3	15.3	16.3	13.1	13.9	8.7	9.5	12.6	11.1	12.5
n-hexane	15.1	12.7	24.4	41.0	44.8	9.9	16.9	34.3	36.7	41.1
mecycchexane	12.3	15.0	13.3	13.7	16.8	8.2	9.9	12.2	11.8	11.6
n-heptane	11.1	9.8	18.7	23.0	27.4	9.7	14.0	24.0	27.5	26.6
n-octane	9.0	10.4	8.2	8.7	10.1	7.0	9.2	14.9	14.8	14.5
n-nonane	8.0	9.4	9.2	8.5	9.8	7.9	8.3	11.8	12.1	11.5
n-decane	7.7	9.9	10.9	7.8	10.7	8.3	11.1	16.4	17.8	17.2
2,2,4-tmp	14.6	15.4	20.5	29.5	28.0	15.4	26.3	30.1	35.7	28.2
2,3-dmb						8.8	13.5	20.9	23.4	18.0
2,4-dmp						7.9	9.8	11.9	12.5	11.1
2-mepentane						11.8	34.1	55.0	66.5	59.4
3-mepentane						13.5	34.5	51.5	64.7	49.6
ethyne	164.3	171.6	212.9	297.4	326.8	106.2	224.0	314.0	377.4	363.5
ethene	74.2	88.8	134.0	176.0	135.5	46.2	169.9	260.8	286.8	235.1
propene	9.0	9.8	22.9	12.0	12.5	13.1	44.2	59.5	69.6	49.8
trans-2-butene		7.2	7.9	8.2	6.8	5.2	6.3	6.8	6.0	5.8
1-butene	8.4	18.4	16.4	19.1	18.1	8.8	9.3	11.1	13.1	8.7
cis-2-butene		7.4	7.4	9.4	7.8	11.2	6.8	8.5	9.7	5.4
2-me-2-butene	5.7	9.5	10.0	12.3	6.9	6.7	8.2	7.9	6.8	7.9
1-pentene	11.4	16.2	15.0	11.5	12.7	5.7	7.0	8.0	6.9	6.8
benzene	38.6	40.5	52.7	76.6	85.5	20.9	50.1	73.8	74.0	80.3
toluene	49.8	50.9	93.5	135.5	161.7	17.6	80.6	150.3	150.8	157.1
ethylbenzene	10.3	21.6	21.3	16.4	18.5	9.8	16.0	28.2	34.3	27.8
m+p-xylene	17.5	15.1	44.6	40.1	39.9	13.5	35.8	60.2	83.1	52.5
o-xylene	11.4	17.3	19.8	16.7	18.6	10.2	16.3	26.5	35.9	24.0
1,3,5-tmb										
isoprene	60.8	148.7	609.3	186.7	254.2	10.1	74.6	133.4	25.9	36.0
α -pinene	19.5	255.4	130.0	56.8	27.6	21.6	102.8	146.7	21.3	31.2
β -pinene						18.2	70.7	79.3	15.2	21.8
camphene						15.5	45.1	54.4	15.0	14.7
limonene	32.3	226.0	334.6	233.0	53.1	15.6	15.3	15.5	17.8	17.9
3-carene	28.1	84.0	137.7	88.4	35.8					
DMS	44	38	40	41	43	41	35	52	51	76
methanol	1786	2462	3705	2804	4211	1052	2098	2921	995	1610
acetaldehyde	381	535	807	667	981	213	403	648	285	493
acetone	1544	1881	2928	2360	3682	926	1524	2455	1121	1792
MEK	148	177	332	289	520	74	146	259	96	218
MVK+MACR	122	269	835	619	732	41	257	543	119	207
acetonitrile	113	117	138	136	143	75	109	122	82	106
acetic acid	324	543	1243	831	1172	331	518	872	347	545
CO	138	139	165	193	198	122	155	183	182	188
CH ₄	1.82	1.83	1.87	1.86	1.88					

Table 4.1b. Median mixing ratios of VOCs (pptv), CO (ppbv), and CH₄ (ppmv) in the five transport sectors at TF and AI in 2005.

Maximum and minimum hourly average mixing ratios occur ~2-3 hours later at AI compared to TF (Figure 4.4). Under the shallow marine boundary layer at AI, the NMHC mixing ratios reach their highest levels during mid-morning and persist through early afternoon. Mixing ratios probably remain elevated throughout the entire morning because of the absence of a strong nocturnal inversion layer and the time delay between when the morning rush hour emissions begin and when the emissions reach AI. The lowest mixing ratios occur during the early evening hours (16:00-21:00). During 2005, the butanes, ethyne, toluene, and CO (Figure 4.3e) displayed a pronounced morning peak which was primarily associated with transport from the NW and SC sectors (not shown).

4.4 Estimates of Chlorine Atom Concentrations

4.4.1 Lifetime-Variability Relationship

Several studies have shown that the variability and lifetime (τ) of trace gases can be described by the following power law relationship (e.g., Jobson et al., 1998, 1999; Ehhalt et al., 1998; Lenschow and Gurarie, 2002):

$$S_{\ln[X]} = A\tau^{-b} \quad (1)$$

where $S_{\ln[X]}$ is the standard deviation of the natural log of the mixing ratios of a specific compound and describes the variability of the compound. The parameters A and b are found from the fit of $S_{\ln[X]}$ versus τ and provide qualitative information on the distance to sources and the factors (i.e., chemistry, mixing, emissions) controlling mixing ratio variability. Parameter b is a measure of proximity to sources and varies between 0 and 1. Lower values of b are representative of measurements made close to sources where the mixing ratio variability is dominated by varying source strengths. Higher values of b reflect measurements made farther from sources where chemistry controls the variability

(Jobson et al., 1998, 1999). Lifetime-variability analyses have been applied to measurements of NMHCs, OVOCs, and halocarbons in order to characterize sources, relative processing times, and/or to estimate oxidant concentrations in remote, rural, and urban locations (e.g., Jobson et al., 1998, 1999, 2004; Karl et al., 2004; Millet et al., 2004; Pszenny et al., 2007; Williams et al., 2000).

	k_{OH}	k_{Cl}		k_{OH}	k_{Cl}
	Alkanes				
ethane	2.40E-13	5.90E-11	CO	1.50E-13	3.15E-14
propane	1.10E-12	1.40E-10	CH ₄	6.40E-15	1.00E-13
i-butane	2.12E-12	1.43E-10			
n-butane	2.30E-12	2.05E-10		Alkenes	
i-pentane	3.60E-12	2.20E-10	ethene	9.00E-12	1.10E-10
n-pentane	3.80E-12	2.80E-10	propene	3.00E-11	2.70E-10
cyclohexane	6.97E-12	3.50E-10	t-2-butene	6.40E-11	3.31E-10
n-hexane	5.20E-12	3.40E-10	1-butene	3.14E-11	3.38E-10
2-mepentane	5.20E-12	2.90E-10	c-2-butene	5.64E-11	3.76E-10
3-mepentane	5.20E-12	2.80E-10	2-me-2-butene	8.69E-11	3.95E-10
2,3-dmb	5.78E-12	2.30E-10	1-pentene	3.14E-11	3.97E-10
2,4-dmp	4.80E-12	2.90E-10			
mecyhexane	9.60E-12	3.90E-10		Biogenics	
n-heptane	6.76E-12	3.90E-10	isoprene	1.00E-10	5.10E-10
2,2,4-tmp	3.34E-12	2.60E-10	α -pinene	5.30E-11	5.30E-10
n-octane	8.11E-12	4.60E-10	β -pinene	7.90E-11	5.30E-10
n-nonane	9.70E-12	4.80E-10	limonene	1.70E-10	6.40E-10
n-decane	1.10E-11	5.50E-10	3-carene	8.80E-11	5.20E-10
	Aromatics			OVOCs	
benzene	1.23E-12	4.00E-12	methanol	9.30E-13	5.50E-11
toluene	5.96E-12	5.90E-11	acetaldehyde	1.50E-11	7.90E-11
ethylbenzene	7.10E-12	1.22E-10	acetone	1.70E-13	2.50E-12
m+p-xylene	1.90E-12	1.45E-10	MEK	1.20E-12	3.80E-11
o-xylene	1.37E-11	1.50E-10	MVK+MACR	2.45E-11	2.15E-10
1,3,5-tmb	5.67E-11	2.42E-10	acetonitrile	2.20E-14	1.20E-14
			acetic acid	7.30E-13	2.65E-14
ethyne	1.00E-12	5.20E-11			
DMS	4.80E-12	3.40E-10			

References: Anderson et al. (2007); Atkinson et al. (1990, 1997, 2003, 2006a); Atkinson and Arey, (2003); Canosa-Mas et al. (2001); Ezell et al. (2002); Finlayson-Pitts et al. (1999); Shi and Bernard, (1997); Timerghazin et al. (2001); Wang et al. (2005).

Notes: mecyhexane=methylcyclohexane; dmb=dimethylbutane; dmp=dimethylpentane; tmp=trimethylpentane; tmb=trimethylbenzene; MEK=methyl ethyl ketone; MVK+MACR=methyl vinyl ketone + methacrolein.

Table 4.2. VOC, CO, and CH₄ rate constants for reaction with OH and Cl (cm³ molecule⁻¹ s⁻¹).

The lifetime of a specific NMHC against reaction with OH or Cl (τ_{OH} and τ_{Cl} , respectively) is: $\tau_z = \{1/(k_z[Z])\}$ where $Z = \text{OH}$ or Cl . The lifetime against reaction with both OH and Cl was calculated from equation (2) (rate constants are given in Table 4.2):

$$\tau_{\text{OH} + \text{Cl}} = \left[\left(\frac{1}{\tau_{\text{OH}}} \right) + \left(\frac{1}{\tau_{\text{Cl}}} \right) \right]^{-1} \quad (2)$$

By keeping $[\text{OH}]$ constant, an optimum value for $[\text{Cl}]$ which maximizes the correlation coefficient between $S_{\ln[X]}$ and $\tau_{\text{OH}+\text{Cl}}$ can be obtained. The optimization was performed using the ‘solver’ tool in Microsoft Excel, following Pszeny et al. (2007). Variability-lifetime relationships were constructed for each transport sector using measurements of eight NMHCs (propane, i-butane, n-butane, i-pentane, n-pentane, ethyne, benzene, and toluene) from TF and AI in 2004 and 2005 (Figure 4.5). These eight NMHCs were chosen because they have similar sources (vehicular and gasoline emissions) and sinks (reaction with OH or Cl). Furthermore, the lifetime of each NMHC against reaction with OH or Cl is longer than ~1 day (assuming $[\text{OH}] = 2.5 \times 10^6$ and $[\text{Cl}] = 4 \times 10^4$ molecules cm^{-3}) which minimizes complications arising from variable sources and sinks.

As discussed in Pszeny et al. (2007), coherent and similar lifetime-variability relationships were found for the southern and western sectors at AI in 2004 and were characterized by lower b values suggesting the influence from nearby sources (Table 4.3). This is consistent with the location of upwind source regions to the west-southwest of AI and shorter transport distances as indicated by the lower values of the A parameter. In contrast, higher b values were found for the marine and NNE sectors indicating a stronger influence from chemical processing and air mass mixing. In the present study, similar results were found for TF in 2004 with the highest b values, and thus the most processed

air masses, corresponding to the marine and NNE sectors (Table 4.3). However, the b values were lower in each sector at TF which illustrates the narrower range of $S_{\ln[X]}$ values (i.e., lower variability) and suggests that varying source strengths had a stronger influence than at AI. Note that six transport sectors were discussed in Pszenny et al. (2007), whereas in this work, a separate midwest sector is not used. Samples corresponding to the midwest sector of Pszenny et al. (2007) were classified into either the NW or SW sectors in this work.

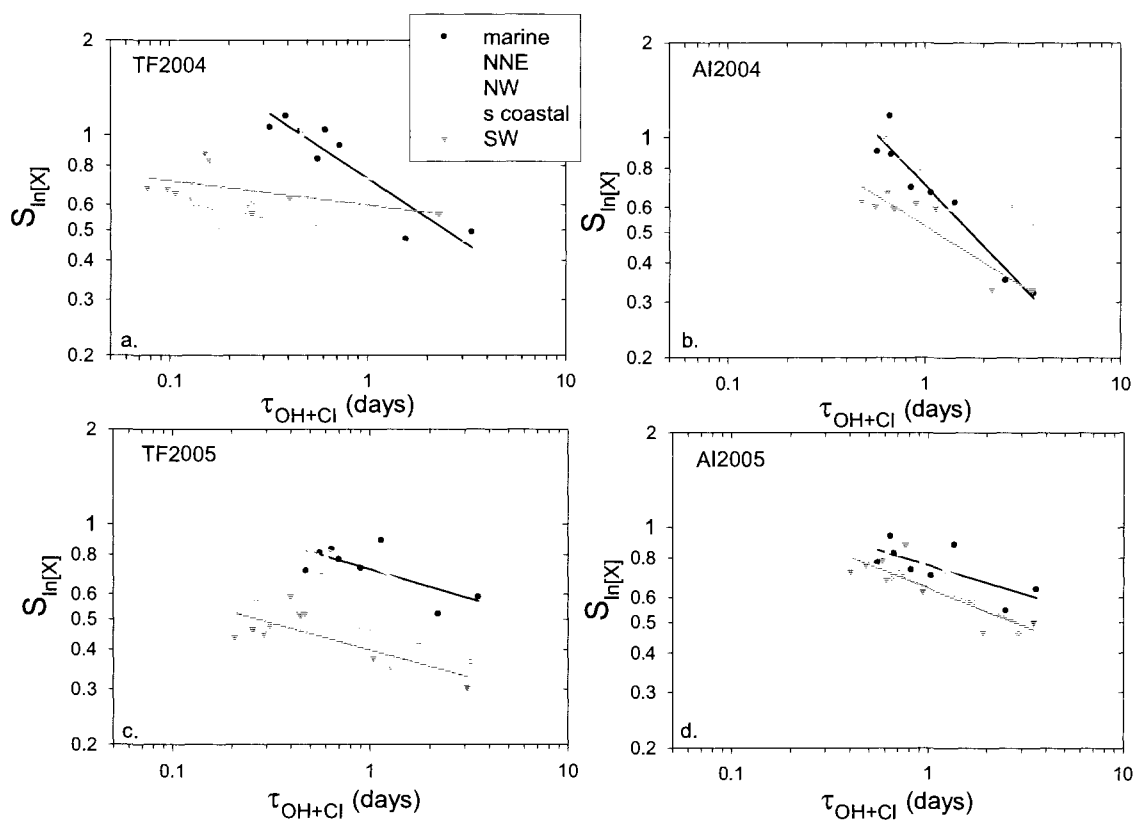


Figure 4.5. Lifetime-variability relationships for NMHCs in the five transport sectors at TF in (a) 2004 and (c) 2005, and at AI in (b) 2004 and (d) 2005.

		AI2004						TF2004						
	[Cl]	A	b	r ²	Ψ	N	[OH]/[Cl]	[Cl]	A	b	R ²	Ψ	N	[OH]/[Cl]
marine	3.84E+04	0.71	0.65	0.93	14.2	85	65	9.42E+04	0.73	0.42	0.84	11.3	155	27
NNE	4.59E+04	0.82	0.40	0.86	14.6	149	54	1.60E+05	0.59	0.29	0.64	3.9	290	16
NW	5.15E+04	0.63	0.22	0.81	2.9	168	49	1.55E+05	0.73	0.21	0.73	5.4	469	16
SC	3.15E+04	0.87	0.36	0.92	16.3	162	79	2.87E+05	0.48	0.11	0.66	0.03	193	9
SW	5.33E+04	0.52	0.38	0.84	4.3	76	47	-	-	-	-	-	-	-

		AI2005						TF2005						
	[Cl]	A	b	r ²	Ψ	N	[OH]/[Cl]	[Cl]	A	b	R ²	Ψ	N	[OH]/[Cl]
marine	4.09E+04	0.76	0.19	0.51	5.7	107	61	5.3E+04	0.72	0.19	0.51	4	115	47
NNE	5.72E+04	0.65	0.25	0.73	4.3	157	44	7.5E+04	0.67	0.29	0.59	6	244	33
NW	3.24E+04	0.77	0.27	0.89	9.1	197	77	8.4E+04	0.73	0.27	0.54	7	236	30
SC	2.94E+04	0.66	0.26	0.87	4.9	78	85	1.3E+05	0.46	0.17	0.30	0.25	130	20
SW	6.86E+04	0.64	0.25	0.67	4.0	123	36	1.7E+05	0.40	0.17	0.53	0.11	154	15

Table 4.3. Estimated chlorine atom concentrations ([Cl]) (molecules cm⁻³) in the five transport sectors at TF and AI in 2004 and 2005. The A, b, and Ψ (= A^{1/b} x 24; indicator of transport times from source regions) parameters were derived from the optimized fit between the standard deviation of the natural log of eight NMHC mixing ratios in each transport sector with the lifetime of each NMHC with respect to reaction with OH and Cl (S_{ln[X]} versus τ_(OH+Cl)). N is the number of samples included in each sector. The [OH]/[Cl] ratio was obtained using [OH] = 2.5 x 10⁶ molecules cm⁻³ and the corresponding [Cl] in each sector.

In contrast to 2004, a narrow range of low b values (0.17-0.29) was obtained for both TF and AI in all transport sectors during 2005. This suggests a stronger relative impact from local or recent emissions in 2005 and/or a weaker influence from aged air masses. This is consistent with the more frequent transport of aged air masses to New England in 2004 discussed in section 4.3.2. The lifetime-variability relationships were similar in each sector at AI in 2005. The nearly identical A and b values is likely a consequence of the more uniform mixing ratios in the NNE, NW, SC, and SW sectors during 2005 compared to 2004 (Table 4.3, Figure 4.5).

4.4.2 Comparison between [Cl] Estimates at TF and AI in 2004 and 2005

Atomic chlorine concentrations ([Cl]) determined by optimizing the variability-lifetime relationship exhibited similar trends in 2004 and 2005. At AI, the highest and lowest [Cl] were estimated for the SW and SC sectors, respectively, in both 2004 and 2005 (Table 4.3). Overall, a similar range of [Cl] was obtained for 2004 $(3.2-5.3) \times 10^4$ molecules cm^{-3} and 2005 $(2.9-6.9) \times 10^4$ molecules cm^{-3} . The highest [Cl] was also found for the SW sector at TF; however, the lowest [Cl] was in the marine sector in both years. The Cl concentrations in the marine sector were comparable to AI $((5-9) \times 10^4$ molecules cm^{-3}), but were higher in the other four sectors ($\sim 10^5$ molecules cm^{-3}) (Table 4.3). It is counterintuitive that the concentrations were higher at TF than at the offshore location because sea-salt aerosol is the major source of Cl in the atmosphere (Graedel and Keene, 1995). However, according to the EPA 2004 and 2005 Toxics Release Inventories, $\sim 3000-4000$ tons/year of chlorine is released in New England from chemical and industrial plants and paper mills (www.epa.gov/tri). Thus, even though anthropogenic sources are believed to be minor, Cl or HCl emissions from power plant cooling towers,

water treatment plants, waste incineration, or other chemical treatment processes may contribute to the composition of air masses observed at TF. Furthermore, a possible explanation for the variations in [Cl] between sectors and sampling sites is the use of a constant OH concentration. The OH radical has a very short lifetime (~1 second) and highly variable concentrations which strongly depend upon solar radiation and water vapor concentrations. However, by keeping OH constant, the lifetime-variability trends should provide information on the relative differences in the source-sink distributions of NMHCs.

Pszenny et al. (2007) suggested that the high [Cl] in the SW sector may reflect enhanced sea-salt aerosol concentrations caused by high wind speeds. At AI in 2004, the highest sea-salt chloride, HCl, total nitrate, and HNO₃ concentrations were observed in the SW sector (Fischer et al., 2006; Keene et al., 2007). Moreover, the highest median wind speeds were in the SW sector (second highest after the NNE sector at TF in 2005). Air masses originating to the SW typically travel over the ocean or coastal areas along the East Coast urban corridor before arriving in the seacoast region of NH (e.g., Mao and Talbot, 2004b; Angevine et al., 2004) and likely reflect a combination of marine and urban emissions. The scavenging of less volatile acids (HNO₃, H₂SO₄) into sea-salt aerosol causes the acidity to increase (lowers the pH) and releases HCl or other photolabile reactive halogen compounds (i.e., Cl₂, ClONO₂, ClNO₂, BrCl) (Keene et al., 1990; Finlayson-Pitts, 2003; Platt and Honninger, 2003). Reaction between sea-salt chloride and oxidized nitrogen species (i.e., NO₂, NO₃, N₂O₅) in urban air masses may also produce gaseous chlorine species. Therefore, a combination of higher wind speeds

and enhanced chloride displacement from acidified sea-salt aerosols likely contributed to the high [Cl] in the SW sector during both summers at TF and AI.

These results have important implications for the processing of continental outflow over the Atlantic Ocean. A modeling study that was initialized to represent the conditions at AI during July 2004 demonstrated that significant concentrations of Cl₂ (up to ~100 pptv) could be produced in polluted air masses that are advected over the ocean (Pechtl and von Glasow, 2007). Modeling studies and chamber experiments focused on air quality in heavily urbanized coastal areas, such as Houston, TX (Tanaka et al., 2000, 2003; Chang and Allen, 2006) or Southern California (Knipping and Dabdub, 2003) have reported that the enhanced oxidation of NMHCs from reaction with Cl can lead to enhanced O₃ formation.

4.4.3 Comparison to [Cl] Estimates based on Hydrocarbon Ratios

A separate estimate of both OH radical and Cl atom concentrations was made using a more common technique which involves plotting the natural log of the ratio of the change in NMHC mixing ratios during a specified time versus their rate constants with OH and/or Cl (Jobson et al., 1994; Rudolph et al., 1996, 1997; Ariya et al., 1998; Ramacher et al., 1999; Blake et al., 2003b). The estimates were based on the ratio of the average mixing ratios of ethane, propane, i-butane, n-butane, i-pentane, n-pentane, ethyne, and benzene in the AI 2004 marine sector and during the marine sector event on July 13-14, 2004 to their average in the NNE, NW, SC, and SW sectors (Figures 4.6a, b). The range of OH concentrations derived using the ratio method ((1-3) x 10⁶ molecules cm⁻³) indicate that our choice of a constant [OH] = 2.5 x 10⁶ molecules cm⁻³ was valid. Furthermore, the Cl concentrations ((1.5-4) x 10⁴ molecules cm⁻³) agree with the

estimates made in section 4.4.2 suggesting that the lifetime-variability relationship is a useful method for the indirect determination of Cl concentrations. The correlations between the NMHC ratios and their respective k_{OH} and k_{Cl} were similar ($r^2 \sim 0.7-0.8$) providing additional evidence that chlorine chemistry influenced the composition of air masses observed at AI (Figures 4.6a, b).

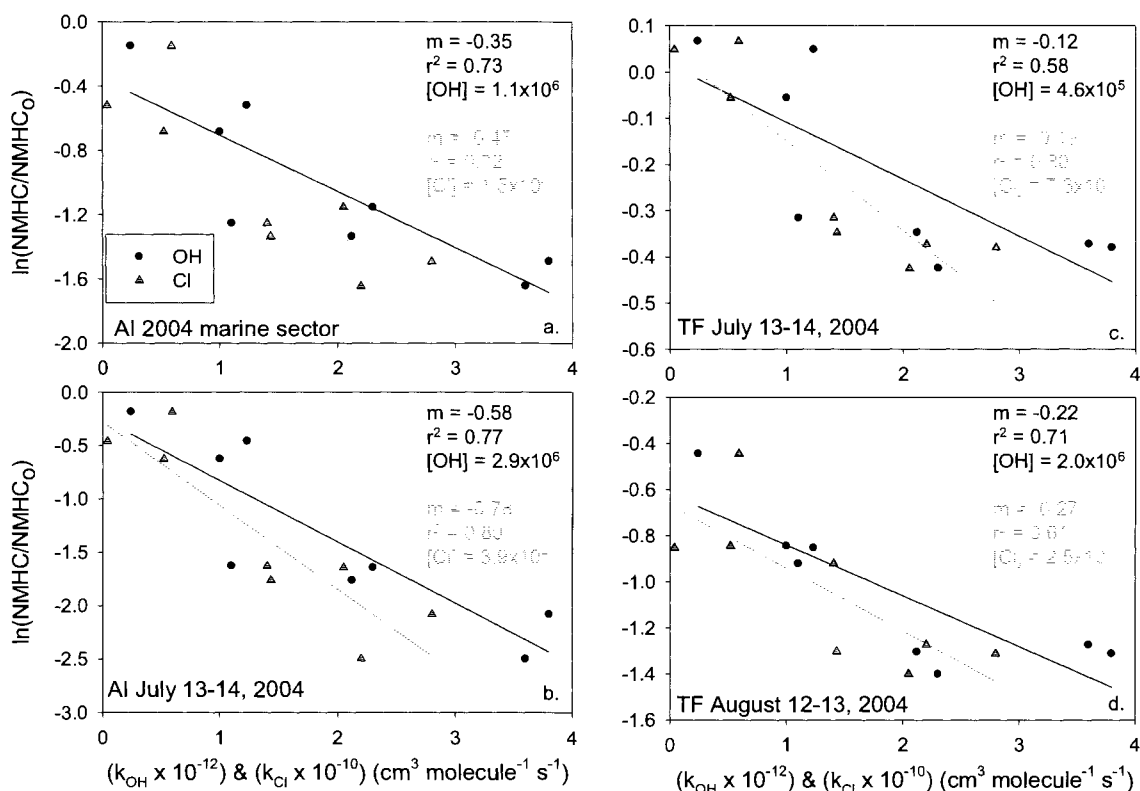


Figure 4.6. Correlation between $\ln(\text{NMHC}/\text{NMHC}_0)$ during a specific time period (Δt) and k_{OH} and k_{Cl} ($m = \text{slope} = [Z]\Delta t$ where $Z = \text{OH}$ or Cl) using data from AI during (a) all times with transport from the marine sector in 2004, (b) July 13-14, 2004, and TF during (c) July 13-14, 2004, and (d) August 12-13, 2004. NMHC is the mean mixing ratio during Δt ; NMHC_0 is the mean mixing ratio in the NNE, NW, SC, and SW sectors.

Application of the ratio method to two specific marine events at TF (July 13-14 and August 12-13, 2004) gave estimates of $[\text{OH}]$ and $[\text{Cl}]$ ranging from $(0.5-2) \times 10^6$ and $(0.73-2.5) \times 10^4$ molecules cm^{-3} , respectively (Figures 4.6c, d). These $[\text{Cl}]$ estimates are slightly lower than those obtained from the lifetime-variability relationships.

Nonetheless, the fairly strong correlations provide supporting evidence for the influence of Cl chemistry under certain conditions. In fact, during the July 13-14 episode, the correlation between the NMHC ratios and k_{Cl} ($r^2=0.80$) was stronger than the correlation with k_{OH} ($r^2=0.58$).

4.5 VOC Contributions to OH and Cl Removal over Coastal NH

The contribution of a specific VOC to O_3 production depends on several factors, including (1) the mixing ratio of the VOC, (2) the concentration of available oxidants (OH, O_3 , NO_3 , halogens), (3) the rate of reaction between the VOC and oxidant, and (4) the NO_x availability (Carter, 1994). One common method for assessing the potential contribution of VOCs to O_3 formation is to calculate the loss rate of the VOC. This also represents the loss rate of the oxidant. The individual OH (or Cl) loss rate (L_{OH} or L_{Cl} in molecules $cm^{-3} s^{-1}$) can be calculated by multiplying the concentration of the VOC ($[X]$) by the OH (or Cl) concentration and k_{OH} (or k_{Cl}). The loss rate for the specific compound is the sum of the OH and Cl contributions ($L_X = L_{OH} + L_{Cl} = k_{OH}[OH][X] + k_{Cl}[Cl][X]$). Additionally, the kinetic reactivity ($KR=L_X/L_{total}$) is the fraction of VOC oxidized to produce peroxy radicals (RO_2) and is an indicator of the rate that the radicals are formed following VOC oxidation (Carter, 1994). The total loss rate of VOCs, CO, and CH_4 , and consequently of OH and Cl, is the sum of the individual removal rates ($L_{total} = L_{VOCs} + L_{CO} + L_{CH_4}$) where $L_{VOCs} = L_{alkanes} + L_{alkenes} + L_{aromatics} + L_{ethyne} + L_{biogenics} + L_{DMS} + L_{OVOCs}$.

During summers 2004 and 2005 at both TF and AI, the lowest and highest L_{total} was in the marine and NW sectors, respectively (Figure 4.7). These two sectors were chosen as representative examples of marine and continental air masses for an in depth comparison of OH and Cl removal and kinetic reactivity. The total loss rate was higher in

the NW sector ($(0.6-1.7) \times 10^7$ molecules $\text{cm}^{-3} \text{s}^{-1}$) than in the marine sector ($(3-5) \times 10^6$ molecules $\text{cm}^{-3} \text{s}^{-1}$) reflecting the direct influence from continental emissions at both sites. Reaction with Cl contributed $\sim 20-35\%$ and $\sim 13-20\%$ to the total KR at TF and AI, respectively. This agrees with the range of 16-30% reported by Pszenny et al. (2007) based on the AI 2004 data. Methane and CO dominated L_{total} in the marine sector, and they were among the top 5 largest contributors to OH+Cl loss in the NW sector (Table 4.4). The rest of the discussion will focus on the VOCs.

The VOC KR was enhanced by $\sim 20-40\%$ and $\sim 20-30\%$ at TF and AI, respectively, by including Cl. In addition, L_{VOC} was higher at TF in the NW and marine sectors because of the larger contribution from $L_{\text{biogenics}}$, L_{alkanes} , L_{ethyne} , and L_{OVOCs} . In the NW sector, L_{alkenes} and $L_{\text{aromatics}}$ were higher at AI presumably because of the higher median aromatic, ethene, and propene mixing ratios in this sector discussed in section 4.3.3. At TF, isoprene made the largest contribution to L_{VOC} in the NW and marine sectors while acetaldehyde was the major contributor at AI (Table 4.4).

The chlorine removal rate at AI was dominated by the alkanes and OVOCs, specifically ethane, propane, and methanol, in the marine sector, and also by MVK+MACR in the NW sector. In the marine sector during 2004, the Cl removal rate of DMS was higher than the alkene, aromatic, biogenic, and ethyne rates (Figure 4.7a). Overall, L_{OH} of the alkanes, alkenes, and aromatics was comparable within a specific sector and year at both AI and TF. The alkanes and OVOCs (ethane, propane, methanol) also made the largest contributions to L_{Cl} at TF in the marine sector. However, in the NW sector, L_{Cl} was dominated by the biogenics (Figure 4.7). Furthermore, during 2005, isoprene and its oxidation products (MVK+MACR) made comparable or larger

contributions to the oxidation capacity of air masses from the NW sector than the more abundant compounds, CO and CH₄ (Table 4.4). This indicates that VOCs derived from biogenic sources must be considered in photochemical models in order to accurately predict the oxidation capacity and O₃ budget of coastal regions in the northeast U.S.

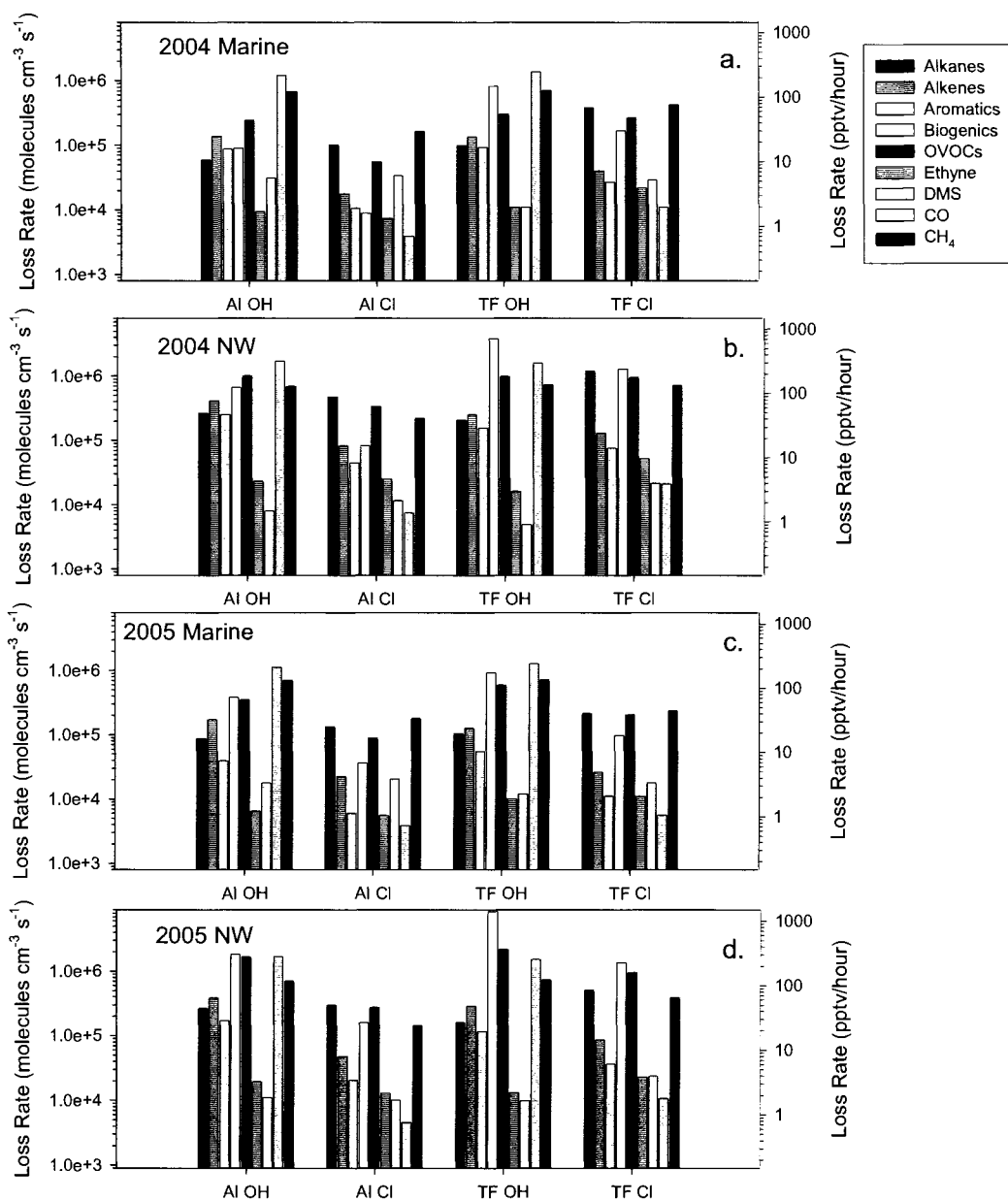


Figure 4.7. VOC, CO, and CH₄ loss rates (left axis: molecules cm⁻³ s⁻¹; right axis: pptv/hour) with respect to reaction with OH and Cl during 2004 at TF and AI in the (a) marine and (b) NW sectors and during 2005 in the (c) marine and (d) NW sectors.

AI2004 marine				TF2004 marine			
Compound	OH+Cl			Compound	OH+Cl		
	Loss Rate	%OH	%Cl		Loss Rate	%OH	%Cl
CO	1.2E+06	1.00	0.00	CO	1.4E+06	0.99	0.01
CH ₄	8.5E+05	0.81	0.19	CH ₄	1.1E+06	0.63	0.37
acetaldehyde	1.7E+05	0.93	0.07	isoprene	7.9E+05	0.84	0.16
methanol	7.6E+04	0.52	0.48	methanol	2.9E+05	0.31	0.69
DMS	6.5E+04	0.48	0.52	MVK+MACR	1.8E+05	0.75	0.25
ethane	5.9E+04	0.21	0.79	ethane	1.5E+05	0.10	0.90
m+p-xylene	5.8E+04	0.89	0.11	propane	1.1E+05	0.17	0.83
isoprene	4.6E+04	0.93	0.07	limonene	7.4E+04	0.88	0.12
β-pinene	3.9E+04	0.91	0.09	acetaldehyde	7.3E+04	0.83	0.17
propane	3.5E+04	0.34	0.66	i-pentane	6.6E+04	0.30	0.70
Ethane	3.5E+04	0.84	0.16	β-pinene	6.6E+04	0.80	0.20
propene	3.3E+04	0.88	0.12	α-pinene	6.2E+04	0.73	0.27
MVK+MACR	3.0E+04	0.88	0.12	m+p-xylene	5.3E+04	0.78	0.22
2-me-2-butene	2.6E+04	0.93	0.07	DMS	4.0E+04	0.27	0.73
Ethyne	1.7E+04	0.56	0.44	propene	3.3E+04	0.75	0.25
α-pinene	1.5E+04	0.87	0.13	ethyne	3.3E+04	0.34	0.66
o-xylene	1.5E+04	0.86	0.14	2-me-2-butene	3.3E+04	0.85	0.15
1,3,5-tmb	1.3E+04	0.94	0.06	n-butane	2.8E+04	0.23	0.77
acetic acid	1.3E+04	1.00	0.00	toluene	2.7E+04	0.73	0.27
t-2-butene	1.0E+04	0.93	0.07	1,3,5-tmb	2.6E+04	0.86	0.14
c-2-butene	9.7E+03	0.91	0.09	c-2-butene	2.3E+04	0.80	0.20
1-pentene	9.5E+03	0.84	0.16	n-pentane	2.3E+04	0.26	0.74
1-butene	9.1E+03	0.86	0.14	n-hexane	2.1E+04	0.29	0.71
Acetone	8.5E+03	0.82	0.18	1-pentene	1.8E+04	0.68	0.32
n-butane	7.9E+03	0.42	0.58	1-butene	1.7E+04	0.71	0.29
n-decane	6.9E+03	0.57	0.43	acetone	1.7E+04	0.64	0.36
n-octane	6.5E+03	0.53	0.47	ethene	1.6E+04	0.68	0.32
mecycchexane	6.1E+03	0.62	0.38	t-2-butene	1.6E+04	0.84	0.16
2-mepentane	5.8E+03	0.54	0.46	n-heptane	1.5E+04	0.31	0.69
toluene	4.9E+03	0.87	0.13	MEK	1.4E+04	0.46	0.54
MEK	4.8E+03	0.67	0.33	n-decane	1.4E+04	0.35	0.65
i-pentane	4.4E+03	0.52	0.48	mecycchexane	1.4E+04	0.40	0.60
i-butane	4.0E+03	0.49	0.51	2,2,4-tmp	1.2E+04	0.25	0.75
3-mepentane	3.6E+03	0.55	0.45	i-butane	1.1E+04	0.28	0.72
n-nonane	3.5E+03	0.57	0.43	n-octane	1.0E+04	0.32	0.68
n-pentane	3.5E+03	0.47	0.53	cyclohexane	1.0E+04	0.35	0.65
2,2,4-tmp	3.5E+03	0.46	0.54	ethylbenzene	8.6E+03	0.61	0.39
Benzene	3.4E+03	0.95	0.05	benzene	5.0E+03	0.89	0.11
n-hexane	3.4E+03	0.50	0.50	acetic acid	4.8E+03	1.00	0.00
Cyclohexane	3.3E+03	0.56	0.44	acetonitrile	1.8E+02	0.98	0.02
ethylbenzene	3.3E+03	0.79	0.21				
n-heptane	3.0E+03	0.53	0.47				
2,4-dmp	2.5E+03	0.52	0.48				
acetonitrile	1.2E+02	0.99	0.01				

Table 4.4a. The OH+Cl loss rates (molecules cm⁻³ s⁻¹) and kinetic reactivity (%OH, %Cl) of VOCs, CO, and CH₄ in the (a) marine and (b) NW sectors at TF and AI in 2004 and 2005. The compounds are listed from highest to lowest loss rate.

AI2005 marine				TF2005 marine			
Compound	OH+Cl			Compound	OH+Cl		
	Loss Rate	%OH	%Cl		Loss Rate	%OH	%Cl
CO	1.1E+06	1.00	0.00	CO	1.3E+06	1.00	0.00
CH ₄	8.9E+05	0.80	0.20	CH ₄	9.5E+05	0.75	0.25
acetaldehyde	2.1E+05	0.92	0.08	isoprene	4.1E+05	0.90	0.10
limonene	1.7E+05	0.94	0.06	limonene	3.6E+05	0.93	0.07
methanol	1.2E+05	0.51	0.49	acetaldehyde	3.0E+05	0.90	0.10
β-pinene	9.8E+04	0.90	0.10	methanol	2.3E+05	0.45	0.55
α-pinene	8.2E+04	0.86	0.14	MVK+MACR	2.2E+05	0.84	0.16
MVK+MACR	7.0E+04	0.87	0.13	3-carene	1.7E+05	0.89	0.11
isoprene	6.7E+04	0.92	0.08	propane	8.4E+04	0.27	0.73
ethane	5.5E+04	0.20	0.80	α-pinene	7.7E+04	0.83	0.17
c-2-butene	4.3E+04	0.90	0.10	ethane	7.4E+04	0.16	0.84
propane	4.3E+04	0.32	0.68	ethene	5.2E+04	0.80	0.20
2-me-2-butene	3.8E+04	0.93	0.07	2-me-2-butene	3.3E+04	0.91	0.09
DMS	3.8E+04	0.46	0.54	i-pentane	3.3E+04	0.44	0.56
ethene	3.1E+04	0.83	0.17	DMS	3.0E+04	0.40	0.60
propene	2.8E+04	0.87	0.13	1-pentene	2.8E+04	0.79	0.21
t-2-butene	2.2E+04	0.92	0.08	m+p-xylene	2.4E+04	0.86	0.14
1-butene	2.0E+04	0.85	0.15	toluene	2.2E+04	0.83	0.17
M+p-xylene	1.8E+04	0.89	0.11	acetone	2.1E+04	0.76	0.24
acetic acid	1.5E+04	1.00	0.00	ethyne	2.1E+04	0.48	0.52
1-pentene	1.3E+04	0.83	0.17	n-pentane	2.1E+04	0.39	0.61
n-butane	1.3E+04	0.41	0.59	n-butane	2.0E+04	0.35	0.65
ethyne	1.2E+04	0.54	0.46	1-butene	2.0E+04	0.82	0.18
acetone	1.2E+04	0.81	0.19	propene	2.0E+04	0.84	0.16
i-pentane	1.0E+04	0.50	0.50	MEK	1.9E+04	0.60	0.40
n-decane	1.0E+04	0.55	0.45	mecyclohexane	1.3E+04	0.54	0.46
o-xylene	1.0E+04	0.85	0.15	o-xylene	1.2E+04	0.81	0.19
n-nonane	8.5E+03	0.55	0.45	n-hexane	1.1E+04	0.42	0.58
MEK	8.3E+03	0.66	0.34	n-decane	1.1E+04	0.49	0.51
3-mepentane	8.1E+03	0.53	0.47	n-heptane	1.0E+04	0.45	0.55
mecyclohexane	8.1E+03	0.60	0.40	acetic acid	1.0E+04	1.00	0.00
n-heptane	7.8E+03	0.51	0.49	n-octane	9.9E+03	0.46	0.54
toluene	7.5E+03	0.86	0.14	n-nonane	9.8E+03	0.49	0.51
2-mepentane	7.2E+03	0.52	0.48	i-butane	8.7E+03	0.41	0.59
2,2,4-tmp	7.2E+03	0.44	0.56	cyclohexane	8.2E+03	0.49	0.51
i-butane	7.1E+03	0.48	0.52	2,2,4-tmp	7.9E+03	0.38	0.62
cyclohexane	6.8E+03	0.55	0.45	ethylbenzene	6.1E+03	0.73	0.27
n-octane	6.8E+03	0.52	0.48	benzene	3.1E+03	0.94	0.06
n-hexane	6.6E+03	0.48	0.52	acetonitrile	1.5E+02	0.99	0.01
n-pentane	6.3E+03	0.45	0.55				
ethylbenzene	5.5E+03	0.78	0.22				
2,3-dmb	5.1E+03	0.61	0.39				
2,4-dmp	4.6E+03	0.50	0.50				
1,3,5-tmb	2.8E+03	0.93	0.07				
benzene	1.7E+03	0.95	0.05				
acetonitrile	1.0E+02	0.99	0.01				

Table 4.4a. continued. The loss rates (molecules cm⁻³ s⁻¹) and kinetic reactivity of VOCs, CO, and CH₄ in the marine sector at TF and AI in 2005.

AI2004 NW				TF2004 NW			
Compound	OH+Cl			Compound	OH+Cl		
	Loss Rate	%OH	%Cl		Loss Rate	%OH	%Cl
CO	1.7E+06	1.00	0.00	isoprene	4.1E+06	0.76	0.24
CH ₄	9.2E+05	0.76	0.24	CO	1.6E+06	0.99	0.01
acetaldehyde	5.4E+05	0.90	0.10	CH ₄	1.5E+06	0.51	0.49
methanol	3.8E+05	0.45	0.55	MVK+MACR	8.5E+05	0.65	0.35
isoprene	3.7E+05	0.90	0.10	methanol	6.7E+05	0.21	0.79
MVK+MACR	3.6E+05	0.85	0.15	propane	4.3E+05	0.11	0.89
β-pinene	2.0E+05	0.88	0.12	α-pinene	3.9E+05	0.62	0.38
propane	2.0E+05	0.28	0.72	β-pinene	3.5E+05	0.71	0.29
ethene	1.9E+05	0.80	0.20	acetaldehyde	3.3E+05	0.75	0.25
propene	1.4E+05	0.84	0.16	ethane	2.6E+05	0.06	0.94
m+p-xylene	1.3E+05	0.86	0.14	limonene	2.5E+05	0.81	0.19
α-pinene	1.1E+05	0.83	0.17	i-pentane	2.4E+05	0.21	0.79
i-pentane	1.0E+05	0.44	0.56	n-butane	1.0E+05	0.15	0.85
ethane	9.4E+04	0.16	0.84	n-pentane	9.9E+04	0.18	0.82
toluene	8.3E+04	0.83	0.17	m+p-xylene	9.5E+04	0.68	0.32
limonene	7.0E+04	0.93	0.07	propene	9.1E+04	0.64	0.36
n-butane	5.7E+04	0.35	0.65	ethene	7.0E+04	0.57	0.43
ethyne	4.8E+04	0.48	0.52	ethyne	6.8E+04	0.24	0.76
n-pentane	4.8E+04	0.40	0.60	toluene	6.8E+04	0.62	0.38
2-mepentane	3.9E+04	0.47	0.53	n-hexane	6.0E+04	0.20	0.80
o-xylene	3.3E+04	0.82	0.18	2-me-2-butene	5.0E+04	0.78	0.22
3-mepentane	3.1E+04	0.47	0.53	MEK	4.8E+04	0.34	0.66
n-hexane	3.1E+04	0.43	0.57	1,3,5-tmb	4.3E+04	0.79	0.21
MEK	2.8E+04	0.61	0.39	2,2,4-tmp	4.3E+04	0.17	0.83
i-butane	2.5E+04	0.42	0.58	acetone	4.2E+04	0.52	0.48
2-me-2-butene	2.5E+04	0.91	0.09	c-2-butene	3.7E+04	0.71	0.29
acetone	2.4E+04	0.77	0.23	i-butane	3.5E+04	0.19	0.81
1,3,5-tmb	2.4E+04	0.92	0.08	n-heptane	3.4E+04	0.22	0.78
2,2,4-tmp	2.4E+04	0.38	0.62	1-butene	3.2E+04	0.60	0.40
1-butene	2.4E+04	0.82	0.18	t-2-butene	3.1E+04	0.76	0.24
acetic acid	2.2E+04	1.00	0.00	mecychexane	2.9E+04	0.28	0.72
n-decane	2.0E+04	0.49	0.51	n-decane	2.8E+04	0.24	0.76
DMS	2.0E+04	0.41	0.59	1-pentene	2.8E+04	0.56	0.44
1-pentene	1.9E+04	0.79	0.21	DMS	2.6E+04	0.19	0.81
n-heptane	1.8E+04	0.46	0.54	cyclohexane	2.3E+04	0.24	0.76
c-2-butene	1.7E+04	0.88	0.12	n-octane	2.1E+04	0.22	0.78
t-2-butene	1.7E+04	0.90	0.10	ethylbenzene	1.9E+04	0.48	0.52
ethylbenzene	1.4E+04	0.74	0.26	acetic acid	1.3E+04	1.00	0.00
mecychexane	1.3E+04	0.54	0.46	benzene	6.7E+03	0.83	0.17
cyclohexane	1.2E+04	0.49	0.51	acetonitrile	1.6E+02	0.97	0.03
n-nonane	1.1E+04	0.50	0.50				
n-octane	9.8E+03	0.46	0.54				
2,4-dmp	8.2E+03	0.45	0.55				
benzene	7.6E+03	0.94	0.06				
acetonitrile	1.4E+02	0.99	0.01				

Table 4.4b. continued. The loss rates (molecules cm⁻³ s⁻¹) and kinetic reactivity of VOCs, CO, and CH₄ in the (b) NW sector at TF and AI in 2004.

AI2005 NW				TF2005 NW			
Compound	OH+Cl			Compound	OH+Cl		
	Loss Rate	%OH	%Cl		Loss Rate	%OH	%Cl
CO	1.7E+06	1.00	0.00	isoprene	4.4E+06	0.85	0.15
MVK+MACR	9.1E+05	0.90	0.10	limonene	3.9E+06	0.89	0.11
isoprene	8.7E+05	0.94	0.06	MVK+MACR	1.7E+06	0.77	0.23
CH ₄	8.5E+05	0.83	0.17	CO	1.5E+06	0.99	0.01
acetaldehyde	6.4E+05	0.94	0.06	CH ₄	1.1E+06	0.66	0.34
α-pinene	5.4E+05	0.89	0.11	β-pinene	8.9E+05	0.83	0.17
β-pinene	4.2E+05	0.92	0.08	acetaldehyde	6.6E+05	0.85	0.15
methanol	3.0E+05	0.57	0.43	methanol	6.3E+05	0.34	0.66
limonene	1.7E+05	0.95	0.05	α-pinene	5.7E+05	0.75	0.25
ethene	1.7E+05	0.86	0.14	propane	2.2E+05	0.19	0.81
propane	1.5E+05	0.38	0.62	ethane	1.3E+05	0.11	0.89
propene	1.2E+05	0.90	0.10	ethene	1.0E+05	0.71	0.29
m+p-xylene	7.7E+04	0.91	0.09	i-pentane	7.2E+04	0.33	0.67
i-pentane	6.7E+04	0.56	0.44	m+p-xylene	6.5E+04	0.80	0.20
toluene	6.2E+04	0.89	0.11	2-me-2-butene	6.2E+04	0.87	0.13
ethane	5.9E+04	0.24	0.76	propene	5.5E+04	0.77	0.23
n-butane	4.6E+04	0.46	0.54	MEK	5.3E+04	0.49	0.51
2-me-2-butene	4.4E+04	0.94	0.06	n-pentane	5.1E+04	0.29	0.71
acetic acid	3.9E+04	1.00	0.00	acetone	4.6E+04	0.67	0.33
n-pentane	3.5E+04	0.51	0.49	toluene	4.6E+04	0.75	0.25
Ethyne	3.2E+04	0.60	0.40	n-butane	4.3E+04	0.25	0.75
c-2-butene	3.2E+04	0.92	0.08	1-butene	4.3E+04	0.74	0.26
Acetone	3.1E+04	0.84	0.16	acetic acid	4.1E+04	1.00	0.00
2-mepentane	3.0E+04	0.58	0.42	1-pentene	4.1E+04	0.70	0.30
t-2-butene	2.9E+04	0.94	0.06	t-2-butene	3.7E+04	0.85	0.15
3-mepentane	2.8E+04	0.59	0.41	ethyne	3.6E+04	0.36	0.64
MEK	2.7E+04	0.71	0.29	DMS	3.3E+04	0.30	0.70
o-xylene	2.6E+04	0.88	0.12	c-2-butene	3.2E+04	0.82	0.18
1-butene	2.4E+04	0.88	0.12	n-hexane	2.5E+04	0.31	0.69
DMS	2.1E+04	0.52	0.48	n-heptane	2.3E+04	0.34	0.66
i-butane	2.1E+04	0.53	0.47	o-xylene	2.3E+04	0.73	0.27
n-hexane	2.0E+04	0.54	0.46	n-decane	2.0E+04	0.37	0.63
n-decane	1.8E+04	0.61	0.39	cyclohexane	1.9E+04	0.37	0.63
1-pentene	1.8E+04	0.86	0.14	mecychexane	1.8E+04	0.42	0.58
n-heptane	1.7E+04	0.57	0.43	i-butane	1.7E+04	0.31	0.69
ethylbenzene	1.5E+04	0.82	0.18	2,2,4-tmp	1.5E+04	0.28	0.72
n-octane	1.3E+04	0.58	0.42	ethylbenzene	1.5E+04	0.63	0.37
2,2,4-tmp	1.2E+04	0.50	0.50	n-nonane	1.5E+04	0.38	0.62
n-nonane	1.2E+04	0.61	0.39	n-octane	1.2E+04	0.35	0.65
2,3-dmb	1.1E+04	0.66	0.34	benzene	4.4E+03	0.90	0.10
mecychexane	1.1E+04	0.65	0.35	acetonitrile	1.9E+02	0.98	0.02
cychexane	8.9E+03	0.61	0.39				
2,4-dmp	6.3E+03	0.56	0.44				
Benzene	5.8E+03	0.96	0.04				
1,3,5-tmb	5.5E+03	0.95	0.05				
Acetonitrile	1.7E+02	0.99	0.01				

Table 4.4b. continued. The loss rates (molecules cm⁻³ s⁻¹) and kinetic reactivity of VOCs, CO, and CH₄ in the (b) NW sector at TF and AI in 2005.

4.6 DMS Trends and Oxidation

Dimethyl sulfide is produced by marine phytoplankton and is the dominant biogenic sulfur compound emitted from the ocean. The oxidation of DMS in the atmosphere is the major precursor of non-sea-salt sulfate (nss-SO₄) aerosol. Thus, DMS also serves as an important gas-phase precursor of cloud condensation nuclei (CCN). As a result, the biogeochemical cycling of DMS influences cloud formation and residence times, precipitation rates, cloud and surface albedo, the radiative balance of the earth, and aerosol production, growth, and acidity (e.g., Charlson et al., 1987; Pandis et al., 1994). Therefore, it is essential that the emission and removal processes of DMS in marine and coastal regions are accurately quantified.

4.6.1 Diurnal Cycle and Removal Mechanisms of DMS at AI

The diurnal cycle of a compound in the atmosphere reflects the combined effects of emission, chemical production, chemical loss (oxidation, photolysis, heterogeneous reactions), deposition (wet and/or dry), advection, and vertical mixing. Therefore, analyzing the diurnal cycle of a compound provides information on the relative contributions of these various processes. At AI during 2004, DMS exhibited a pronounced diurnal cycle in the marine sector with peak mixing ratios occurring at night (>100 pptv) that decreased throughout the morning to mid afternoon (06:00-15:00) (Figure 4.8). Enhanced emission rates of DMS from the ocean typically coincide with increasing wind speed (e.g., Carpenter et al., 2004; Huebert et al., 2004; Marandino et al., 2008). However, the hourly average wind speed in the marine sector increased from ~6 m/s at 05:00 to 8.5 m/s at 09:00 (Figure 4.8). The coincident decrease in DMS between 06:00-09:00 indicates that removal processes were dominant.

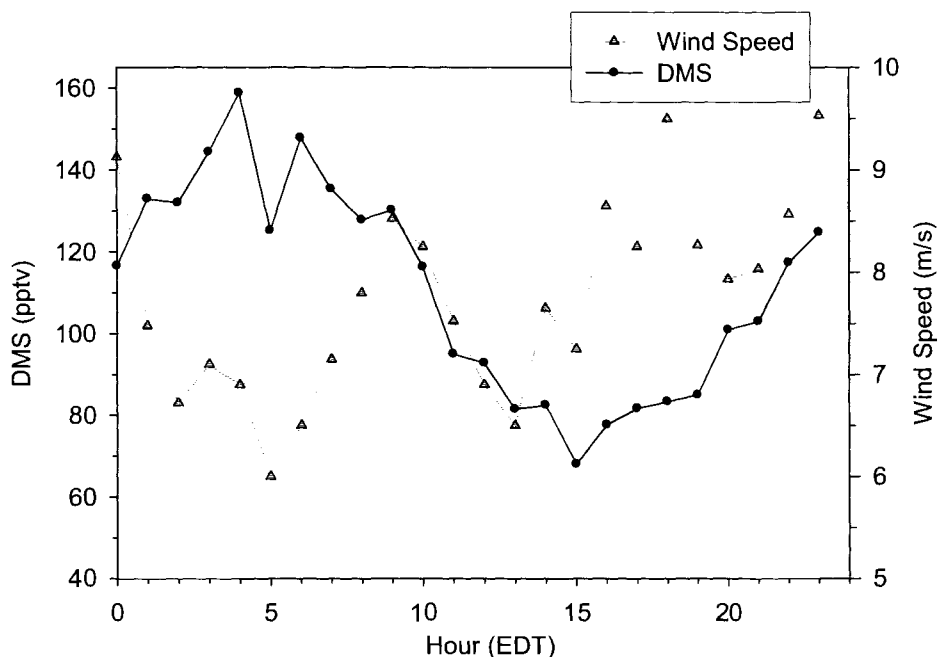


Figure 4.8. Hourly average DMS (pptv) and wind speed (m/s) at AI during 2004 in the marine sector. The yellow curve is the hourly average J_{NO_2} (s^{-1}) from TF.

The possible removal mechanisms of DMS from the atmosphere are oxidation, advection, and mixing. DMS may react with several different oxidants, including OH ($k_{\text{OH}} = 4.8 \times 10^{-12} \text{ cm}^3 \text{ molecule}^{-1} \text{ s}^{-1}$), Cl ($k_{\text{Cl}} = 3.4 \times 10^{-10} \text{ cm}^3 \text{ molecule}^{-1} \text{ s}^{-1}$), the nitrate radical (NO_3 , $k_{\text{NO}_3} = 1 \times 10^{-12} \text{ cm}^3 \text{ molecule}^{-1} \text{ s}^{-1}$), and bromine monoxide (BrO , $k_{\text{BrO}} = 4.3 \times 10^{-13} \text{ cm}^3 \text{ molecule}^{-1} \text{ s}^{-1}$) (Atkinson et al., 2006b). During the AI 2004 campaign, a long path differential optical absorption spectroscopy system was deployed on AI for measuring several trace gases, including NO_3 and BrO (Pikelnaya et al., 2007). The nitrate radical is produced from the reaction between NO_2 and O_3 ($\text{NO}_2 + \text{O}_3 \rightarrow \text{NO}_3 + \text{O}_2$) and is rapidly removed during the day by photolysis and reaction with NO (e.g., Wayne et al., 1991). In this region, NO_3 only builds up at night when sufficient levels of NO_x are available (i.e., in air masses from urban source regions and continental outflow from the eastern U. S.) (e.g., Brown et al., 2006; Ambrose et al., 2007). At AI, NO_3 was

not detected after ~05:00 following nights when enhanced mixing ratios were observed (Ambrose et al., 2007). Therefore, DMS loss by reaction with NO₃ was neglected. The nighttime increase in hourly average DMS mixing ratios in the marine sector reflects continuous emission from the ocean and is consistent with the lack of NO from source regions and thus a lack of NO₃ production. In addition, BrO was not detected (Keene et al., 2007) and was neglected in the following analysis of the chemical processes regulating the DMS diurnal cycle. The following discussion also does not include entrainment from the free troposphere and vertical mixing, which likely made non-negligible contributions. However, it is safe to assume that the DMS mixing ratio in the free troposphere is near zero because it is emitted from the ocean surface and has a short lifetime (<~1 day) with respect to OH, halogens, and NO₃.

The expected mixing ratios of DMS were calculated under the assumption that the only important daytime oxidants of DMS were OH and Cl:

$$[\text{DMS}] = [\text{DMS}_i] \exp(-(\text{k}_{\text{OH}}[\text{OH}] + \text{k}_{\text{Cl}}[\text{Cl}]) * t) \quad (4)$$

where [DMS_i] is the mixing ratio at 06:00 (148 pptv = 3.6 x 10⁹ molecules cm⁻³) and t is time (seconds). Chlorine atom concentrations estimated for the marine sector (Table 4.3) and the constant OH concentration used in the lifetime-variability analysis were used to calculate the DMS mixing ratio. For comparison, a diurnally varying OH concentration was estimated using the parameterization of Ehhalt and Rohrer (2000) (Figure 4.9a). The O₃ photolysis frequency (*J*_{O₃}) for each hour between 05:00-19:00 was obtained from the Tropospheric Ultraviolet and Visible (TUV) radiation model with input values based on July 19, 2004 at the latitude and longitude of AI (<http://cprm.acd.ucar.edu/Models/TUV>). This date was chosen as a representative example of the conditions when transport from

the marine sector influenced TF and AI (Figure 4.2). The hourly average J_{NO_2} from TF in the marine sector was used because J_{NO_2} was not measured at AI. An estimated NO_2 mixing ratio for nights with marine transport of 0.2 ppbv was used (Ambrose et al., 2007). A comparison between $[\text{OH}]$ calculated using measured NMHC and NO_x mixing ratios during NEAQS 2002 in the Gulf of Maine and the Ehhalt and Rohrer (2000) parameterization agreed fairly well (slope = 0.79, $r^2 = 0.84$) and yielded an average $[\text{OH}]$ of 2.5×10^6 molecules cm^{-3} (Warneke et al., 2004).

The DMS mixing ratios calculated using the TUV OH (OH_{calc}) agree (within error bars) with the observations until $\sim 10:00$, but overestimate the DMS removal by $\sim 10\text{-}50\%$ during late morning to mid-afternoon (Figure 4.9b). Additional $[\text{Cl}]$ estimates were obtained using the lifetime-variability relationship for the daytime marine sector data which was separated into three time bins (06:00-09:00, 10:00-13:00, 14:00-17:00). These three groups were chosen to correspond to the rapid morning increase in photolysis frequencies, the midday peak in OH and Cl concentrations, and the afternoon reduction in OH and Cl production (Figure 4.9a). The resulting $[\text{Cl}]$ ($\text{Cl}_{\text{varied}}$) were 6.2×10^4 , 5.3×10^4 , and 8.9×10^3 molecules cm^{-3} , respectively. The higher $[\text{Cl}]$ at 06:00-09:00 is consistent with the build up of photolabile Cl precursors overnight and rapid photolysis after sunrise. When these $[\text{Cl}]$ are used in (4) along with the TUV OH, a similar trend occurs in the calculated DMS as when $[\text{Cl}]=0$ (pink line Figure 4.9b). The agreement between observed and predicted DMS is much better when a constant OH concentration and the $[\text{Cl}]$ derived for the marine sector based on optimizing the variability-lifetime relationships are used. In these cases, the calculated DMS falls within the observed error bars throughout the entire time period of decreasing mixing ratios (Figure 4.9b).

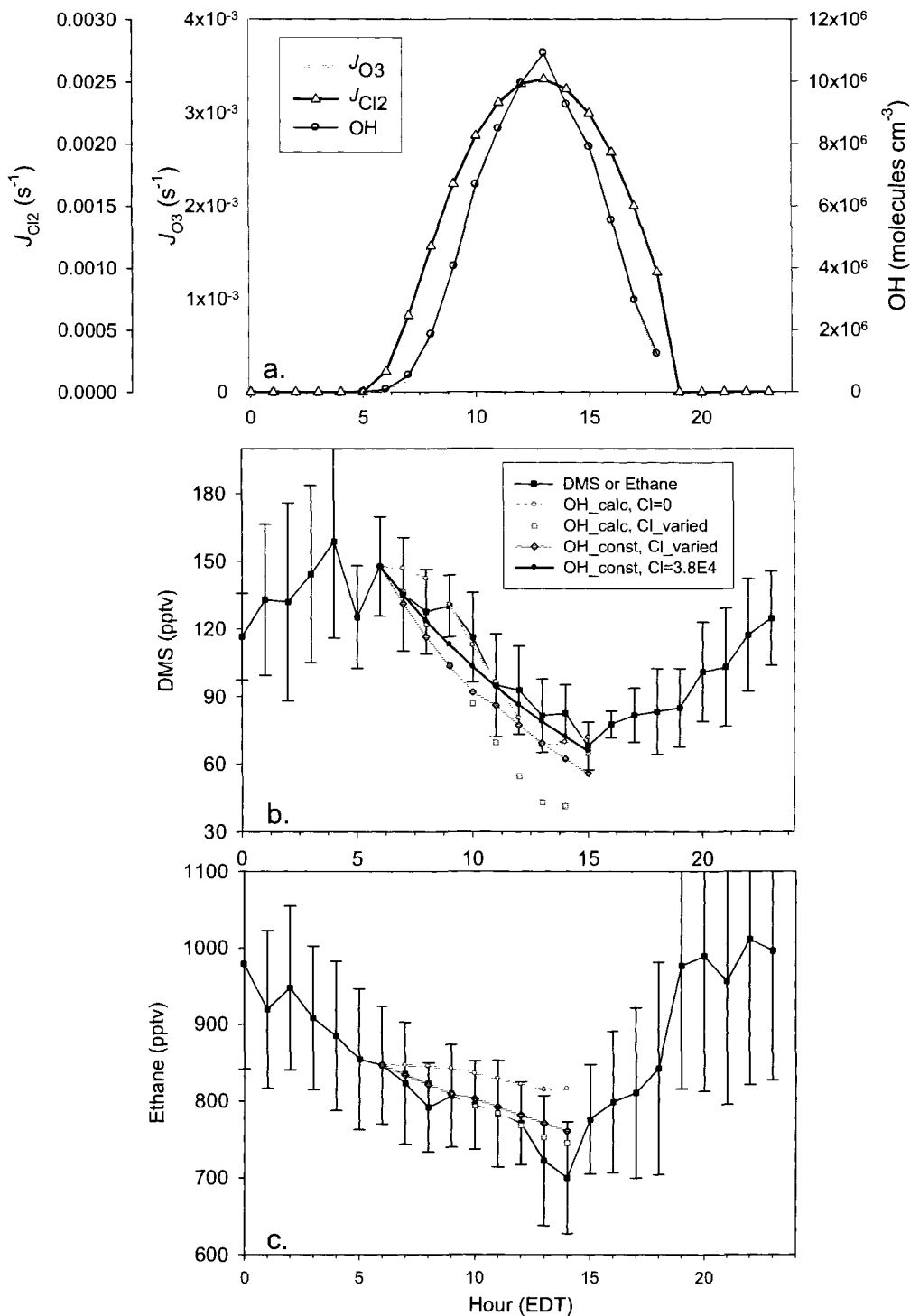


Figure 4.9. (a) Hourly ozone (J_{O_3}) and chlorine (J_{Cl_2}) photolysis frequencies (s^{-1}) and calculated OH concentrations (molecules cm^{-3}), (b) hourly average (\pm standard deviation of the mean) DMS and (c) ethane mixing ratios (pptv) in the marine sector at AI in 2004. The colored lines refer to different sensitivity studies with varying OH and Cl concentrations in equation 4.

The larger discrepancy between observed and calculated DMS mixing ratios when the variable [OH] was used likely indicates that the midday peak [OH] ($\sim 10^7$ molecules cm^{-3}) was overestimated by the TUV model (Figure 4.9a). While it is unrealistic that [OH] was constant throughout the entire day, it is reasonable to assume that [OH] was relatively low. In the marine sector, the mixing ratios of OH precursors were low (Table 4.1), and the median temperature (15.6°C compared to $17\text{-}19^\circ\text{C}$) and J_{NO_2} were lower than the other four sectors. This indicates that the atmospheric conditions were less favorable for OH production and may have resulted in less variable concentrations.

A similar analysis was performed using ethane. It was assumed that any potential marine source of ethane was negligible. Ethane was chosen as a long-lived NMHC with a significantly faster rate of reaction with Cl than OH (Table 4.2). The hourly average ethane mixing ratios in the marine sector decreased throughout the entire night, and by 147 pptv during the time corresponding to the reduction in DMS mixing ratios (Figure 4.9c). In contrast to DMS, the predicted ethane mixing ratios fell within the error bars when the TUV OH was used. This is likely a consequence of the slower rate of reaction between OH and ethane than with DMS (Table 4.2). The predicted ethane mixing ratios were in closer agreement ($\leq 10\%$) with the observed hourly averages when a [Cl] concentration estimated using the lifetime-variability method was used in (4). The increase at 14:00 in the calculated DMS and ethane mixing ratios when the [Cl] for the 3 daytime bins was used reflects the lower estimated [Cl] in the 14:00-17:00 group.

4.6.2 Comparison with Previous Studies

The ambient diurnal cycle of DMS displays considerable regional variability. Unexplained behavior in the DMS diurnal cycle has been hypothesized to reflect both

chemical and dynamical processes. For example, Stark et al. (2007) observed an early morning maximum and an evening minimum in atmospheric DMS mixing ratios in the Gulf of Maine that was modeled more accurately when halogens (Cl, BrO) were included. The best agreement was obtained when an [OH]/[Cl] ratio of 80 was invoked (Stark et al., 2007). This ratio value is within the range of our estimated ratios (~10-85) (Table 4.3). Furthermore, several measurement-modeling studies suggested that discrepancies between observed and predicted DMS diurnal cycles could be explained by including an additional oxidant, most likely Cl or BrO, during the daytime and/or by increasing the oxidation rate of DMS by factors of ~0.5-3 (Yvon et al., 1996; James et al., 2000; Sciare et al., 2000). Moreover, de Bruyn et al. (2006) concluded that dynamic processes (i.e., mixing), as well as oxidation by halogens, likely contributed to the DMS cycle near Hawaii based on inconsistencies between observed and modeled DMS and its major oxidation product, SO₂. The close agreement between the measured DMS with the mixing ratios calculated by including Cl atom concentrations derived from the lifetime-variability relationships of observed NMHCs at AI provides supporting evidence for the importance of halogens in the atmospheric sulfur budget of coastal regions. This additional oxidation of DMS will influence the formation of nss-SO₄ aerosols, and consequently CCN production, and will alter aerosol acidity and thus the phase partitioning of nitrogen and sulfur species.

4.7 Summary

The potential influence of chlorine chemistry on VOCs at an inland (Thompson Farm, Durham, NH) and an offshore (Appledore Island, ME) site during July-August 2004 and 2005 was examined. Chlorine atom concentrations ranging from (2.9-29) x 10⁴

molecules cm^{-3} were estimated by optimizing the fit between the variability and lifetime of eight selected NMHCs (C_3 - C_5 alkanes, ethyne, benzene, toluene). These concentrations are comparable to estimates made using the more common method involving NMHC ratios. In addition, the lifetime-variability analysis demonstrated that the composition of air masses encountered at TF and AI during 2004 reflected a stronger influence from chemical processing and/or mixing. Relative to the results from 2004, local/regional emissions and shorter transport distances characterized the chemical composition of air masses during July-August 2005. These trends are consistent with the more frequent transport of aged Canadian and marine air masses to New England in 2004. Furthermore, observed rates of DMS and ethane loss in marine air masses were best explained by including reaction with Cl (in addition to OH) at the concentrations estimated in this work.

LIST OF REFERENCES

- Altshuller, A. P.: Chemical reactions and transport of alkanes and their products in the troposphere, *J. Atmos. Chem.*, 12, 19-61, 1991.
- Ambrose, J. L., Mao, H., Mayne, H. R., Stutz, J., Talbot, R., and Sive, B. C.: Nighttime nitrate radical chemistry at Appledore Island, Maine during the 2004 International Consortium for Atmospheric Research on Transport and Transformation, *J. Geophys. Res.*, 112, D21302, doi:10.1029/2007JD008756, 2007.
- Anderson, R. S., Huang, L., Iannone, R., and Rudolph, J.: Laboratory measurements of the $^{12}\text{C}/^{13}\text{C}$ kinetic isotope effects in the gas-phase reactions of unsaturated hydrocarbons with Cl atoms at 298 ± 3 K, *J. Atmos. Chem.*, 56, 275-291, 2007.
- Angevine, W. M., Senff, C. J., White, A. B., Williams, E. J., Koerner, J., Miller, S. T. K., Talbot, R., Johnston, P. E., McKeen, S. A., and Downs, T.: Coastal boundary layer influence on pollutant transport in New England, *J. Appl. Meteorol.*, 43, 1425-1437, 2004.
- Arey, J., Aschmann, S. M., Kwok, E. S. C., and Atkinson, R.: Alkyl nitrate, hydroxyalkyl nitrate, and hydroxycarbonyl formation from the NO_x -air photooxidations of C_5 - C_8 n-alkanes, *J. Phys. Chem. A*, 105, 1020-1027, 2001.
- Ariya, P. A., Jobson, B. T., Sander, R., Niki, H., Harris, G. W., Hopper, J. F., and Anlauf, K. G.: Measurements of C_2 - C_7 hydrocarbons during the Polar Sunrise Experiment 1994: Further evidence for halogen chemistry in the troposphere, *J. Geophys. Res.*, 103, 13169-13180, 1998.
- Atkinson, R., Aschmann, S. M., Carter, W. P. L., Winer, A. M., and Pitts, J. N.: Alkyl nitrate formation from the NO_x -air photooxidations of C_2 - C_8 n-alkanes, *J. Phys. Chem.*, 86, 4563-4569, 1982.
- Atkinson, R., Aschmann, S. M., and Winer, A. M.: Alkyl nitrate formation from the reaction of a series of branched RO_2 radicals with NO as a function of temperature and pressure, *J. Atmos. Chem.*, 5, 91-102, 1987.
- Atkinson, R.: Gas-phase tropospheric chemistry of organic compounds- A review, *Atmos. Environ., A-Gen*, 24, 1-41, 1990.
- Atkinson, R.: Gas-phase tropospheric chemistry of volatile organic compounds 1. Alkanes and alkenes, *J. Phys. Chem. Ref. Data*, 26, 215-290, 1997.

Atkinson, R.: Kinetics of the gas-phase reactions of OH radicals with alkanes and cycloalkanes, *Atmos. Chem. Phys.*, 3, 2233-2307, 2003.

Atkinson, R., and Arey, J.: Gas-phase tropospheric chemistry of biogenic volatile organic compounds: A review, *Atmos. Environ.*, 27, S197-S219, 2003.

Atkinson, R., Baulch, D. L., Cox, R. A., Crowley, J. N., Hampson, R. F., Hynes, R. G., Jenkin, M. E., Rossi, M. J., Troe, J.: Evaluated kinetic and photochemical data for atmospheric chemistry: Volume II- gas phase reactions of organic species, *Atmos. Chem. Phys.*, 6, 3625-4055, 2006a.

Atkinson, R., Baulch, D. L., Cox, R. A., Crowley, J. N., Hampson, R. F., Hynes, R. G., Jenkin, M. E., Rossi, M. J., Troe, J.: Summary of Evaluated Kinetic and Photochemical Data for Atmospheric Chemistry, web version, <http://www.iupac-kinetic.ch.cam.ac.uk>, February, 2006b.

Atlas, E., Pollock, W., Greenberg, J., Heidt, L., and Thompson, A. M.: Alkyl nitrates, nonmethane hydrocarbons, and halocarbon gases over the equatorial Pacific ocean during SAGA-3, *J. Geophys. Res.*, 98, 16933-16947, 1993.

Barletta, B., Meinardi, S., Simpson, I. J., Khwaja, H. A., Blake, D. R., and Rowland, F. S.: Mixing ratios of volatile organic compounds (VOCs) in the atmosphere of Karachi, Pakistan, *Atmos. Environ.*, 36, 3429-3443, 2002.

Barletta, B., Meinardi, S., Simpson, I. J., Zou, S. C., Rowland, F. S., and Blake, D. R.: Ambient mixing ratios of nonmethane hydrocarbons (NMHCs) in two major urban centers of the Pearl River Delta (PRD) region: Guangzhou and Dongguan, *Atmos. Environ.*, 42, 4393-4408, 10.1016/j.atmosenv.2008.01.028, 2008.

Barnes, D. H., Wofsy, S. C., Fehrlau, B. P., Gottlieb, E. W., Elkins, J. W., Dutton, G. S., and Montzka, S. A.: Urban/industrial pollution for the New York City - Washington, DC, corridor, 1996-1998: 1. Providing independent verification of CO and PCE emissions inventories, *J. Geophys. Res.*, 108, 4185, doi:10.1029/2001jd001116, 2003.

Becker, K. H., and Wirtz, K.: Gas-phase reactions of alkyl nitrates with hydroxyl radicals under tropospheric conditions in comparison with photolysis, *J. Atmos. Chem.*, 9, 419-433, 1989.

Bertman, S. B., Roberts, J. M., Parrish, D. D., Buhr, M. P., Goldan, P. D., Kuster, W. C., Fehsenfeld, F. C., Montzka, S. A., and Westberg, H.: Evolution of alkyl nitrates with air-mass age, *J. Geophys. Res.*, 100, 22805-22813, 1995.

Blake, D. R., and Rowland, F. S.: Urban leakage of liquefied petroleum gas and its impact on Mexico City air quality, *Science*, 269, 953-956, 1995.

- Blake, N. J., et al.: Aircraft measurements of the latitudinal, vertical, and seasonal variations of NMHCs, methyl nitrate, methyl halides, and DMS during the First Aerosol Characterization Experiment (ACE 1), *J. Geophys. Res.*, 104, 21,803-21,817, 1999.
- Blake, N. J., Blake, D. R., Swanson, A. L., Atlas, E., Flocke, F., and Rowland, F. S.: Latitudinal, vertical, and seasonal variations of C₁-C₄ alkyl nitrates in the troposphere over the Pacific Ocean during PEM-Tropics A and B: Oceanic and continental sources, *J. Geophys. Res.*, 108, 8242, doi:10.1029/2001jd001444, 2003a.
- Blake, N. J., Blake, D. R., Sive, B. C., Katzenstein, A. S., Meinardi, S., Wingenter, O. W., Atlas, E. L., Flocke, F., Ridley, B. A., and Rowland, F. S.: The seasonal evolution of NMHCs and light alkyl nitrates at middle to high northern latitudes during TOPSE, *J. Geophys. Res.*, 108, 8359, doi:10.1029/2001jd001467, 2003b.
- Boissard, C., Bonsang, B., Kanakidou, M., and Lambert, G.: TROPOZ II: Global distributions and budgets of methane and light hydrocarbons, *J. Atmos. Chem.*, 25, 115-148, 1996.
- Bottenheim, J. W., and Shepherd, M. F.: C₂-C₆ hydrocarbon measurements at 4 rural locations across Canada, *Atmos. Environ.*, 29, 647-664, 1995.
- Brasseur, G. P., Orlando, J. J., and Tyndall, G. S.: *Atmospheric chemistry and global change*, Oxford University Press, New York, 1999.
- Brown, S. S., et al.: Nocturnal odd-oxygen budget and its implications for ozone loss in the lower troposphere, *Geophys. Res. Lett.*, 33, L08801, doi:10.1029/2006G1025900, 2006.
- Canosa-Mas, C. E., Cotter, E. S. N., Duffy, J., Thompson, K. C., and Wayne, R. P.: The reactions of atomic chlorine with acrolein, methacrolein and methyl vinyl ketone, *Phys. Chem. Chem. Phys.*, 3, 3075-3084, 2001.
- Carpenter, L. J., Lewis, A. C., Hopkins, J. R., Read, K. A., Longley, I. D., and Gallagher, M. W.: Uptake of methanol to the North Atlantic Ocean surface, *Global Biogeochem. Cy.*, 18, Gb4027, doi:10.1029/2004gb002294, 2004.
- Carter, W. P. L.: Development of ozone reactivity scales for volatile organic compounds, *J. Air & Waste Manage. Assoc.*, 44, 881-899, 1994.
- Chang, S. Y., and Allen, D. T.: Atmospheric chlorine chemistry in southeast Texas: Impacts on ozone formation and control, *Environ. Sci. Technol.*, 40, 251-262, doi:10.1021/es050787z, 2006.
- Charlson, R. J., Lovelock, J. E., Andreae, M. O., and Warren, S. G.: Oceanic phytoplankton, atmospheric sulfur, cloud albedo and climate, *Nature*, 326, 655-661, 1987.

Chen, M., Talbot, R., Mao, H. T., Sive, B., Chen, J. J., and Griffin, R. J.: Air mass classification in coastal New England and its relationship to meteorological conditions, *J. Geophys. Res.*, 112, D10S05, doi:10.1029/2006jd007687, 2007.

Chen, T. Y., Simpson, I. J., Blake, D. R., and Rowland, F. S.: Impact of the leakage of liquefied petroleum gas (LPG) on Santiago air quality, *Geophys. Res. Lett.*, 28, 2193-2196, 2001.

Choi, Y. J., and Ehrman, S. H.: Investigation of sources of volatile organic carbon in the Baltimore area using highly time-resolved measurements, *Atmos. Environ.*, 38, 775-791, 10.1016/j.atmosenv.2003.10.004, 2004.

Chuck, A. L., Turner, S. M., and Liss, P. S.: Direct evidence for a marine source of C₁ and C₂ alkyl nitrates, *Science*, 297, 1151-1154, 2002.

Clemetshaw, K. C., Williams, J., Rattigan, O. V., Shallcross, D. E., Law, K. S., and Cox, R. A.: Gas-phase ultraviolet absorption cross-sections and atmospheric lifetimes of several C₂-C₅ alkyl nitrates, *J. Photoch. Photobio. A*, 102, 117-126, 1997.

Cohan, A., Chang, W., Carreras-Sospedra, M., and Dabdub, D.: Influence of sea-salt activated chlorine and surface-mediated renoxification on the weekend effect in the South Coast Air Basin of California, *Atmos. Environ.*, 42, 3115-3129, 10.1016/j.atmosenv.2007.11.046, 2008.

Conner, T. L., Lonneman, W. A., and Seila, R. L.: Transportation related volatile hydrocarbon source profiles measured in Atlanta, *J. Air & Waste Manage. Assoc.*, 45, 383-394, 1995.

Cornell, S. E., Jickells, T. D., Cape, J. N., Rowland, A. P., and Duce, R. A.: Organic nitrogen deposition on land and coastal environments: a review of methods and data, *Atmos. Environ.*, 37, 2173-2191, 10.1016/s1352-2310(03)00133-x, 2003.

Crutzen P. J., and Lelieveld, J.: Human impacts on atmospheric chemistry, *Annu. Rev. Earth Planet. Sci*, 29, 17-45, 2001.

Dahl, E. E., Yvon-Lewis, S. A., and Saltzman, E. S.: Saturation anomalies of alkyl nitrates in the tropical Pacific Ocean, *Geophys. Res. Lett.*, 32, L20817, doi:10.1029/2005gl023896, 2005.

Dahl, E. E., Yvon-Lewis, S. A., and Saltzman, E. S.: Alkyl nitrate (C₁-C₃) depth profiles in the tropical Pacific Ocean, *J. Geophys. Res.*, 112, C01012, doi:10.1029/2006jc003471, 2007.

de Bruyn, W. J., Dahl, E., and Saltzman, E. S.: DMS and SO₂ measurements in the tropical marine boundary layer, *J. Atmos. Chem.*, 53, 145-154, 10.1007/s10874-005-9000-z, 2006.

de Gouw, J. A., et al.: Budget of organic carbon in a polluted atmosphere: Results from the New England Air Quality Study in 2002, *J. Geophys. Res.*, 110, D16305, doi:10.1029/2004jd005623, 2005.

Dimmer, C. H., McCulloch, A., Simmonds, P. G., Nickless, G., Bassford, M. R., and Smythe-Wright, D.: Tropospheric concentrations of the chlorinated solvents, tetrachloroethene and trichloroethene, measured in the remote northern hemisphere, *Atmos. Environ.*, 35, 1171-1182, 2001.

Doskey, P. V., Kotamarthi, V. R., Fukui, Y., Cook, D. R., Breitbeil, F. W., and Wesely, M. L.: Air-surface exchange of peroxyacetyl nitrate at a grassland site, *J. Geophys. Res.*, 109, D10310, doi:10.1029/2004jd004533, 2004.

Draxler, R.R. and Rolph, G.D.: HYSPLIT (HYbrid Single-Particle Lagrangian Integrated Trajectory) Model, NOAA Air Resources Laboratory, Silver Spring, MD (Available at <http://www.arl.noaa.gov/ready/hysplit4.html>), 2003.

Ehhalt, D. H., Rohrer, F., Wahner, A., Prather, M. J., and Blake, D. R.: On the use of hydrocarbons for the determination of tropospheric OH concentrations, *J. Geophys. Res.*, 103, 18981-18997, 1998.

Ehhalt, D. H., and Rohrer, F.: Dependence of the OH concentration on solar UV, *J. Geophys. Res.*, 105, 3565-3571, 2000.

Elliott, S., et al.: Ventilation of liquefied petroleum gas components from the Valley of Mexico, *J. Geophys. Res.*, 102, 21197-21207, 1997.

Erickson, D. J., Seuzaret, C., Keene, W. C., and Gong, S. L.: A general circulation model based calculation of HCl and ClNO₂ production from sea salt dechlorination: Reactive Chlorine Emissions Inventory, *J. Geophys. Res.*, 104, 8347-8372, 1999.

Ezell, M. J., Wang, W. H., Ezell, A. A., Soskin, G., and Finlayson-Pitts, B. J.: Kinetics of reactions of chlorine atoms with a series of alkenes at 1 atm and 298 K: structure and reactivity, *Phys. Chem. Chem. Phys.*, 4, 5813-5820, 10.1039/b207529f, 2002.

Fehsenfeld, F., et al.: Emissions of volatile organic compounds from vegetation and the implications for atmospheric chemistry, *Global Biogeochem. Cy.*, 6, 389-430, 1992.

Fehsenfeld, F. C., et al.: International Consortium for Atmospheric Research on Transport and Transformation (ICARTT): North America to Europe - Overview of the 2004 summer field study, *J. Geophys. Res.*, 111, D23s01, doi:10.1029/2006jd007829, 2006.

Finkelstein, P. L., Ellestad, T. G., Clarke, J. F., Meyers, T. P., Schwede, D. B., Hebert, E. O., and Neal, J. A.: Ozone and sulfur dioxide dry deposition to forests: Observations and model evaluation, *J. Geophys. Res.*, 105, 15365-15377, 2000.

- Finlayson-Pitts, B. J.: Chlorine atoms as a potential tropospheric oxidant in the marine boundary-layer, *Res. Chem. Intermediat.*, 19, 235-249, 1993.
- Finlayson-Pitts, B. J., Keoshian, C. J., Buehler, B., and Ezell, A. A.: Kinetics of reaction of chlorine atoms with some biogenic organics, *Int. J. Chem. Kinet.*, 31, 491-499, 1999.
- Finlayson-Pitts, B. J.: The tropospheric chemistry of sea salt: A molecular-level view of the chemistry of NaCl and NaBr, *Chem. Rev.*, 103, 4801-4822, 2003.
- Fischer, E. V., Talbot, R. W., Dibb, J. E., Moody, J. L., and Murray, G. L.: Summertime ozone at Mount Washington: Meteorological controls at the highest peak in the northeast, *J. Geophys. Res.*, 109, D24303, doi:10.1029/2004jd004841, 2004.
- Fischer, E., Pszenny, A., Keene, W., Maben, J., Smith, A., Stohl, A., and Talbot, R.: Nitric acid phase partitioning and cycling in the New England coastal atmosphere, *J. Geophys. Res.*, 111, D23S09, doi:10.1029/2006JD007328, 2006.
- Flocke, F., Volzthomas, A., and Kley, D.: Measurements of alkyl nitrates in rural and polluted air masses, *Atmos. Environ. A-Gen*, 25, 1951-1960, 1991.
- Flocke, F., Volz-Thomas, A., Buers, H. J., Patz, W., Garthe, H. J., and Kley, D.: Long-term measurements of alkyl nitrates in southern Germany I. General behavior and seasonal and diurnal variation, *J. Geophys. Res.*, 103, 5729-5746, 1998.
- Fortin, T. J., Howard, B. J., Parrish, D. D., Goldan, P. D., Kuster, W. C., Atlas, E. L., and Harley, R. A.: Temporal changes in US benzene emissions inferred from atmospheric measurements, *Environ. Sci. Technol.*, 39, 1403-1408, 2005.
- Fujita, E. M.: Hydrocarbon source apportionment for the 1996 Paso del Norte Ozone Study, *Sci. Total Environ.*, 276, 171-184, 2001.
- Gautrois, M., Brauers, T., Koppmann, R., Rohrer, F., Stein, O., and Rudolph, J.: Seasonal variability and trends of volatile organic compounds in the lower polar troposphere, *J. Geophys. Res.*, 108, 4393, doi:10.1029/2002jd002765, 2003.
- Giacopelli, P., Ford, K., Espada, C., and Shepson, P. B.: Comparison of the measured and simulated isoprene nitrate distributions above a forest canopy, *J. Geophys. Res.*, 110, D01304, doi:10.1029/2004jd005123, 2005.
- Goldan, P. D., Kuster, W. C., Fehsenfeld, F. C., and Montzka, S. A.: Hydrocarbon measurements in the southeastern United States: The Rural Oxidants in the Southern Environment (ROSE) program 1990, *J. Geophys. Res.*, 100, 25945-25963, 1995.
- Goldan, P. D., Parrish, D. D., Kuster, W. C., Trainer, M., McKeen, S. A., Holloway, J., Jobson, B. T., Sueper, D. T., and Fehsenfeld, F. C.: Airborne measurements of isoprene, CO, and anthropogenic hydrocarbons and their implications, *J. Geophys. Res.*, 105, 9091-

9105, 2000.

Goldstein, A. H., Wofsy, S. C., and Spivakovsky, C. M.: Seasonal variations of nonmethane hydrocarbons in rural New England: Constraints on OH concentrations in northern midlatitudes, *J. Geophys. Res.*, 100, 26273-26274, 1995.

Gong, Q., and Demerjian, K. L.: Measurement and analysis of C₂-C₁₀ hydrocarbons at Whiteface Mountain, New York, *J. Geophys. Res.*, 102, 28059-28069, 1997.

Graedel, T. E., and Keene, W. C.: Tropospheric budget of reactive chlorine, *Global Biogeochem. Cy.*, 9, 47-77, 1995.

Gupta, M. L., Cicerone, R. J., Blake, D. R., Rowland, F. S., and Isaksen, I. S. A.: Global atmospheric distributions and source strengths of light hydrocarbons and tetrachloroethene, *J. Geophys. Res.*, 103, 28219-28235, 1998.

Gusten, H., Heinrich, G., and Sprung, D.: Nocturnal depletion of ozone in the Upper Rhine Valley, *Atmos. Environ.*, 32, 1195-1202, 1998.

Hagerman, L. M., Aneja, V. P., and Lonneman, W. A.: Characterization of non-methane hydrocarbons in the rural southeast United States, *Atmos. Environ.*, 31, 4017-4038, 1997.

Harley, R. A., Hannigan, M. P., and Cass, G. R.: Respeciation of organic gas emissions and the detection of excess unburned gasoline in the atmosphere, *Environ. Sci. Technol.*, 26, 2395-2408, 1992.

Harley, R. A., Coulter-Burke, S. C., and Yeung, T. S.: Relating liquid fuel and headspace vapor composition for California reformulated gasoline samples containing ethanol, *Environ. Sci. Technol.*, 34, 4088-4094, 2000.

Harley, R. A., McKeen, S. A., Pearson, J., Rodgers, M. O., and Lonneman, W. A.: Analysis of motor vehicle emissions during the Nashville/Middle Tennessee Ozone Study, *J. Geophys. Res.*, 106, 3559-3567, 2001.

Harley, R. A., Hooper, D. S., Kean, A. J., Kirchstetter, T. W., Hesson, J. M., Balberan, N. T., Stevenson, E. D., and Kendall, G. R.: Effects of reformulated gasoline and motor vehicle fleet turnover on emissions and ambient concentrations of benzene, *Environ. Sci. Technol.*, 40, 5084-5088, 10.1021/es0604820, 2006.

Hastie, D. R., Shepson, P. B., Sharma, S., and Schiff, H. I.: The influence of the nocturnal boundary layer on secondary trace species in the atmosphere at Dorset, Ontario, *Atmos. Environ. A-Gen*, 27, 533-541, 1993.

Hauff, K., Fischer, R. G., and Ballschmiter, K.: Determination of C₁-C₅ alkyl nitrates in rain, snow, white frost, lake, and tap water by a combined codistillation head-space gas

chromatography technique. Determination of Henry's law constants by head-space GC, *Chemosphere*, 37, 2599-2615, 1998.

Hegarty, J., Mao, H., and Talbot, R.: Synoptic controls on summertime surface ozone in the northeastern United States, *J. Geophys. Res.*, 112, D14306, doi:10.1029/2006JD008170, 2007.

Horii, C. V., Munger, J. W., Wofsy, S. C., Zahniser, M., Nelson, D., and McManus, J. B.: Fluxes of nitrogen oxides over a temperate deciduous forest, *J. Geophys. Res.*, 109, D08305, doi:10.1029/2003jd004326, 2004.

Horii, C. V., Munger, J. W., Wofsy, S. C., Zahniser, M., Nelson, D., and McManus, J. B.: Atmospheric reactive nitrogen concentration and flux budgets at a Northeastern US forest site, *Agr. Forest. Meteorol.*, 136, 159-174, 10.1016/j.agrformet.2006.03.005, 2006.

Huebert, B. J., Blomquist, B. W., Hare, J. E., Fairall, C. W., Johnson, J. E., and Bates, T. S.: Measurement of the sea-air DMS flux and transfer velocity using eddy correlation, *Geophys. Res. Lett.*, 31, L23113, doi:10.1029/2004gl021567, 2004.

Hurst, D. F., Bakwin, P. S., and Elkins, J. W.: Recent trends in the variability of halogenated trace gases over the United States, *J. Geophys. Res.*, 103, 25299-25306, 1998.

IPCC: Summary for Policymakers. In: *Climate Change 2007: The Physical Science Basis. Contribution of Working Group I to the Fourth Assessment Report of the Intergovernmental Panel on Climate Change* (Solomon, S., D. Qin, M. Manning, Z. Chen, M. Marquis, K.B. Averyt, M. Tignor and H.L. Miller (eds.)). Cambridge University Press, Cambridge, United Kingdom and New York, NY, USA, 2007.

James, J. D., Harrison, R. M., Savage, N. H., Allen, A. G., Grenfell, J. L., Allan, B. J., Plane, J. M. C., Hewitt, C. N., Davison, B., and Robertson, L.: Quasi-Lagrangian investigation into dimethyl sulfide oxidation in maritime air using a combination of measurements and model, *J. Geophys. Res.*, 105, 26379-26392, 2000.

Jobson, B. T., Wu, Z., Niki, H., and Barrie, L. A.: Seasonal trends of isoprene, C₂-C₅ alkanes, and acetylene at a remote boreal site in Canada, *J. Geophys. Res.*, 99, 1589-1599, 1994.

Jobson, B. T., Parrish, D. D., Goldan, P., Kuster, W., Fehsenfeld, F. C., Blake, D. R., Blake, N. J., and Niki, H.: Spatial and temporal variability of nonmethane hydrocarbon mixing ratios and their relation to photochemical lifetime, *J. Geophys. Res.*, 103, 13557-13567, 1998.

Jobson, B. T., McKeen, S. A., Parrish, D. D., Fehsenfeld, F. C., Blake, D. R., Goldstein, A. H., Schauffler, S. M., and Elkins, J. C.: Trace gas mixing ratio variability versus

lifetime in the troposphere and stratosphere: Observations, *J. Geophys. Res.*, 104, 16091-16113, 1999.

Jobson, B. T., Berkowitz, C. M., Kuster, W. C., Goldan, P. D., Williams, E. J., Fehsenfeld, F. C., Apel, E. C., Karl, T., Lonneman, W. A., and Riemer, D.: Hydrocarbon source signatures in Houston, Texas: Influence of the petrochemical industry, *J. Geophys. Res.*, 109, D24305, doi:10.1029/2004jd004887, 2004.

Jordan, C., Fitz, E., Hagan, T., Sive, B., Frinak, E., Haase, K., Cottrell, L., Buckley, S., and Talbot, R.: Long-term study of VOCs measured with PTR-MS at a rural site in New Hampshire with urban influences, *Atmos. Chem. Phys. Discuss.*, 9, 4251-4299, 2009.

Kames, J., and Schurath, U.: Alkyl nitrates and bifunctional nitrates of atmospheric interest- Henry Law constants and their temperature dependencies, *J. Atmos. Chem.*, 15, 79-95, 1992.

Kang, D. W., Aneja, V. P., Zika, R. G., Farmer, C., and Ray, J. D.: Nonmethane hydrocarbons in the rural southeast United States national parks, *J. Geophys. Res.*, 106, 3133-3155, 2001.

Karl, T., and Guenther, A.: Atmospheric variability of biogenic VOCs in the surface layer measured by proton-transfer-reaction mass spectrometry, *Int. J. Mass. Spectrom.*, 239, 77-86, 2004.

Keene, W. C., Pszenny, A. A. P., Jacob, D. J., Duce, R. A., Galloway, J. N., Schultz-Tokos, J. J., Sievering, H., and Boatman, J. F.: The geochemical cycling of reactive chlorine through the marine troposphere, *Global. Biogeochem. Cyc.*, 4, 407-430, 1990.

Keene, W. C., et al.: Composite global emissions of reactive chlorine from anthropogenic and natural sources: Reactive Chlorine Emissions Inventory, *J. Geophys. Res.*, 104, 8429-8440, 1999.

Keene, W. C., Stutz, J., Pszenny, A. A. P., Maben, J. R., Fischer, E. V., Smith, A. M., von Glasow, R., Pechtl, S., Sive, B. C., and Varner, R. K.: Inorganic chlorine and bromine in coastal New England air during summer, *J. Geophys. Res.*, 112, D10S12, doi:10.1029/2006jd007689, 2007.

Kindler, T. P., Chameides, W. L., Wine, P. H., Cunnold, D. M., Alyea, F. N., and Franklin, J. A.: The fate of atmospheric phosgene and the stratospheric chlorine loadings of its parent compounds: CCl_4 , C_2Cl_4 , C_2HCl_3 , CH_3CCl_3 , and CHCl_3 , *J. Geophys. Res.*, 100, 1235-1251, 1995.

Kirchstetter, T. W., Singer, B. C., Harley, R. A., Kendall, G. B., and Chan, W.: Impact of oxygenated gasoline use on California light-duty vehicle emissions, *Environ. Sci. Technol.*, 30, 661-670, 1996.

- Kirchstetter, T. W., Singer, B. C., Harley, R. A., Kendall, G. R., and Hesson, J. M.: Impact of California reformulated gasoline on motor vehicle emissions. 2. Volatile organic compound speciation and reactivity, *Environ. Sci. Technol.*, 33, 329-336, 1999.
- Kleiman, G., and Prinn, R. G.: Measurement and deduction of emissions of trichloroethene, tetrachloroethene, and trichloromethane (chloroform) in the northeastern United States and southeastern Canada, *J. Geophys. Res.*, 105, 28875-28893, 2000.
- Kleinman, L. I., et al.: Photochemical age determinations in the Phoenix metropolitan area, *J. Geophys. Res.*, 108, 4096, doi:10.1029/2002jd002621, 2003.
- Kleinman, L. I., Daum, P. H., Lee, Y. N., Nunnermacker, L. J., Springston, S. R., Weinstein-Lloyd, J., and Rudolph, J.: A comparative study of ozone production in five U.S. metropolitan areas, *J. Geophys. Res.*, 110, D02301, doi:10.1029/2004jd005096, 2005.
- Klemp, D., Kley, D., Kramp, F., Buers, H. J., Pilwat, G., Flocke, F., Patz, H. W., and VolzThomas, A.: Long-term measurements of light hydrocarbons (C₂-C₅) at Schauinsland (Black Forest), *J. Atmos. Chem.*, 28, 135-171, 1997.
- Knipping, E. M., and Dabdub, D.: Impact of chlorine emissions from sea-salt aerosol on coastal urban ozone, *Environ. Sci. Technol.*, 37, 275-284, 10.1021/es025793z, 2003.
- Kroll, J. H., and Seinfeld, J. H.: Chemistry of secondary organic aerosol: Formation and evolution of low-volatility organics in the atmosphere, *Atmos. Environ.*, 42, 3593-3624, 10.1016/j.atmosenv.2008.01.003, 2008.
- Kwok, E. S. C., and Atkinson, R.: Estimation of hydroxyl radical reaction rate constants for gas-phase organic compounds using a structure-reactivity relationship: An update, *Atmos. Environ.*, 29, 1685-1695, 1995.
- Lee, B. H., Munger, J. W., Wofsy, S. C., and Goldstein, A. H.: Anthropogenic emissions of nonmethane hydrocarbons in the northeastern United States: Measured seasonal variations from 1992-1996 and 1999-2001, *J. Geophys. Res.*, 111, D20307, doi:10.1029/2005jd006172, 2006.
- Lefer, B. L., Talbot, R. W., and Munger, J. W.: Nitric acid and ammonia at a rural northeastern US site, *J. Geophys. Res.*, 104, 1645-1661, 1999.
- Lenschow, D. H., and Gurarie, D.: A simple model for relating concentrations and fluctuations of trace reactive species to their lifetimes in the atmosphere, *J. Geophys. Res.*, 107, 4805, doi:10.1029/2002jd002526, 2002.
- Lough, G. C., Schauer, J. J., Lonneman, W. A., and Allen, M. K.: Summer and winter nonmethane hydrocarbon emissions from on-road motor vehicles in the Midwestern United States, *J. Air & Waste Manage. Assoc.*, 55629-55646, 2005.

- Luke, W. T., Dickerson, R. R., and Nunnermacker, L. J.: Direct measurements of the photolysis rate coefficients and Henry Law constants of several alkyl nitrates, *J. Geophys. Res.*, 94, 14905-14921, 1989.
- Mao, H. T., and Talbot, R.: O₃ and CO in New England: Temporal variations and relationships, *J. Geophys. Res.*, 109, D21304, doi:10.1029/2004jd004913, 2004a.
- Mao, H. T., and Talbot, R.: Role of meteorological processes in two New England ozone episodes during summer 2001, *J. Geophys. Res.*, 109, D20305, doi:10.1029/2004jd004850, 2004b.
- Mao, H., Talbot, R. W., Sigler, J. M., Sive, B. C., and Hegarty, J. D.: Seasonal and diurnal variations of Hg⁰ over New England, *Atmos. Chem. Phys.*, 8, 1403-1421, 2008.
- Marandino, C. A., De Bruyn, W. J., Miller, S. D., and Saltzman, E. S.: DMS air/sea flux and gas transfer coefficients from the North Atlantic summertime coccolithophore bloom, *Geophys. Res. Lett.*, 35, L23812, doi:10.1029/2008gl036370, 2008.
- McCarthy, M. C., Hafner, H. R., and Montzka, S. A.: Background concentrations of 18 air toxics for North America, *J. Air & Waste Manage. Assoc.*, 56, 3-11, 2006.
- McCulloch, A., and Midgley, P. M.: The production and global distribution of emissions of trichloroethene, tetrachloroethene and dichloromethane over the period 1988-1992, *Atmos. Environ.*, 30, 601-608, 1996.
- McCulloch, A., Aucott, M. L., Graedel, T. E., Kleiman, G., Midgley, P. M., and Li, Y-F.: Industrial emissions of trichloroethene, tetrachloroethene, and dichloromethane: Reactive Chlorine Emissions Inventory, *J. Geophys. Res.*, 104, 8417-8427, 1999.
- McGaughey, G. R., Desai, N. R., Allen, D. T., Seila, R. L., Lonneman, W. A., Fraser, M. P., Harley, R. A., Pollack, A. K., Ivy, J. M., and Price, J. H.: Analysis of motor vehicle emissions in a Houston tunnel during the Texas Air Quality Study 2000, *Atmos. Environ.*, 38, 3363-3372, 10.1016/j.atmosenv.2004.03.006, 2004.
- McKeen, S. A., Liu, S. C., Hsie, E. Y., Lin, X., Bradshaw, J. D., Smyth, S., Gregory, G. L., and Blake, D. R.: Hydrocarbon ratios during PEM-WEST A: A model perspective, *J. Geophys. Res.*, 101, 2087-2109, 1996.
- McLaren, R., Singleton, D. L., Lai, J. Y. K., Khouw, B., Singer, E., Wu, Z., and Niki, H.: Analysis of motor vehicle sources and their contribution to ambient hydrocarbon distributions at urban sites in Toronto during the Southern Ontario Oxidants Study, *Atmos. Environ.*, 30, 2219-2232, 1996.
- Miller, S. T. K., Keim, B. D., Talbot, R. W., and Mao, H.: Sea breeze: Structure, forecasting, and impacts, *Rev. Geophys.*, 41, 1011, doi:10.1029/2003rg000124, 2003.

Millet, D. B., et al.: Volatile organic compound measurements at Trinidad Head, California, during ITCT 2K2: Analysis of sources, atmospheric composition, and aerosol residence times, *J. Geophys. Res.*, 109, D23S16, doi:10.1029/2003JD004026, 2004.

Mohamed, M. F., Kang, D. W., and Aneja, V. P.: Volatile organic compounds in some urban locations in United States, *Chemosphere*, 47, 863-882, 2002.

Moody, J. L., Munger, J. W., Goldstein, A. H., Jacob, D. J., and Wofsy, S. C.: Harvard forest regional-scale air mass composition by Patterns in Atmospheric Transport History (PATH), *J. Geophys. Res.*, 103, 13181-13194, 1998.

Monod, A., Sive, B. C., Avino, P., Chen, T., Blake, D. R., and Rowland, F. S.: Monoaromatic compounds in ambient air of various cities: a focus on correlations between the xylenes and ethylbenzene, *Atmos. Environ.*, 35, 135-149, 2001.

Moore, R. M., and Blough, N. V.: A marine source of methyl nitrate, *Geophys. Res. Lett.*, 29, 1737, doi:10.1029/2002gl014989, 2002.

Munger, J. W., Wofsy, S. C., Bakwin, P. S., Fan, S. M., Goulden, M. L., Daube, B. C., Goldstein, A. H., Moore, K. E., and Fitzjarrald, D. R.: Atmospheric deposition of reactive nitrogen oxides and ozone in a temperate deciduous forest and a subarctic woodland I. Measurements and mechanisms, *J. Geophys. Res.*, 101, 12639-12657, 1996.

Munger, J. W., Fan, S. M., Bakwin, P. S., Goulden, M. L., Goldstein, A. H., Colman, A. S., and Wofsy, S. C.: Regional budgets for nitrogen oxides from continental sources: Variations of rates for oxidation and deposition with season and distance from source regions, *J. Geophys. Res.*, 103, 8355-8368, 1998.

Muthuramu, K., Shepson, P. B., Bottenheim, J. W., Jobson, B. T., Niki, H., and Anlauf, K. G.: Relationships between organic nitrates and surface ozone destruction during Polar Sunrise Experiment 1992, *J. Geophys. Res.*, 99, 25369-25378, 1994.

Neu, J. L., Lawler, M. J., Prather, M. J., and Saltzman, E. S.: Oceanic alkyl nitrates as a natural source of tropospheric ozone, *Geophys. Res. Lett.*, 35, L13814, doi:10.1029/2008gl034189, 2008.

Nielsen, T., Egelov, A. H., Granby, K., and Skov, H.: Observations on particulate organic nitrates and unidentified components of NO_y, *Atmos. Environ.*, 29, 1757-1769, 1995.

National Climatic Data Center, Climatological Data Summary: New England, July and August 2004, July and August 2005, Vols. 116, 117 (07, 08), <http://www7.ncdc.noaa.gov/IPS/cd/cd.html>.

Odum, J. R., Jungkamp, T. P. W., Griffin, R. J., Forstner, H. J. L., Flagan, R. C., and Seinfeld, J. H.: Aromatics, reformulated gasoline, and atmospheric organic aerosol formation, *Environ. Sci. Technol.*, 31, 1890-1897, 1997.

Ostling, K., Kelly, B., Bird, S., Bertman, S., Pippin, M., Thornberry, T., and Carroll, M. A.: Fast-turnaround alkyl nitrate measurements during the PROPHET 1998 summer intensive, *J. Geophys. Res.*, 106, 24439-24449, 2001.

Pandis, S. N., Russell, L. M., and Seinfeld, J. H.: The relationship between DMS flux and CCN concentration in remote marine, *J. Geophys. Res.*, 99, 16945-16957, 1994.

Parrish, D. D., et al.: Internal consistency tests for evaluation of measurements of anthropogenic hydrocarbons in the troposphere, *J. Geophys. Res.*, 103, 22339-22359, 1998.

Parrish, D. D.: Critical evaluation of US on-road vehicle emission inventories, *Atmos. Environ.*, 40, 2288-2300, 10.1016/j.atmosenv.2005.11.033, 2006.

Parrish, D., Goldan, P., de Gouw, J., Shao, M., Kondo, Y., Shirai, T., Yokouchi, Y., and Koike, M., Comparison of air pollutant emissions among mega-cities, *IGAC Activities Newsletter*, 38, 22-29, April 2008.

Pechtl, S., and von Glasow, R.: Reactive chlorine in the marine boundary layer in the outflow of polluted continental air: A model study, *Geophys. Res. Lett.*, 34, L11813, doi:10.1029/2007gl029761, 2007.

Pikel'naya, O., Hurlock, S. C., Trick, S., and Stutz, J.: Intercomparison of multi-axis and long-path differential optical absorption spectroscopy measurements in the marine boundary layer, *J. Geophys. Res.*, 112, D10S01, doi:10.1029/2006JD007727, 2007.

Platt, U., and Honninger, G.: The role of halogen species in the troposphere, *Chemosphere*, 52, 325-338, 10.1016/s0045-6535(03)00216-9, 2003.

Pszenny, A. A. P., Fischer, E. V., Russo, R. S., Sive, B. C., and Varner, R. K.: Estimates of Cl atom concentrations and hydrocarbon kinetic reactivity in surface air at Appledore Island, Maine (USA), during International Consortium for Atmospheric Research on Transport and Transformation/Chemistry of Halogens at the Isles of Shoals, *J. Geophys. Res.*, 112, D10S13, doi:10.1029/2006JD007725, 2007.

Qin, Y., Walk, T., Gary, R., Yao, X., and Elles, S.: C₂-C₁₀ nonmethane hydrocarbons measured in Dallas, USA - Seasonal trends and diurnal characteristics, *Atmos. Environ.*, 41, 6018-6032, 10.1016/j.atmosenv.2007.03.008, 2007.

Ramacher, B., Rudolph, J., and Koppmann, R.: Hydrocarbon measurements during tropospheric ozone depletion events: Evidence for halogen atom chemistry, *J. Geophys. Res.*, 104, 3633-3653, 1999.

Ranschaert, D. L., Schneider, N. J., and Elrod, M. J.: Kinetics of the C₂H₅O₂+NO_x reactions: Temperature dependence of the overall rate constant and the C₂H₅ONO₂ branching channel of C₂H₅O₂+NO, *J. Phys. Chem. A*, 104, 5758-5765, 2000.

- Reeves, C. E., et al.: Alkyl nitrates in outflow from North America over the North Atlantic during Intercontinental Transport of Ozone and Precursors 2004, *J. Geophys. Res.*, 112, D10s37, doi:10.1029/2006jd007567, 2007.
- Ridley, B. A., et al.: The behavior of some organic nitrates at Boulder and Niwot Ridge, Colorado, *J. Geophys. Res.*, 95, 13949-13961, 1990.
- Roberts, J. M., Fehsenfeld, F. C., Liu, S. C., Bollinger, M. J., Hahn, C., Albritton, D. L., and Sievers, R. E.: Measurements of aromatic hydrocarbon ratios and NO_x concentrations in the rural troposphere: Observation of air-mass photochemical aging and NO_x removal, *Atmos. Environ.*, 18, 2421-2432, 1984.
- Roberts, J. M.: The atmospheric chemistry of organic nitrates, *Atmos. Environ. A-Gen*, 24, 243-287, 1990.
- Roberts, J. M., Bertman, S. B., Parrish, D. D., Fehsenfeld, F. C., Jobson, B. T., and Niki, H.: Measurement of alkyl nitrates at Chebogue Point, Nova Scotia during the 1993 North Atlantic Regional Experiment (NARE) intensive, *J. Geophys. Res.*, 103, 13569-13580, 1998.
- Rogak, S. N., Pott, U., Dann, T., and Wang, D.: Gaseous emissions from vehicles in a traffic tunnel in Vancouver, British Columbia, *J. Air & Waste Manage. Assoc.*, 48, 604-615, 1998.
- Rudolph, J., Koppmann, R., and PlassDulmer, C.: The budgets of ethane and tetrachloroethene: Is there evidence for an impact of reactions with chlorine atoms in the troposphere?, *Atmos. Environ.*, 30, 1887-1894, 1996.
- Rudolph, J., Ramacher, B., PlassDulmer, C., Muller, K. P., and Koppmann, R.: The indirect determination of chlorine atom concentration in the troposphere from changes in the patterns of non-methane hydrocarbons, *Tellus B*, 49, 592-601, 1997.
- Russo, R. S., et al.: Chemical composition of Asian continental outflow over the western Pacific: Results from Transport and Chemical Evolution over the Pacific (TRACE-P), *J. Geophys. Res.*, 108, 8804, doi:10.1029/2002jd003184, 2003.
- Russo, R. S., Zhou, Y., Haase, K., Wingenter, O. W., Frinak, E. K., Mao, H., Talbot, R., and Sive, B. C.: Temporal variability, sources, and sinks of C₁-C₅ alkyl nitrates in coastal New England, *Atmos. Chem. Phys. Discuss.*, submitted, 2009.
- Russo, R. S., Zhou, Y., White, M. L., Talbot, R., and Sive, B. C.: Long-term (2004-2008) Measurements of Nonmethane Hydrocarbons and Halocarbons in New Hampshire: Seasonal Variations and Regional Sources, *Atmos. Chem. Phys. Discuss.*, in preparation, 2009.

Sagebiel, J. C., Zielinska, B., Pierson, W. R., and Gertler, A. W.: Real-world emissions and calculated reactivities of organic species from motor vehicles, *Atmos. Environ.*, 30, 2287-2296, 1996.

Sander, R.: Compilation of Henry's law constants for inorganic and organic species of potential importance in environmental chemistry, version 3, <http://www.mpch-mainz.mpg.de/~sander/res/henry.html>, 1999.

Schauffler, S. M., Atlas, E. L., Donnelly, S. G., Andrews, A., Montzka, S. A., Elkins, J. W., Hurst, D. F., Romashkin, P. A., Dutton, G. S., and Stroud, V.: Chlorine budget and partitioning during the Stratospheric Aerosol and Gas Experiment (SAGE) III Ozone Loss and Validation Experiment (SOLVE), *J. Geophys. Res.*, 108, 4173, doi:10.1029/2001JD002040, 2003.

Schlesinger, W. H.: On the fate of anthropogenic nitrogen, *P. Natl. Acad. Sci. USA*, 106, 10.1073/pnas.0810193105, 2009.

Schrimpf, W., Lienaerts, K., Muller, K. P., Rudolph, J., Neubert, R., Schussler, W., and Levin, I.: Dry deposition of peroxyacetyl nitrate (PAN): Determination of its deposition velocity at night from measurements of the atmospheric PAN and ²²²Rn concentration gradient, *Geophys. Res. Lett.*, 23, 3599-3602, 1996.

Sciare, J., Baboukas, E., Kanakidou, M., Krischke, U., Belviso, S., Bardouki, H., and Mihalopoulos, N.: Spatial and temporal variability of atmospheric sulfur-containing gases and particles during the Albatross campaign, *J. Geophys. Res.*, 105, 14433-14448, 2000.

Shepson, P. B., Bottenheim, J. W., Hastie, D. R., and Venkatram, A.: Determination of the relative ozone and PAN deposition velocities at night, *Geophys. Res. Lett.*, 19, 1121-1124, 1992.

Shepson, P. B., Anlauf, K. G., Bottenheim, J. W., Wiebe, H. A., Gao, N., Muthuramu, K., and Mackay, G. I.: Alkyl nitrates and their contribution to reactive nitrogen at a rural site in Ontario, *Atmos. Environ. A-Gen*, 27, 749-757, 1993.

Shepson, P. B., Mackay, E., and Muthuramu, K.: Henry's law constants and removal processes for several atmospheric beta-hydroxy alkyl nitrates, *Environ. Sci. Technol.*, 30, 3618-3623, 1996.

Shi, J. C., and Bernhard, M. J.: Kinetic studies of Cl-atom reactions with selected aromatic compounds using the photochemical reactor-FTIR spectroscopy technique, *Int. J. Chem. Kinet.*, 29, 349-358, 1997.

Shipham, M. C., Crill, P. M., Bartlett, K. B., Goldstein, A. H., Czepiel, P. M., Harriss, R. C., and Blaha, D.: Methane measurements in central New England: An assessment of regional transport from surrounding sources, *J. Geophys. Res.*, 103, 21985-22000, 1998.

Sillman, S., and He, D. Y.: Some theoretical results concerning O₃-NO_x-VOC chemistry and NO_x-VOC indicators, *J. Geophys. Res.*, 107, 4659, doi:10.1029/2001jd001123, 2002.

Simmonds, P. G., et al.: Global trends, seasonal cycles, and European emissions of dichloromethane, trichloroethene, and tetrachloroethene from the AGAGE observations at Mace Head, Ireland, and Cape Grim, Tasmania, *J. Geophys. Res.*, 111, D18304, doi:10.1029/2006jd007082, 2006.

Simpson, I. J., Meinardi, S., Blake, D. R., Blake, N. J., Rowland, F. S., Atlas, E., and Flocke, F.: A biomass burning source of C₁-C₄ alkyl nitrates, *Geophys. Res. Lett.*, 29, 2168, doi:10.1029/2002gl016290, 2002.

Simpson, I. J., Blake, N. J., Blake, D. R., Atlas, E., Flocke, F., Crawford, J. H., Fuelberg, H. E., Kiley, C. M., Meinardi, S., and Rowland, F. S.: Photochemical production and evolution of selected C₂-C₅ alkyl nitrates in tropospheric air influenced by Asian outflow, *J. Geophys. Res.*, 108, 8808, doi:10.1029/2002jd002830, 2003.

Simpson, I. J., Meinardi, S., Blake, N. J., Rowland, F. S., and Blake, D. R.: Long-term decrease in the global atmospheric burden of tetrachloroethene (C₂Cl₄), *Geophys. Res. Lett.*, 31, L08108, doi:10.1029/2003gl019351, 2004.

Simpson, I. J., Wang, T., Guo, H., Kwok, Y. H., Flocke, F., Atlas, E., Meinardi, S., Rowland, F. S., and Blake, D. R.: Long-term atmospheric measurements of C₁-C₅ alkyl nitrates in the pearl river delta region of southeast China, *Atmos. Environ.*, 40, 1619-1632, 10.1016/j.atmosenv.2005.10.062, 2006.

Singh, H. B., and Zimmerman, P. B.: Atmospheric distribution and sources of nonmethane hydrocarbons, *Gaseous Pollutants: Characterization and Cycling*, Jon Wiley & Sons, Inc, 1997-235, 1992.

Sistla, G., and Aleksic, N.: A comparison of PAMS and air toxics measurements, *Atmos. Environ.*, 41, 5719-5731, 10.1016/j.atmosenv.2007.02.041, 2007.

Sive, B. C., Zhou, Y., Troop, D., Wang, Y. L., Little, W. C., Wingenter, O. W., Russo, R. S., Varner, R. K., and Talbot, R.: Development of a cryogen-free concentration system for measurements of volatile organic compounds, *Anal. Chem.*, 77, 6989-6998, doi:10.1021/ac0506231, 2005.

Sive, B. C., Varner, R. K., Mao, H., Blake, D. R., Wingenter, O. W., and Talbot, R.: A large terrestrial source of methyl iodide, *Geophys. Res. Lett.*, 34, L17808, doi:10.1029/2007gl030528, 2007.

Sommariva, R., et al.: A study of organic nitrates formation in an urban plume using a Master Chemical Mechanism, *Atmos. Environ.*, 42, 5771-5786, 10.1016/j.atmosenv.2007.12.031, 2008.

Smyth, S., et al.: Characterization of the chemical signatures of air masses observed during the PEM experiments over the western Pacific, *J. Geophys. Res.*, 104, 16243-16254, 1999.

Sparks, J. P., Roberts, J. M., and Monson, R. K.: The uptake of gaseous organic nitrogen by leaves: A significant global nitrogen transfer process, *Geophys. Res. Lett.*, 30, 2189, doi:10.1029/2003gl018578, 2003.

Spivakovsky, C. M., et al.: Three-dimensional climatological distribution of tropospheric OH: Update and evaluation, *J. Geophys. Res.*, 105, 8931-8980, 2000.

Stark, H., Brown, S. S., Goldan, P. D., Aldener, M., Kuster, W. C., Jakoubek, R., Fehsenfeld, F. C., Meagher, J., Bates, T. S., and Ravishankara, A. R.: Influence of nitrate radical on the oxidation of dimethyl sulfide in a polluted marine environment, *J. Geophys. Res.*, 112, D10s10, doi:10.1029/2006jd007669, 2007.

Stroud, C. A., et al.: Alkyl nitrate measurements during STERAO 1996 and NARE 1997: Intercomparison and survey of results, *J. Geophys. Res.*, 106, 23043-23053, 2001.

Stutz, J., Pikelnaya, O., Hurlock, S. C., Trick, S., Pechtl, S., and von Glasow, R.: Daytime OIO in the Gulf of Maine, *Geophys. Res. Lett.*, 34, L22816, doi:10.1029/2007G1031332, 2007.

Swanson, A. L., Blake, N. J., Atlas, E., Flocke, F., Blake, D. R., and Rowland, F. S.: Seasonal variations of C₂-C₄ nonmethane hydrocarbons and C₁-C₄ alkyl nitrates at the Summit research station in Greenland, *J. Geophys. Res.*, 108, 4065, doi:10.1029/2001jd001445, 2003.

Talbot, R. W., Dibb, J. E., Scheuer, E. M., Bradshaw, J. D., Sandholm, S. T., Singh, H. B., Blake, D. R., Blake, N. J., Atlas, E., and Flocke, F.: Tropospheric reactive odd nitrogen over the South Pacific in austral springtime, *J. Geophys. Res.*, 105, 6681-6694, 2000.

Talbot, R., Mao, H. T., and Sive, B.: Diurnal characteristics of surface level O₃ and other important trace gases in New England, *J. Geophys. Res.*, 110, D09307, doi:10.1029/2004jd005449, 2005.

Talukdar, R. K., Burkholder, J. B., Hunter, M., Gilles, M. K., Roberts, J. M., and Ravishankara, A. R.: Atmospheric fate of several alkyl nitrates 2. UV absorption cross-sections and photodissociation quantum yields, *J. Chem. Soc. Faraday T.*, 93, 2797-2805, 1997.

Tanaka, P. L., Oldfield, S., Neece, J. D., Mullins, C. B., and Allen, D. T.: Anthropogenic sources of chlorine and ozone formation in urban atmospheres, *Environ. Sci. Technol.*, 34, 4470-4473, 2000.

Tanaka, P. L., et al.: Direct evidence for chlorine-enhanced urban ozone formation in Houston, Texas, *Atmos. Environ.*, 37, 1393-1400, 10.1016/s1352-2310(02)01007-5, 2003.

Thompson, T. M., et al.: Halocarbons and other atmospheric trace species, CMDL Summary Report #27, 115-135, <http://www.esrl.noaa.gov/gmd/publications/annrpt27/>, 2004.

Thornberry, T., et al.: Observations of reactive oxidized nitrogen and speciation of NO_y during the PROPHET summer 1998 intensive, *J. Geophys. Res.*, 106, 24359-24386, 2001.

Timerghazin, Q. K., and Ariya, P. A.: Kinetics of the gas-phase reaction of atomic chlorine with selected monoterpenes, *Phys. Chem. Chem. Phys.*, 3, 3981-3986, 2001.

Turnipseed, A. A., Huey, L. G., Nemitz, E., Stickel, R., Higgs, J., Tanner, D. J., Slusher, D. L., Sparks, J. P., Flocke, F., and Guenther, A.: Eddy covariance fluxes of peroxyacetyl nitrates (PANs) and NO_y to a coniferous forest, *J. Geophys. Res.*, 111, D09304, doi:10.1029/2005jd006631, 2006.

U.S. Environmental Protection Agency, National Air Quality and Emissions Trends Report, EPA 454/R-03-005, 2003.

U.S. Environmental Protection Agency, National Air Emission Standards for Hazardous air pollutants: Halogenated solvent cleaning; Final Rule, 40 CFR Part 63, 2007.

U.S. Environmental Protection Agency, Fuel Trends Report: Gasoline 1995-2005, EPA420-R-08-002, 2008.

Varner, R. K., Zhou, Y., Russo, R. S., Wingenter, O. W., Atlas, E., Stroud, C., Mao, H., Talbot, R., and Sive, B. C.: Controls on atmospheric chloriodomethane (CH₂ClI) in marine environments, *J. Geophys. Res.*, 113, D10303, doi:10.1029/2007jd008889, 2008.

Velasco, E., et al.: Distribution, magnitudes, reactivities, ratios and diurnal patterns of volatile organic compounds in the Valley of Mexico during the MCMA 2002 & 2003 field campaigns, *Atmos. Chem. Phys.*, 7, 329-353, 2007.

Wang, C. J. L., Blake, D. R., and Rowland, F. S.: Seasonal variations in the atmospheric distribution of a reactive chlorine compound, tetrachloroethene (CCl₂=CCl₂), *Geophys. Res. Lett.*, 22, 1097-1100, 1995.

Wang, L., Arey, J., and Atkinson, R.: Reactions of chlorine atoms with a series of aromatic hydrocarbons, *Environ. Sci. Technol.*, 39, 5302-5310, 10.1021/es0479437, 2005.

- Warneke, C., et al.: Comparison of daytime and nighttime oxidation of biogenic and anthropogenic VOCs along the New England coast in summer during New England Air Quality Study 2002, *J. Geophys. Res.*, 109, D10309, doi:10.1029/2003JD004424, 2004.
- Warneke, C., et al.: Determination of urban volatile organic compound emission ratios and comparison with an emissions database, *J. Geophys. Res.*, 112, D10S47, doi:10.1029/2006jd007930, 2007.
- Watson, J. G., Chow, J. C., and Fujita, E. M.: Review of volatile organic compound source apportionment by chemical mass balance, *Atmos. Environ.*, 35, 1567-1584, 2001.
- Wayne, R. P., et al.: The nitrate radical- physics, chemistry, and the atmosphere, *Atmos. Environ. A-Gen.*, 25, 1-203, 1991.
- White, A. B., et al.: Comparing the impact of meteorological variability on surface ozone during the NEAQS (2002) and ICARTT (2004) field campaigns, *J. Geophys. Res.*, 112, D10214, doi:10.1029/2006JD007590, 2007.
- White, M. L., et al.: Volatile organic compounds in northern New England marine and continental environments during the ICARTT 2004 campaign, *J. Geophys. Res.*, 113, D08S90, doi:10.1029/2007jd009161, 2008.
- White, M. L., et al.: Are biogenic emissions a significant source of summertime atmospheric toluene in the rural Northeastern United States?, *Atmos. Chem. Phys.*, 9, 81-92, 2009.
- Williams, J., et al.: Variability-lifetime relationship for organic trace gases: A novel aid to compound identification and estimation of HO concentrations, *J. Geophys. Res.*, 105, D16, 20473-20486, 2000.
- Wolfe, G. M., Thornton, J. A., Yatavelli, R. L. N., McKay, M., Goldstein, A. H., LaFranchi, B., Min, K.-E., Cohen, R. C.: Eddy covariance fluxes of acyl peroxy nitrates (PAN, PPN and MPAN) above a Ponderosa pine forest, *Atmos. Chem. Phys.*, 9, 615-635, 2009.
- Yorks, J. E., Thompson, A. M., Joseph, E., and Miller, S. K.: The variability of free tropospheric ozone over Beltsville, Maryland (39N, 77W) in the summers 2004-2007, *Atmos. Environ.*, 43, 1827-1838, 10.1016/j.atmosenv.2008.12.049, 2009.
- Yvon, S. A., Saltzman, E. S., Cooper, D. J., Bates, T. S., and Thompson, A. M.: Atmospheric sulfur cycling in the tropical Pacific marine boundary layer (12 degrees S, 135 degrees W): A comparison of field data and model results 1. Dimethylsulfide, *J. Geophys. Res.*, 101, 6899-6909, 1996.

Zhang, L., Vet, R., O'Brien, J. M., Mihele, C., Liang, Z., and Wiebe, A.: Dry deposition of individual nitrogen species at eight Canadian rural sites, *J. Geophys. Res.*, 114, D02301, doi:10.1029/2008jd010640, 2009.

Zhou, Y., Varner, R. K., Russo, R. S., Wingenter, O. W., Haase, K. B., Talbot, R., and Sive, B. C.: Coastal water source of short-lived halocarbons in New England, *J. Geophys. Res.*, 110, D21302, doi:10.1029/2004jd005603, 2005.

Zhou, Y., Mao, H. T., Russo, R. S., Blake, D. R., Wingenter, O. W., Haase, K. B., Ambrose, J., Varner, R. K., Talbot, R., and Sive, B. C.: Bromoform and dibromomethane measurements in the seacoast region of New Hampshire, 2002-2004, *J. Geophys. Res.*, 113, D08305, doi:10.1029/2007jd009103, 2008.